

현대물리실험

2011년 2학기

대구대학교 사범대학
과학교육학부 물리교육전공

목차

1. 전자의 비전하(e/m) 측정실험	1
2. Frank-Herz 실험	5
3. ESR 장치를 이용한 g -factor 측정실험	9
4. Zeeman 효과 측정실험	23
5. X-선 실험: Duane-Hunt의 법칙	33
6. Hall 계수 측정실험	43
*참고자료(매뉴얼 영문원본)	51

1. 전자의 비전하(e/m) 측정실험

(1) 실험목적

전자의 전하와 질량의 비를 측정하며 대전입자가 자기장 내에서 운동할 때 받는 로렌츠 힘(Lorentz force)을 이해한다.

(2) 실험원리

가열된 필라멘트 음극에 의해서 방출된 전자는 양극에 가해진 전위차에 의해 가속된다. 양극에 있는 작은 구멍을 통하여 전자가 자기장이 있는 곳으로 들어가면 전자는 속도와 자기장에 수직인 방향으로 힘을 받아 원운동을 한다. 이 실험기구의 관 내부에는 저압의 헬륨Gas가 들어 있어서 전자가 수은과 충돌하여 헬륨Gas를 여기(또는 들뜸, excitation) 시킨다. 여기 된 헬륨Gas에서 나오는 형광에 의하여 전자의 궤도와 위치를 결정할 수 있다.

전하량이 e 인 전자가 전위차 V 인 곳에서 가속될 때 얻는 운동 에너지는 $E = \frac{mv^2}{2} = eV$ 이므로 전자의 질량을 m 이라고 할 때 전자의 속도는 다음과 같이 주어진다.

$$v = \sqrt{\frac{2E}{m}} = \sqrt{\frac{2eV}{m}} \quad (1)$$

자기장 B 속에서 속도 v 로 운동하는 전자가 받는 로렌츠 힘 F 는

$$F = -e v \times B \quad (2)$$

이다. 이 힘은 속도에 수직인 방향으로 작용하므로 구심력이 되어 전자를 원운동하게 한다. 원운동의 반경을 r 이라고 하면 전자에 작용하는 힘은 다음과 같이 주어진다.

$$F = \frac{mv^2}{r} = evB \quad (3)$$

이다. 식 (I)과 (III)으로부터

$$\frac{e}{m} = \frac{2V}{B^2 r^2} \quad (4)$$

이 된다. 균일한 자기장은 헬름홀츠(Helmholtz) 코일에 의하여 생긴다. 코일의 반경이 R이고, 코일로부터 x만큼 떨어진 점에서의 자기장의 크기는 다음과 같다.

$$B = \frac{\mu_0 N I R^2}{(R^2 + x^2)^{3/2}} \quad (5)$$

위 식에서 μ_0 는 진공 상태의 투자율($4\pi \times 10^{-7} H/M$), N은 코일의 감은 총 횟수, I는 코일에 흐르는 전류이다.

(3) 실험기자재

전자의 비전하 측정장치(SG-6132D)

전자의 비전하 전원장치(SG-6134D)

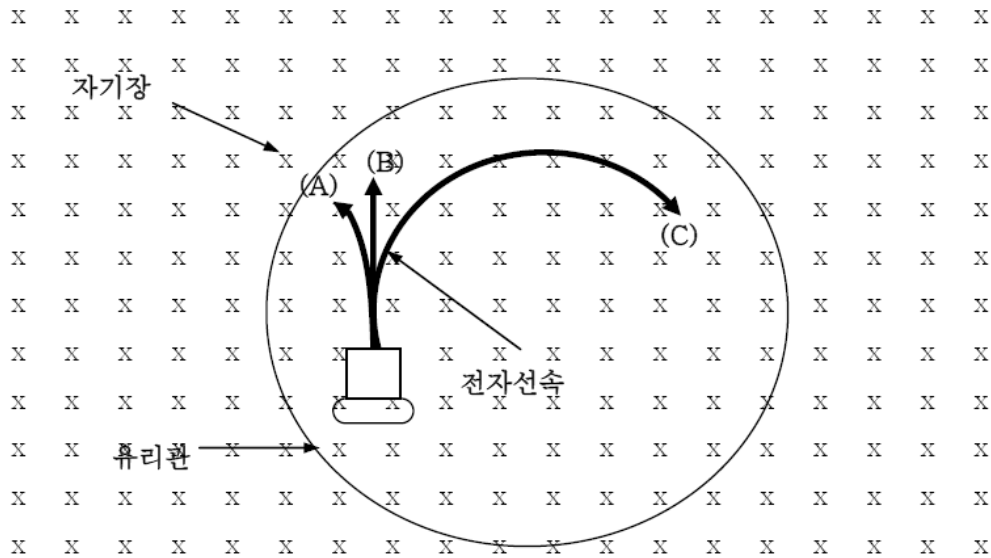


그림 1. e/m 측정관의 구조

사용 주의사항

- 램프가 코일에 평행하게 고정되어 있지 않으면 전자선속이 안쪽이나 바깥쪽으로 나선형을 그리면서 휘어질 것이다. 이는 램프를 조금만 돌림으로서 원형으로 교정할 수 있다.

(4) 실험방법

- ① 전자의 비전하 측정장치에 전자의 비전하 전원장치를 연결한다.
- ② 필라멘트에 6.3V AC전원을 가한다. 필라멘트가 달구어질 때까지 2~3분 기다린다.
- ③ 전자 가속 전압을 0 V에서부터 서서히 증가 시켜 가속 전압이 150V가 되게 한다.
- ④ 필라멘트가 달구어지면 양전극의 작은 구멍을 통과하는 전자선 속이 관찰된다. 양전극에 흐르는 전류를 측정한다.
- ⑤ 헬름홀츠 코일의 전원에서 전류 조정 나사를 돌려 전류를 변화시키면 전자선 속의 방향이 변하는 것을 관찰할 수 있다.
- ⑥ 헬름홀츠 코일에 흐르는 전류를 차단시켰을 때 전자선 속이 직선으로 진행하는지를 관찰하라. 만일, 직선으로 진행하지 않을 경우에는 코일에 흐르는 전류를 미소 변화시켜 전자선 속이 직선으로 진행하게 하고 이때 코일에 흐르는 전류 I_0 를 기록한다.
- ⑦ 헬름홀츠 코일의 전류를 증가시켜 전자선 속의 제일 바깥 부분이 눈금자의 끝 눈금에 도달하게 하고 이때의 전류 I' 를 기록하라.
- ⑧ 다른 눈금에 대해서도 과정 ⑦을 반복해서 측정한다.
- ⑨ 다른 가속 전압에 대해서도 과정 ⑥, ⑦, ⑧을 반복해서 측정한다.
- ⑩ 측정값으로부터 식(4), (5)를 이용하여 e/m 를 구하고 $\frac{e}{m} = 1.76 \times 10^{11} C/kg$ 과 비교한다.

(5) 측정 예

측정값

① 코일의 반경 : m, 코일의 간격(2×) : m, 감의 횟수(N) :

② 가속 전압 : V, $I_0 =$ A

	반경(r)	I'	$I = I' - I_0$	B	e/m
1					
2					
3					
4					
5					
평균					

② 가속 전압 : V, $I_0 =$ A

	반경(r)	I'	$I = I' - I_0$	B	e/m
1					
2					
3					
4					
5					
평균					

2. Frank-Hertz 실험

(1) 실험목적

전자를 가속시켜 원자에 충돌시켰을 때 전자들의 에너지 변화를 관찰하여 본다.

(2) 실험원리

열 음극에서 방출된 전자들은 수은 (또는 다른 기체)이 들어있는 관 내의 음극 C와 양극 A사이에서 가속되면서 수은 원자들과의 탄성충돌에 의해 산란 된다. 양극전압이 약 4.9 V가 되면 전자들의 운동에너지는 수은 원자의 가전자들을 비 탄성충돌에 의해 6^3P^1 레벨까지 올려놓기에 충분한 에너지가 된다. 이 때 전자들은 에너지를 잃어버리기 때문에 더 이상 전위가 양극보다 약간 낮은 전극 S까지 다다르지 못하게 된다. 이 때 전류 I_S 는 최소가 된다. 양극전압을 더 높여가면 전자들의 운동에너지는 더욱 높아져서 여분의 에너지에 의한 전류 I_S 의 증가가 시작된다. 양극의 전위가 $U_A = 2 \times 4.9 V$ 가 될 때까지 전자들의 운동에너지는 한 전자가 계속해서 두 개의 원자를 여기시킬 수 있게 된다. 이 때 두 번째의 낮은 전류 상태가 일어난다. U_A 에 따른 I_S 의 그래프를 그리면 전류가 높은 점들과 낮은 점들끼리의 간격이 일정하게 나타난다.

양극과 음극 사이의 전압 U_A 는

$$U_A = U + (\Phi_A - \Phi_C) \quad (1)$$

로 나타낼 수 있다. 여기서 U 는 가해진 전압이고 Φ_A 와 Φ_C 는 각각 양극과 음극의 일함수이다. 여기에너지 E_A 는 낮은 점들 간의 전위차로 결정되기 때문에 여기서 일함수들은 별 의미가 없다. 고전적인 이론에 의하면 수은 원자들이 여기 되는 에너지 레벨은 임의적이다. 그러나 양자이론에 의하면 기본적인 과정에서 원자들은 어떤 에너지 간격이 있어야만 한다. 이러한 견지에서 에 다른 곡선의 의미가 처음으로 설명되었고 이것이 곧 양자이론을 뒷받침해 주는 계기가 되었다.

여기 된 수은 원자들은 흡수한 에너지를 빛으로 방출하게 되는데 여기에너지가 4.9 eV일 때 이에 해당하는 광자의 파장은

$$\lambda = \frac{Ch}{E_A} = 253 \text{ nm} \quad (2)$$

가 된다.

여기서 $C = 2.9979 \times 10^8 \text{ m/s}$ 이고, $h = 4.136 \times 10^{-15} \text{ eV} \cdot \text{s}$ 이다.

이 파장은 자외선영역(UV)에 해당한다.

(3) 실험기자재

프랑크-헤르츠 실험 장치(SG-6142)

구성 및 규격

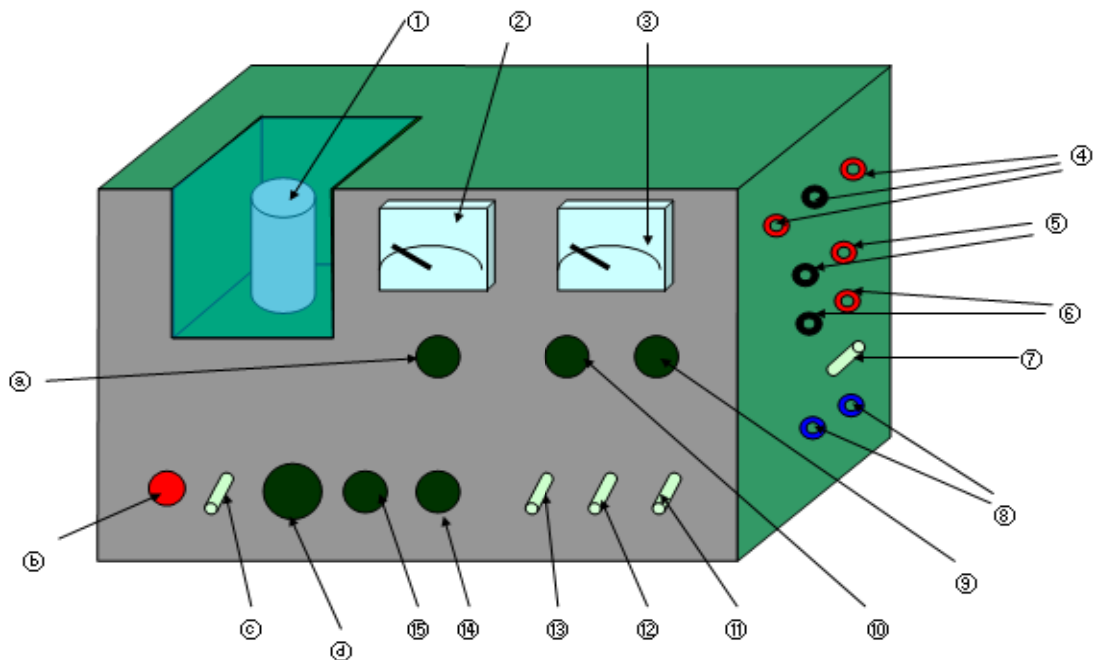


그림 1. Frank-Hertz 실험장치의 구성 및 규격

- ① 프랑크-헤르츠 관 (네온 봉 입)
- ② 전압계
- ③ 전류계
- ④ 오실로스코프 연결 단자
- ⑤ G1(2)-P 전류 외부 측정 단자
- ⑥ G2-K 전압 외부 측정 단자
- ⑦ Heater 전류 측정 mode (측정 시 open mode, 미 측정 시 short mode)
- ⑧ Heater 전류 측정 단자

- ⑨ Gain 조절 손잡이 : 전류계의 전류 변동 조정 (지시 눈금이 위를 향하도록 하는 것이 적당)
- ⑩ 영점 조절 손잡이 : 전류계의 영점을 조정한다.
- ⑪ OSC-Meter mode 선택 스위치
- ⑫ EXT - INT mode 선택 스위치 : 외부 전압계와 전류계 사용 시 EXT mode, 내부 전압계와 전류계 사용 시 INT mode
- ⑬ AUTO-MANU mode 선택 스위치 : X-Y 기록계를 사용할 때나, 자동으로 전압을 증가 시키며 전류의 변화를 관측할 때에는 AUTO mode를 선택하고, 수동으로 전압을 상승 시킬 때에는 MANU mode를 선택 한다.
- ⑭ G2-P 조절 손잡이 : 프랑크-헤르츠 관의 제2그리드와 플레이트 간의 전압 조절 손잡이
- ⑮ G2-K 조절 손잡이 : 프랑크-헤르츠 관의 제2그리드와 캐소드 간의 전압 조절 손잡이
- ㉑ G1-K 조절 손잡이 : 프랑크-헤르츠 관의 제1그리드와 캐소드 간의 전류 조절 손잡이
- ㉒ 전원 램프
- ㉓ 전원 스위치
- ㉔ Heater 전류 조절 손잡이

사용 주의사항

- 프랑크-헤르츠 관을 다룰 때에는 관이 파손되지 않도록 주의하고, 관의 유리부분을 손과 직접 접촉되지 않도록 주의한다.
- Heater 전류는 많이 흐르지 않도록 하여 실험하도록 한다.

(4) 실험방법

- ① 장치는 다음과 같이 초기 설정을 한다.
전원 스위치는 OFF, 각각의 조절 손잡이는 최소, 모드 선택 스위치는 아래로 하여 각각 MANUAL, INT, OSC를 선택한다.
우측 면에 있는 HEATER 전류 측정 선택 스위치는 SHORT로 선택한다. (OPEN으로 선택할 때에는 교류 전류계를 반드시 연결해야 한다.)
- ② 판넬면의 뚜껑을 열어 프랑크-헤르츠 관을 삽입 한다. (유리관을 삽입할 때는 유리관에 지문이 생기지 않도록 주의한다.)
**장치가 삽입되어 있으므로 눈으로 확인만 한다.*
- ③ 전원코드를 연결하고, 전원 스위치를 켜다.
- ④ 영점 조절 손잡이(ZERO. ADJ)를 조절하여 전류계의 영점을 조절한다.

- ⑤ GAIN 조절 손잡이를 적당히 조절한다. (표시된 부분이 위쪽을 향할 때가 대체로 적합하다.)
이 조절 손잡이는 G2-P 전류의 증폭을 조절하는 손잡이이다.
- ⑥ G2-K 조절 손잡이를 조절하여 전압계가 약30V가 되도록 한다.
- ⑦ HEATER 전류 조절 손잡이를 중간으로 조절하고, G1-K 조절 손잡이를 조금씩 증가 시켰을 때 전류계의 눈금이 가장 잘 움직이는 위치에서 HEATER와 G1-K의 손잡이를 고정한다. (G1-K 손잡이를 조절하여도 전류계의 변화가 적으면, G1-K 조절 손잡이를 최소로 한 후, HEATER 전류를 조금 증가 시키고, G1-K 조절 손잡이를 조절하여 보아라. 전류계의 눈금이 영역을 벗어나면 HEATER 전류를 감소 시킨 후, G1-K 조절 손잡이를 조절하여 보아라. 단, HEATER 전류는 될 수 있는 한 적게 하는 것이 좋다.)
- ⑧ 다시 G2-K 조절 손잡이를 최소로 하고, 영점 조절 손잡이를 조절하여 전압계의 영점을 조정한다.
- ⑨ G2-K 조절 손잡이를 돌려 전압계의 눈금이 30V가 되게 조작한다.
- ⑩ G2-P 조절 손잡이를 돌려 전류계의 눈금이 30uA가 되게 조정한다. (현재 G1-K 의 전압 조절에 의해 전류계의 눈금은 30uA이상에 있을 것이다. 이때 G2-P를 이용해 전류계의 눈금을 30uA가 되게 조정한다.)
- ⑪ G2-K 조절 손잡이를 최소로 하고, 다시 영점 조정한다.
- ⑫ 이제 G2-K조절 손잡이를 돌려 전압을 증가 시키면서 전압에 따른 전류계의 눈금의 변화를 측정 기록한다. 그 결과를 이용하여 전압과 전류에 따른 그래프를 그린다. (X-Y기록계를 이용한 측정 시 : Mode 선택 스위치를 Auto로 조정하고 G2-K스위치를 최대로 하고, 전압과 전류의 변화를 관찰한다.)
- ⑬ 전압의 증가에 따른 전류의 증가 감소의 변화가 일어나지 않을 때에는 G2-P조절 손잡이와 Heater 전류 조절 손잡이를 조절한다.

3. ESR 장치를 이용한 g-factor 측정실험

(1) 실험목적

- 선택한 주기 ν 의 함수인 공명 자기장 B_0 측정
- DPPH의 g-factor 측정
- 공명 신호의 선폭 δB_0 측정

(2) 기본원리

1945년 E. K. Zavoisky에 의해 발견된 이후, 전자스핀공명(Electron Spin Resonance, ESR)은 물리, 화학, 생물 그리고 의학 분야에서 분자와 결정의 구조, 화학반응 그리고 다른 여러 가지 문제를 조사하는 중요한 방법으로 현재까지 발전되고 있다. 전자스핀공명은 전자의 스핀상태를 분할시켜주는 외부 자기장내에 있는 상자성체 물질에 의한 고주파 복사의 흡수에 기초한다.

전자스핀공명은 상자성체 물질로 제한되는데 그 이유는 상자성체 물질에서는 전자의 궤도 각운동량과 전자의 스핀이 총각운동량이 0이 되지 않도록 결정한다. 적절한 화합물의 예는 원자의 내부껍질이 완전히 채워지지 않은 전이금속과 희토류이고, 상자성체 상태에서는 격자빈자리를 가진 결정 혹은 개별 홀전자(unpaired electron)를 포함하는 유기 분자(자유 라디칼)이다.

총 각운동량 \vec{J} 와 관련된 자기 모멘트는

$$\vec{\mu}_J = -g_J \cdot \frac{\mu_B}{\hbar} \cdot \vec{J} \quad (1)$$

$$\left(\mu_B = \frac{\hbar \cdot e}{2 \cdot m_e}, \hbar = \frac{h}{2\pi}, \mu_B: \text{Bohr 마그네톤}, h: \text{Plank 상수}, \right.$$

$g_J: \text{Landé splitting factor}, m_e: \text{전자의 질량}, e: \text{전자의 전하량} \left. \right)$

이며, 자기장 \vec{B}_0 내에서 자기 모멘트 $\vec{\mu}_J$ 는 퍼텐셜 에너지

$$E = -\vec{\mu}_J \cdot \vec{B}_0 \quad (2)$$

를 얻는다.

E 는 양자화 되어있는데 그 이유는 자기 모멘트와 총 각운동량이 자기장에 비례하여 불연속적인 방향만을 할 수 있기 때문이다. 각각의 각운동량의 방향은 자기장 내의 특정 궤선을 가진 상태에 상응한다. 총 각운동량의 성분 J_z 는 자기장에 평행하며,

$$J_z = \hbar \cdot m_J \quad (m_J = -J, -(J-1), \dots, J) \quad (3)$$

와 같이 주어지는데, 이 때 각운동량의 양자수는 정수 혹은 반정수이다. 즉, 궤선 에너지는

$$E = g_J \cdot \mu_B \cdot B_0 \cdot m_J \quad (m_J = -J, -(J-1), \dots, J) \quad (4)$$

와 같이 불연속적인 Zeeman 준위에 따라 분리된다.

에너지 분리는 전자스핀공명법으로 직접 측정될 수 있다. 측정을 위해 고주파 교류 자기장은 $\vec{B}_1 = \vec{B}_{HF} \cdot \sin(2\pi\nu \cdot t)$ 이며, 시료에서 방출되는 정적 자기장 \vec{B}_0 에 수직인 고주파 교류자기장 B_1 는 시료와 관련되어 있다. 교류 자기장의 에너지 $h \cdot \nu$ 가 이웃하고 있는 두 개의 에너지 준위 사이의 에너지차이 ΔE 와 같다면, 즉, 조건이

$$\Delta m_J = \pm 1 \quad (5)$$

$$h \cdot \nu = \Delta E = g_J \cdot \mu_B \cdot B_0 \quad (6)$$

로 만족하면, 교류자기장은 자기장 B_0 내에서 하나의 방향으로부터 다른 방향으로 자기 모멘트의 “들뜸”을 유도한다. 즉, 이웃한 준위 사이에서 전이가 유도되고, 시료 내로 방출되는 교류 자기장으로부터 에너지의 흡수로 나타나는 공명효과가 관찰된다.

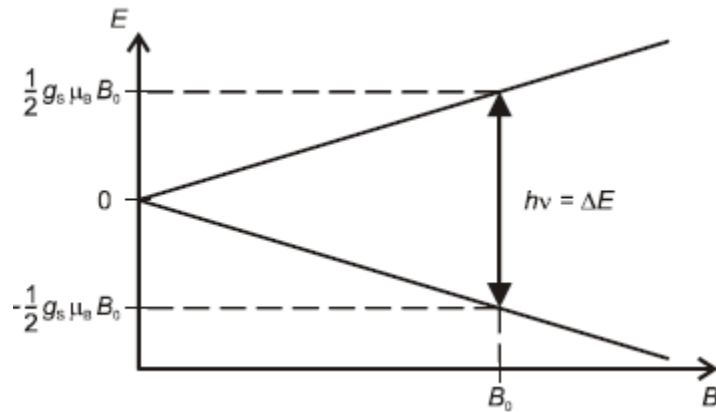


그림 1. 자기장에서 자유전자의 에너지 분리와 전자스핀 공명의 공명조건

수많은 화합물에서 궤도각운동량은 별로 중요하지 않으며, 전자의 스핀만 고려하자. 문제를 단순화하기 위해, 상황을 그림 4.1의 자유전자로 표현해보자. 여기서 총 각운동량은 단지 전자의 스핀 \vec{s} 이다. 각운동량 양자수는

$$J = s = \frac{1}{2} \text{이며, Landé 인자는 } g_J = g_s \approx 2.0023 \text{ 이다.}$$

자기장 내에서 전자의 에너지는

$$E = g_s \cdot \mu_B \cdot B_0 \cdot m_s = -\frac{1}{2}, \frac{1}{2} \quad (4a)$$

의 두 에너지로 분리되며, 이 두 에너지는 자기장에 따라 전자 스핀의 방향이 반평행과 평행에 해당된다. 두 개의 준위 사이의 전이에서 선택률 (4.5)는 자동으로 만족한다: 식 (4.6)과 같은 방법으로, 공명조건은

$$h \cdot \nu = g_s \cdot \mu_B \cdot B_0 \quad (6a)$$

와 같다.

만약 교류 자기장으로부터 흡수된 에너지를 자기장 B_0 의 함수로서 고정 주파수 ν 에서 측정하였을 때, 반치폭 δB_0 를 가진 흡수선을 측정된다. 가장 단순한 경우에, 균일한 자기장내에서 선폴은 전이의 불확정성 δE 를 나타낸다. 불확정성의 원리에 따라

$$\delta E \cdot T \geq \frac{\hbar}{2} \quad (7)$$

가 되며, 여기서 T는 준위의 수명이다. 식 (5)로 인해,

$$\delta E = g \cdot \mu_B \cdot \delta B_0 \quad (8)$$

이 된다. 그래서 관계식

$$\delta B_0 = \frac{\hbar}{2 \cdot g_J \cdot \mu_B \cdot T} \quad (9)$$

는 진동수 ν 에 의존하지 않는다. 이 실험에서 시료의 ESR 스펙트럼내의 흡수선의 위치와 폭이 평가된다. ESR 스펙트럼 흡수선의 위치로부터, 시료의 Landé 인자 g_J 는 식 (6)에 따라 결정된다. 자유 원자 혹은 이온의 경우에, 만약 자성이 전적으로 궤도 각운동량에 기인하면, Landé 인자 $g_J = 1$ 이 되며, 만약 스핀만이 자성에 기여한다면, Landé 인자는 $g_J \approx 2.0023$ 이 된다. 그러나 실제로 전자스핀공명 법에 의해 연구된 상자성체 중심은 이러한 사실과 잘 맞지 않는다. 상자성체가 결정격자에 삽입되거나 혹은 상자성체가 용액 안에 있는 용매화층으로 둘러싸일 때, 상자성체는 둘러싸인 원자에 의해 발생한 강한 전기장과 자기장을 받는다. 이들 전기장과 자기장은 에너지 이동을 유도하고 전자의 Zeeman 분리에 영향을 준다. 그렇게 함으로써 g-factor의 값이 변하게 된다. g-factor의 값은 자주 이방성이 되고 미세구조가 ESR 스펙트럼 내에서 발생한다. 그러므로 g-factor는 시료의 화학 구조와 전자결합을 나타낸다고 결론 지을 수 있다.

선폭으로부터 동적 특성이 유추될 수 있다. 만약 성분으로 분리되지 않은 미세구조를 무시한다면, 선폭은 자기모멘트의 정렬과는 반대되는 몇 가지 과정들에 의해 결정된다. 서로 정렬된 자기모멘트 사이의 상호작용은 스핀-스핀 완화(spin-spin relaxation)라고 하고, 자기모멘트와 전자기장의 요동은 자기모멘트와 전자기장의 요동 사이의 상호작용은 스핀-격자 완화(spin-lattice relaxation)이라고 하는데, 고체내의 격자 진동과 액체내의 원자의 열운동에 의한 것이다.

어떤 경우에는 선폭이 이른바 교환 상호작용(exchange interaction)에 의해 영향을 받고, 그리고나서 만약 스핀의 순수한 쌍극자-쌍극자 간 상호작용이 있다면 선폭은 기대한 것보다 훨씬 작다.

실제적인 응용을 위해 개발된 ESR 스펙트로미터는 약 10 GHz의 주파수에서 대체로 작동한다. 이에 상응하여 자기장은 0.1 T에서 1T에 이르는 크기이다. 이 실험에서 자기장 B_0 는 상당히 약하다. 자기장은 헬륨홀츠 코일법으로 발생되며, 적절한 코일전류를 적절히 선택함으로써 0 mT와 4 mT사이의 값으로 조절될 수 있다. 50 Hz로 변조되는 전류는

일정한 코일 전류가 더해진다. 이에 상응하게 변조되는 자기장 B는 동일한 방향의 자기장 B_0 와 50 Hz B_{mod} 로 구성된다. 시료는 고용량 진동회로의 부분인 HF(고주파용) 코일 내에 놓인다. 진동회로는 15 MHz와 130 MHz사이의 주파수를 갖는 가변주파수 HF 발전기에 의해 들뜬다.

만약 공명조건 식 (5)를 만족하면, 시료는 에너지를 흡수하고 진동회로는 만들어진다. 그 결과, 진동회로의 임피던스는 변하고 코일에 있는 전압은 감소한다. 이 전압은 정류와 증폭에 의해 측정신호로 변환된다.

측정신호는 변조 자기장에 대해 상대적인 시간지연을 가지고 조절부의 출력으로 나타낸다. 시간지연은 조절부 내에 있는 위상 변위로서 보상될 수 있다. X-Y 작동이 되는 2채널 오실로스코프를 사용하면, 자기장에 비례하는 전압과 함께 측정신호를 공명신호로서 나타낼 수 있다. 만약 동일한 방향의 자기장 B_0 가 공명조건을 만족하고 위상 변위 ϕ 가 측정신호와 변조된 자기장이 상쇄된다면, 공명신호는 대칭적이 된다(그림 2).

사용된 시료물질은 1,1-diphenyl-2picryl-hydrazyl(DPPH) 이다. 이 유기화합물은 질소와 질소 결합다리의 한 원자에서 짝을 짓지 못한 가전자를 갖는 비교적 안정된 자유라디칼이다(그림 3을 참조).

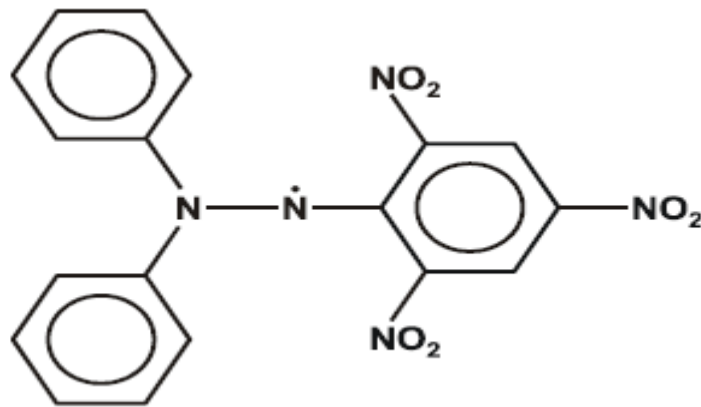
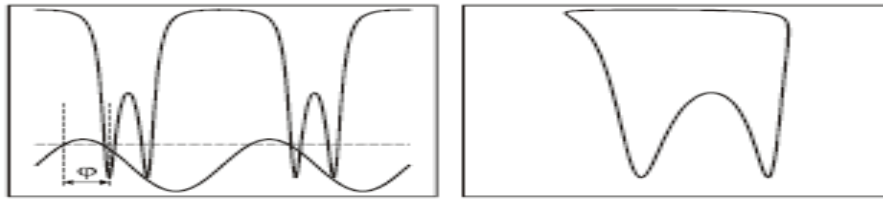
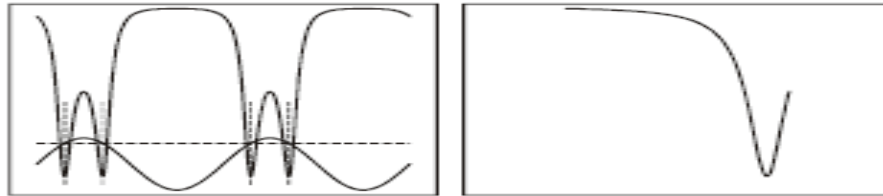


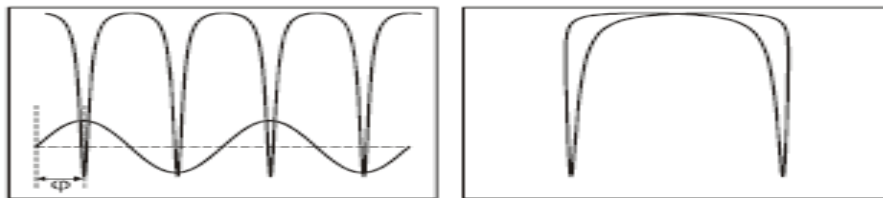
그림 3. 1,1-diphenyl-2picryl-hydrazyl(DPPH)의 화학구조



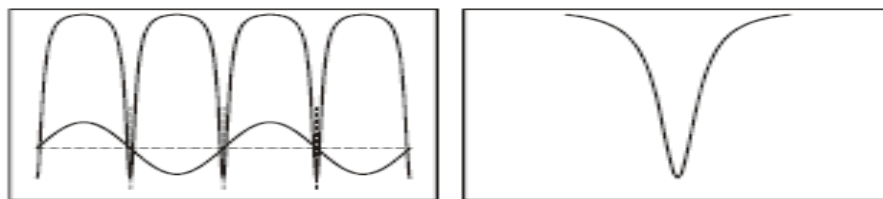
2a



2b



2c



2d

그림 2. 오실로스코프는 측정신호 중의 하나(각각 Y 혹은 I)와 변조 자기장(X 혹은 II)을 보여준다.

왼쪽: 2-채널은 채널 II에 연결된 DC를 보여준다.

오른쪽: XY는 채널 II에 연결된 AC를 보여준다.

그림 2a. 위상 이동 ϕ 는 상쇄되지 않았고, 동일한 방향의 자기장 B_0 는 매우 약하다.

그림 2b. 위상 이동 ϕ 는 상쇄되었으며, 동일한 방향의 자기장 B_0 는 매우 약하다.

그림 2c. 위상 이동 ϕ 는 상쇄되지 않았고, 동일한 방향의 자기장 B_0 는 적절하다.

그림 2d. 위상 이동 ϕ 는 상쇄되었으며, 동일한 방향을의 자기장 B_0 는 적절하다.

전자의 궤도운동은 분자구조에 의해 거의 상쇄된다. 그러므로 전자의 g-factor는 자유 전자의 g-factor와 거의 같다. 다결정질 형태의 물질은 전자스핀공명을 보여주기에는 아주 적절한데 그 이유는 강한 ESR 선을 갖는 좁은 선폭 때문이다.

(3) 실험기자재

- ① ESR 기본장치, ② ESR조절부, ③ 헬름홀츠 코일 1쌍, ④ 2-채널 오실로스코프, ⑤ 1m 인 BNC 케이블 2개, ⑥ 새들 베이스 3개, ⑦ 25cm인 검정색 연결 전선 1개, ⑧ 50cm인 붉은색 연결전선 1개, ⑨ 50cm인 파란색 연결전선 1개.

(4) 설치

*그림 4와 5는 실험을 위한 장치도이다.

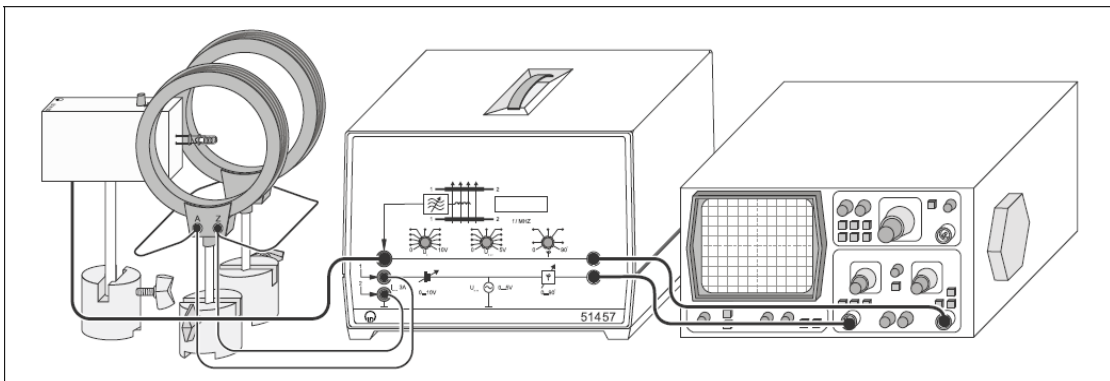


그림 4. 시료 DPPH를 사용한 전자스핀 공명의 실험설정

- 각각의 헬름홀츠 코일은 평균 거리가 6.8 cm가 되도록 역학적으로 평행하게 놓는다.
(평균 반경 r은 같다.)
- 각각의 헬름홀츠 코일은 직렬로, 전류계는 ESR 조절부에 직렬로 연결한다.
- 6-pole 케이블은 ESR 조절부의 ESR 기본장치에 연결한다.
- BNC 케이블로 2채널 오실로스코프의 채널 I 에 ESR 조절부의 Y출력을 연결하고, 오실로스코프의 채널 II 에 ESR 조절부의 X출력에 연결한다.
- 오실로스코프는
 $Y_I : AC; 0.5 \text{ V/cm}, \quad X : AC; 2 \text{ V/cm}$
 로 설정한다.

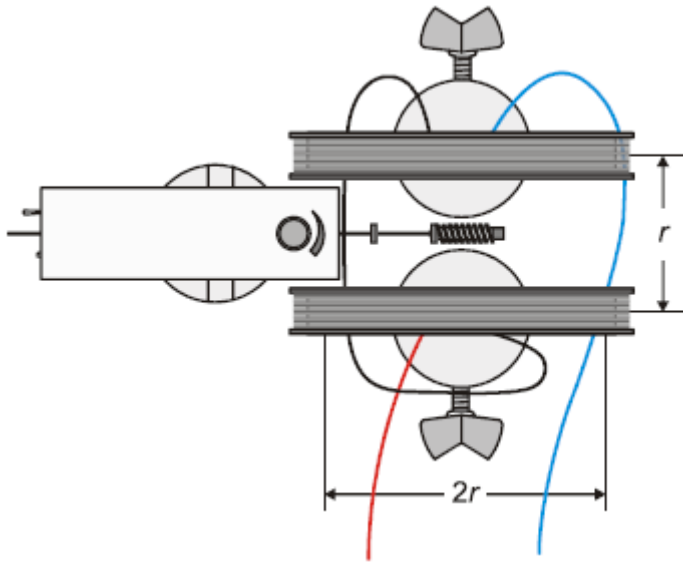


그림 5. 위에서 본 헬름홀츠 코일의 배열

(5) 실험수행

공명자기장 B_0 측정:

-교류 전류장의 진동범위에 해당되는 아래의 플러그인 타입의 코일을 하나 선택한다.



선택한 코일 내부에 DPPH 시료 **DPPH sample** 를 넣는다.

-교류 전류장의 진폭이 너무 작은 자석의 직류전류장과 겹쳐지면, 신호가 화면에 보일 때까지 자석의 직류전류장을 천천히 증가시킨다.

*참고: 일반적으로 두 개의 공명신호가 보인다. 이것은 자석의 교류전류가 각 위상에 대하여 두 번의 공명점을 지나고, 오실로스코프에 나타난 전압들 사이에 위상상쇄가 있기 때문이다.

-위상이동자로 공명신호를 일치시키고, 직류전류장을 변화시킴으로서 화면의 중심에 공명신호가 대칭이 되도록 설정한다(그림 6 참조).

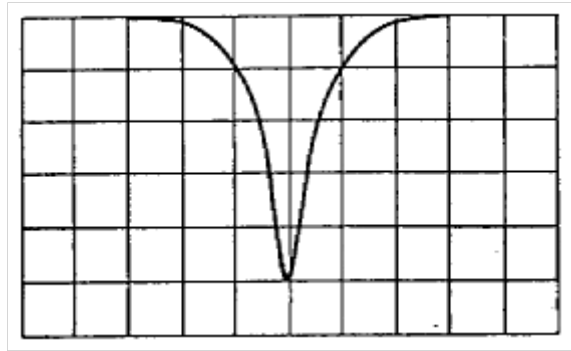


그림 6. 오실로스코프에 나타난 도형

- 고주파 발전기의 진동수 f 를 증가시켜라
자기력선속밀도 B 가 클 때에만 공명선이 오실로스코프 화면에 나타난다.
- 직접 자석의 전류장을 증가시킴으로서 공명선이 원래의 위치로 재설정한다(화면의 정중점으로 $X = 0$ 에서 대칭이 되도록).
- 주기 f 와 B 에 비례하는 직류의 진폭 I 를 측정하고, I 의 정확한 측정을 한다.
외부자기장의 변조진폭을 감소시킴으로서 낮은 ESR 신호를 선택하고, 직류전류장이 있는 화면의 중심에서 대칭이 나타나도록 나머지 ESR 신호를 조절한다(그림 7 참조).
- 설명한 방법에 따라 f 와 I 를 측정한다(그림 8 참조).

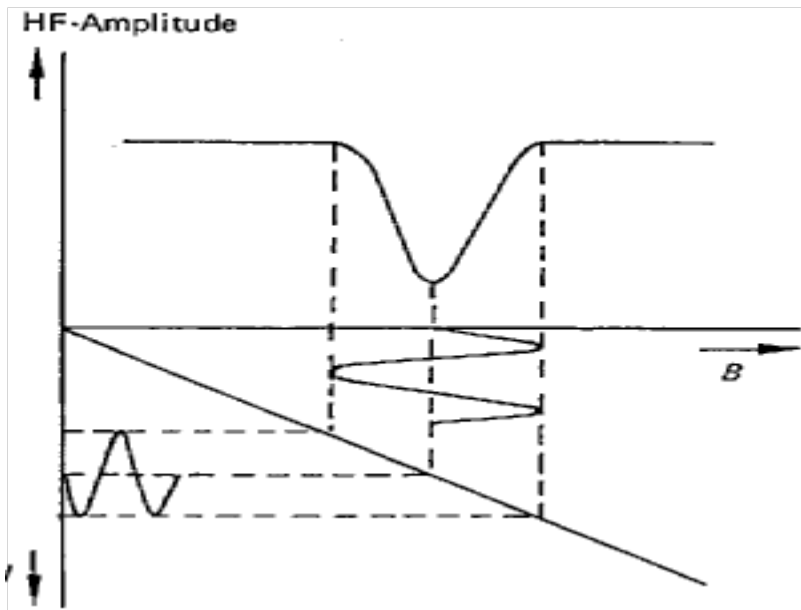


그림 7. 대칭인 공명 신호의 경우에 공명신호의 최대값은 I에 비례하는 자기력 선속밀도 B와 함께 자석의 직류전류장의 진폭을 표시한다.

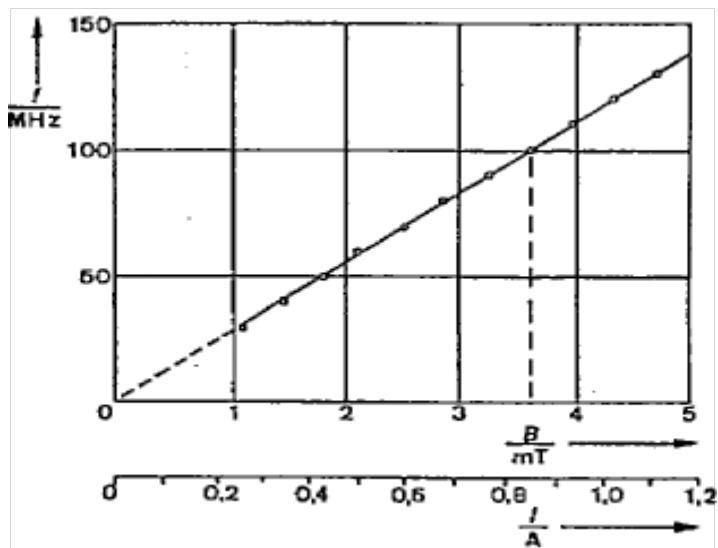


그림 8. 헬름홀츠 코일에 측정전류에 비례하는 자석의 공명자기장 강도 B의 함수로서 공명주기 f

(6) 측정 예

공명자기장 B_0 측정

표 1에서 공명의 경우, 직렬로 연결된 헬름홀츠 코일을 통하는 전류 I_0 는 교류 고주파 영역의 주파수 ν 의 함수로 표시된다.

$\frac{\nu}{\text{MHz}}$	$\frac{I}{\text{A}}$	Plug-in coil
15	0.13	big
20	0.17	big
25	0.21	big
30	0.26	big
30	0.26	medium
35	0.30	medium
40	0.34	medium
45	0.38	medium
50	0.43	medium
55	0.47	medium
60	0.51	medium
65	0.55	medium
70	0.60	medium
75	0.64	medium
75	0.64	small
80	0.68	small
85	0.72	small
90	0.77	small
95	0.81	small
100	0.85	small
105	0.89	small
110	0.94	small
115	0.98	small
120	1.02	small
125	1.06	small
130	1.11	small

표 1. 교류 자기장의 주파수 ν 의 함수인 전류 I_0

반치폭 δB_0 측정

오실로스코프로부터 읽은 반치폭은 1.5 cm이며, 이에 해당하는 $\delta U = 1.5 \text{ cm} \cdot 0.2 \frac{V}{\text{cm}} = 0.3 \text{ V}$ 이다.

전체 변조 전압 U_{mod} 의 보정은 $U_{\text{mod}} = 10 \text{ cm} \cdot 0.5 \frac{V}{\text{cm}} = 5 \text{ V}$ 이며, $I_{\text{mod}} = 0.28 \text{ A}$ (교류 전류의 RMS 값)에 해당한다. 피크와 피크 사이의 진폭은 RMS값의 $2\sqrt{2}$ 이다.

(7) 수치계산

헬름홀츠 코일의 자기장 B는 각각의 코일을 통하는 전류로부터 계산될 수 있다.

$$B = \mu_0 \cdot \left(\frac{4}{5}\right)^2 \cdot \frac{n}{r} \cdot I, \quad \mu_0 = 4\pi \cdot 10^{-7} \frac{Vs}{Am} \quad (n: \text{코일당 감긴 횟수}, r: \text{코일의 반경})$$

$n=320$ 이고, $r=6.8 \text{ cm}$ 이면, $B = 4.23 \text{ mT} \cdot \frac{I}{A}$ 가 얻어진다.

공명자기장 B_0 측정

자기장에 대해 계산된 수치가 표 2에 작성되었다.

$\frac{\nu}{\text{MHz}}$	$\frac{B_0}{\text{mT}}$
15	0.55
20	0.74
25	0.93
30	1.08
35	1.27
40	1.46
45	1.63
50	1.82
55	1.99
60	2.12
65	2.33
70	2.54
75	2.75
80	2.86
85	3.07
90	3.28
95	3.38
100	3.60
105	3.81
110	4.02
115	4.12
120	4.23
125	4.44
130	4.65

표 2. 교류 자기장의 주파수 ν 의 함수인 자기장 B_0

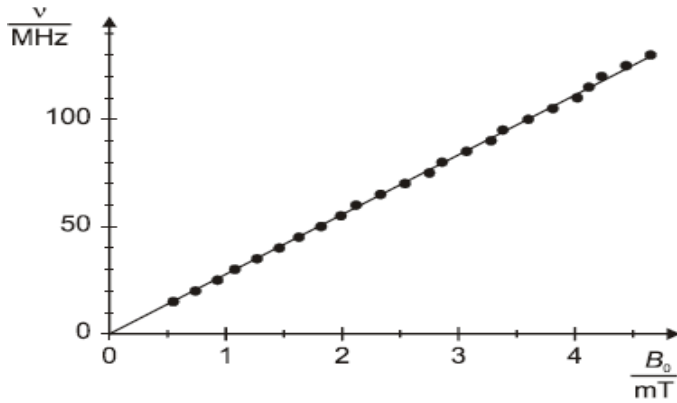


그림 9. 시료 DPPH에 대해 측정된 자기장의 함수인 공명 주파수

그림 9는 측정된 수치의 그래프를 보여준다. 그래프에서 원점을 지나는 직선의 기울기는

$$\frac{\nu}{B_0} = 27.8 \frac{MHz}{mT} \text{ 이다.}$$

이로부터 g-factor는 아래와 같다:

$$g = \frac{h \cdot \nu}{\mu_B \cdot B_0} = \frac{6.625 \cdot 10^{-34} \text{ Js}^2}{9.273 \cdot 10^{-24} \text{ Am}^2} \cdot 27.8 \frac{MHz}{mT} = 1.99$$

문헌에서 인용되는 수치: g-factor(DPPH) = 2.0036

반치폭 δB_0 측정

$$\delta I = \frac{\delta U}{U_{\text{mod}}} \cdot I_{\text{mod}} = \frac{0.3 \text{ V}}{5 \text{ V}} \cdot 0.28 \text{ A} \cdot 2 \cdot \sqrt{2} = 0.049 \text{ A}$$

$$\text{이로부터 } \delta B_0 = 4.23 \text{ mT} \cdot \frac{\delta I}{A} = 0.21 \text{ mT} \text{로 얻어진다.}$$

문헌에서 인용되는 수치: δB_0 (DPPH) = 0.15 ~ 0.81 mT

선폭은 재결정화되는 물질 내에서 용매에 강하게 의존한다. 문헌에서 인용되는 가장 작은 값을 가진 물질은 용매로서 CS_2 (이황화탄소)이다.

4. Zeeman 효과 측정실험

(1) 실험목적

- 정상 가로 Zeeman 효과에 대한 삼중분리선 관찰
- 삼중분리선 성분의 분극 상태 측정
- 정상 세로 Zeeman 효과에 대한 이중분리선 관찰
- 이중분리선의 분극 상태 측정

(2) 기본원리

정상 Zeeman 효과

Zeeman 효과는 외부 자기장의 작용으로 인한 스펙트럼 선 혹은 원자의 에너지 준위의 분리를 의미한다. Zeeman 효과는 전자의 고전이론의 한 부분으로서 1856년에 H. A. Lorentz에 의해 처음으로 예측되었고, 실험적으로는 수 년 후에 Zeeman에 의해 확증되었다. Zeeman은 자기장에 수직인 각도에서 단일 스펙트럼 선 대신에 삼중분리선(Triplet)을, 자기장에 평행인 각도에서는 이중분리선(Doublet)을 관찰했다. 이후에, 더욱 복잡한 스펙트럼선의 분리가 관찰되었는데, 이것은 비정상 Zeeman 효과로 알려지게 되었다. 이 같은 현상을 설명하기 위해, Goudsmit와 Uhlenbeck은 1925년에 처음으로 전자스핀에 대한 가설을 도입했다. 결국, 비정상 Zeeman 효과는 실제적인 법칙이며, 정상 Zeeman 효과는 하나의 예외라는 것이 명백해졌다.

정상 Zeeman 효과는 오직 총 스핀 $S=0$ 을 갖는 원자상태들 사이의 전이에서만 발생한다. 그런 뒤 이 상태의 총 각운동량 $J=L+S$ 는 순수한 궤도각운동량 $J=L$ 이 된다. 이에 해당하는 자기장에 대해, 우리는 다음과 같이 말할 수 있다.

$$\mu = \frac{\mu_B}{\hbar} J \quad (1)$$

$$\text{여기서, } \mu_B = \frac{\hbar e}{2m_e} \quad (2)$$

(μ_B = Bore 마그네톤, m_e =전자의 질량, e =기본전하, \hbar =Plank 상수)

외부 자기장 B 내에서 자기 모멘트는 에너지

$$E = -\mu \cdot B \quad (3)$$

를 갖는다.

자기장의 방향내에서 각운동량 성분은

$$J_z = M_J \cdot \hbar \quad (M_J = J, J-1, \dots, -J) \quad (4)$$

의 값을 가질 수 있다.

그러므로, 각운동량 J 는 M_J 의 값에 의해 달라지는 $2J+1$ 인 등간격의 Zeeman 성분으로 분리된다. 인접 성분 M_J, M_{J+1} 의 에너지 간격은

$$\Delta E = \mu_B \cdot B \quad (5)$$

이다.

예를 들면, 카드뮴의 붉은색 스펙트럼선($\lambda_0 = 643.8 \text{ nm}$, $f_0 = 465.7 \text{ THz}$)에서 우리는 정상 Zeeman 효과를 관찰할 수 있다. 이것은 5번째 껍질의 전자의 $^1D_2 (J=2, S=0) \rightarrow ^1P_1 (J=1, S=0)$ 전이에 해당한다.

자기장에서 1D_2 준위는 5개의 Zeeman 성분으로 분리되고 1P_1 은 식 (5)를 사용하여 계산된 3개의 Zeeman 성분으로 분리된다.

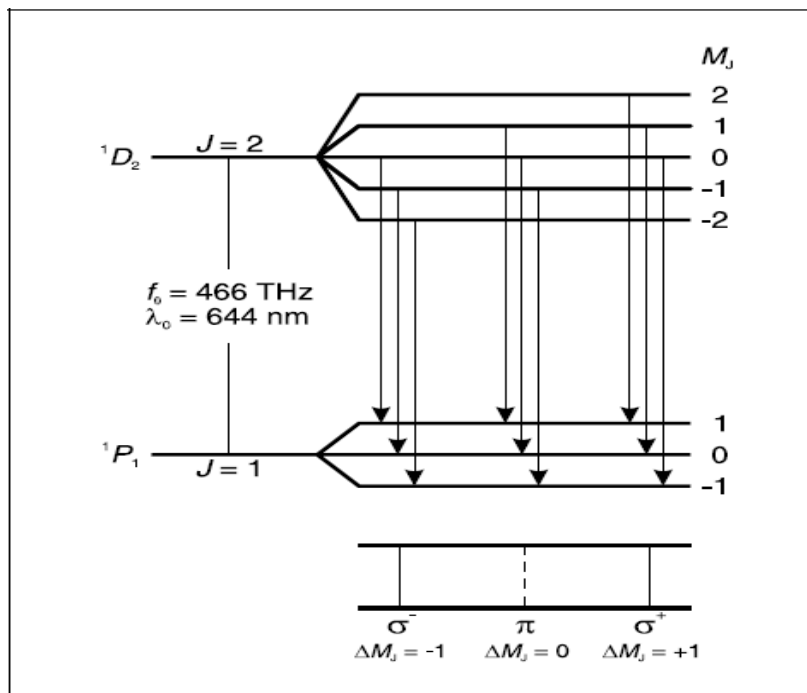


그림 1. 카드뮴 내에서 정상 Zeeman 효과의 준위 분리와 전이

이들 준위 사이에서 광학 전이는 오직 전기쌍극자 복사선의 형태로만 가능하다. 이 상태의 자기 양자수 M_J 에 적용한 선택률은 아래와 같다.

$$\Delta M_J \begin{cases} = \pm 1 & \sigma \text{ 성분} \\ = 0 & \pi \text{ 성분} \end{cases} \quad (6)$$

따라서, 우리는 모두 3개의 스펙트럼선을 관찰한다(그림 1을 참고). 즉, π 성분은 이동하지 않고, 두 개의 σ 성분은 원래 주파수에 대하여

$$\Delta f = \pm \frac{\Delta E}{h} \quad (7)$$

만큼 이동하는데, 위의 식에서 ΔE 는 식(5)에서 계산된 등간격 에너지 분리이다.

각분포와 편광

자기장의 방향에서 각운동량 성분 ΔM 에 따라서, 방출된 광자는 서로 다른 각분포를 보인다. 그림 5.2는 2차원 극성 그림의 한 형태로 각분포를 보여준다. 자기장이 모든 카드뮴 원자에 대한 공통 축에 의해 나타내어지기 때문에 이들은 실험적으로 관찰될 수 있다.

고전적인 측면에서 $\Delta M_J = 0$ 인 경우는 자기장에 평행한 극미한 쌍극자 진동에 해당한다. 양자들은 자기장의 방향대로 방출되지 않는다. 즉, π 성분은 자기장에 평행한 방향에서 관찰될 수 없다. 자기장에 수직으로 방출되는 빛은 선형적으로 편광되고, 그에 따라 E 벡터는 자기장에 평행한 방향과 쌍극자의 방향에서 진동한다(그림 3을 참고).

반대로, $\Delta M_J = \pm 1$ 의 경우에 대부분의 양자들은 자기장의 방향으로 이동한다. 고전적인 측면에서, 이 경우는 90° 의 위상차를 갖는 두 개의 나란한 쌍극자 진동에 해당한다. 두 쌍극자의 중첩은 순환전류를 발생시킨다. 따라서 자기장의 방향내에서 원편광 빛이 방출된다. 양의 방향에서, $\Delta M_J = +1$ 의 경우 시계방향이고 $\Delta M_J = -1$ 의 경우 반시계 방향이다(그림 3을 참고).

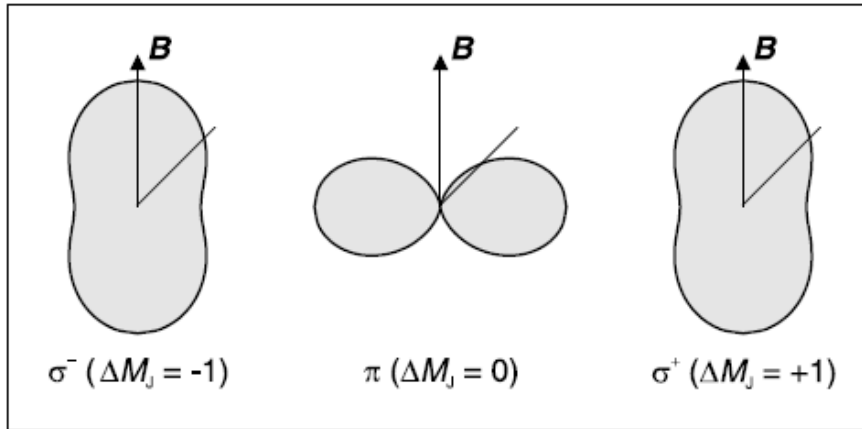


그림 2. 전기 쌍극자 복사선의 각분포(ΔM_j : 자기장의 방향에서 방출되는 광자의 각운동량 성분)

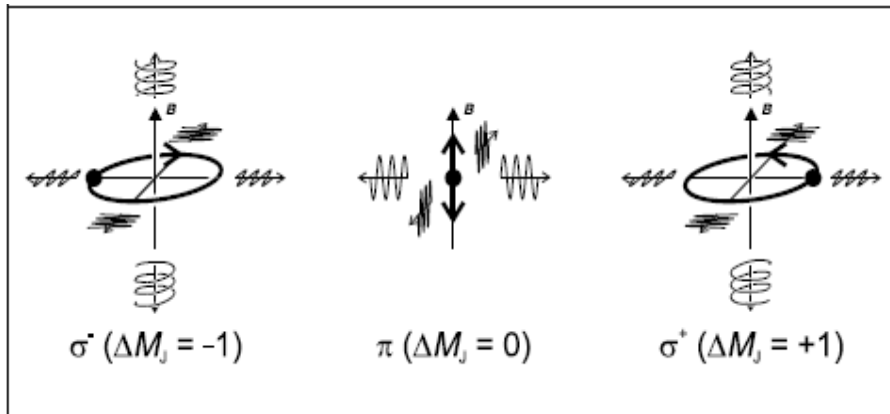


그림 3. Zeeman 성분의 분극 그림

Zeeman 성분의 분광학

Zeeman 효과는 다르게 편광된 성분의 스펙트럼 분리가 가능하게 한다. 그러나 스펙트럼의 분리를 보이기 위해, 극히 높은 해상도를 갖는 스펙트럼 장치가 필요한데, 예를 들면, 각각 $\Delta\lambda = 0.02\text{nm}$, $\Delta f = 14\text{GHz}$ 에 의한 자기선속밀도(magnetic flux density) $B = 1\text{T}$ 에서만 붉은색 카드뮴 선의 두 σ 성분이 이동된다.

Lummer-Gercke plate는 이 실험을 위해서 사용된다. 이 구성품은 표면의 편평함과 평행함에 대해 아주 큰 정밀도를 갖도록 제작되었다. 수직방향으로 발산하는 빛은 길고 평행한 유리판에 붙어 있는 프리즘을 거쳐 수평방향으로 통과한다(그림 4를 참조).

유리판 내부에서 빛은 매번 곧바로 생겨난 빛의 일부와 함께 앞, 뒤로 반사된다.

$\alpha = 90^\circ$ 의 각도에서 관찰 할 때, 유리판 내부의 반사는 전반사의 한계각도 내에서 거의 발생된다. 이 같은 결과는 높은 반사계수 때문인데 즉, 유리판이 충분히 길 때 많은

광선들이 서로 간섭을 일으킬 수 있기 때문이다. 간섭된 광선들은 무한대에 초점을 맞춘 망원경을 사용하여 관찰할 수 있다. 주어진 파장 λ 에 대하여 수평선의 동일한 계에 있는 두 개의 거울상은 유리판 위와 아래에서 관찰될 수 있다. 각각의 간섭 선은 Lummer-gerhcke plate 으로부터 나오는 성분광선 α 와 프리즘으로 들어가는 입사각 β 로부터 광선으로 할당된다.

α_k 의 각도로 나오는 광선은 아래와 같은 조건을 만족할 때 보강간섭이 일어난다.

$$\Delta = 2d \cdot (n^2 - \sin^2 \alpha_k)^{1/2} = k \cdot \lambda, \quad k = 1, 2, 3, \dots \quad (8)$$

(Δ = 광 경로차, d = plate의 두께, n = 유리의 굴절률, k = 간섭 차수)

$\delta \lambda$ 에 의한 파장내에서의 변화는 $\delta \alpha$ 의 각도만큼의 간섭 선의 이동으로 나타난다. 만약 스펙트럼선이 거리 $\delta \lambda$ 를 갖는 많은 광선 성분들을 포함한다면, 각각의 간섭 선들은 $\delta \alpha$ 를 갖는 성분의 수에 따라 갈라질 것이다. 따라서 Doublet 구조 내에서는 Doublet 스펙트럼선, Triplet 구조 내에서는 Triplet 스펙트럼선으로 나타난다.

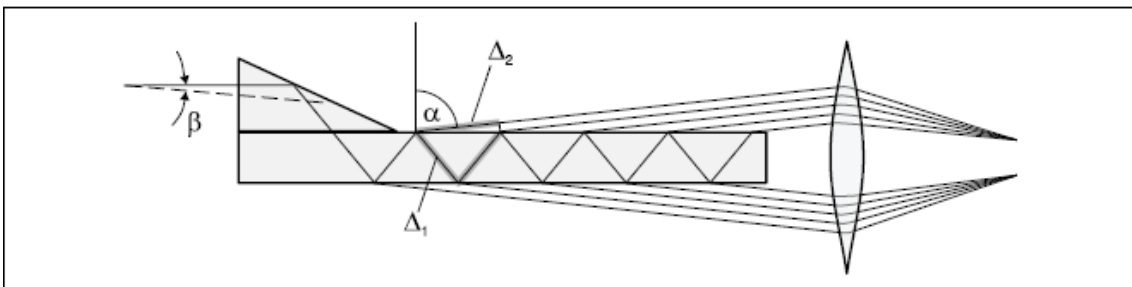


그림 4. 간섭분광계로서 Lummer-Gehrcke plate(입사각 $\beta=0$ 에 대한 빛다발은 굴절되지 않은 선들로 그려졌음). 두 인접 광선 사이의 광경로차는 $\Delta = n\Delta_1 - \Delta_2$ 이다.

(3) 실험기자재

- ① Zeeman 효과용 카드뮴 램프, ② Zeeman 효과 관찰용 광학시스템,
- ③ Lummer-Gehrcke plate, ④ Zeeman 효과용 전자석, ⑤ 고전류 전원공급장치

(4) 설치

처음설정:

그림 5는 수평으로 배치하기 위한 장치도이다.

- 광학시스템의 밑판(base plate)위에 Zeeman 효과 실험을 위한 전자석을 올려놓는다. 육각나사를 밑판 아래와 고정시킨다.
- 10 mm 간격으로 전자석들을 올려놓는다.
- 카드뮴 램프(cadmium lamp) (b)를 전자석의 전기 연결부분에 설치한다.
- 전자석들과 유지 스트랩(retaining straps)을 사용한 카드뮴 램프(cadmium lamp)의 받침대가 고정되어 있는지 확인한다.
- 전선이 광선 다발의 경로를 막지 않도록 하기 위해 전기적으로 연결되어 측면으로 향하는 스펙트럼 램프위의 fused point를 돌린다.
- 광학 시스템의 지지대를 고정한다. 가능한 한 전자석에서 멀리 떨어지도록 설치한다.
- 덮개 (d)를 제거하고 velour-lined base위에 Lummer-Gehrcke plate를 조심스럽게 놓는다. 이 plate가 수평으로 잘 정렬되도록 설치하고 빛이 들어오는 쪽에 가능한 한 가깝게 프리즘을 밀어 넣는다.
- 덮개를 망원경 (e)를 향하는 원통부와 함께 돌리고, Lummer-Gehrcke plate가 불안정하지 않도록 망원경의 반대방향으로 조심스럽게 놓는다.
- 플러그 타입의 받침대 (c)에 적색필터를 설치한다.
- 외부 빛으로부터 간섭을 막기 위해, 덮개의 원통 위에 있는 빛 차단 screen을 끼워 넣고, 망원경 위에 고무링을 밀어 넣는다.

수평배치에서 수직배치로 바꾸기

- 기둥 받침대 위의 멈춤나사 (i)를 풀고, 광학 시스템을 전자석으로부터 가능한 한 멀리 움직인다.
- 플러그 타입의 받침대로부터 붉은색 필터를 제거한다.
- 카드뮴 램프와 함께 전자석을 원하는 위치로 돌린다(그림 6 참고). 그리고 전자석의 받침대가 광학 시스템 받침대의 뒤쪽 가장자리에 평행하도록 놓기 위해 그림 6과 같이 정렬한다.
- 플러그 타입의 받침대에 적색필터를 설치한다.
- 광학시스템의 받침대를 가능한 한 전자석에 가깝게 놓는다.

전기 연결

- 카드뮴 램프(cadmium lamp)를 universal choke에 연결한다. 스위치를 켜 뒤, 충분히 강한 빛 강도를 얻을 때 까지 5분 정도 기다린다.
- 전자석의 코일을 병렬로 연결한다(socket 1은 socket 3에, socket 2는 socket 4에 연결한다). 그리고 이것을 고전류 전원공급장치에 연결한다.

Zeeman 효과 관찰을 위한 광학시스템 조절

수직배치에서 광학 시스템의 높이를 조절하고, 수평배치로 바꿀 때는 광학시스템의 높이를 변경하지 않는다.

광학 시스템은 Lummer-Gehrcke plate의 위와 아래로 간섭무늬가 최대 밝기와 대비를 보일 때 최적화된 것이다.

-망원경 (f)의 접안렌즈를 제거하라; 밝기와 대조를 선택적으로 최적화하기 위해서임.

- a) 받침대 위에 있는 광학 시스템을 왼쪽과 오른쪽으로 이동시킨 뒤 돌린다.
- b) 전자석의 구멍과 카드뮴램프 사이의 완벽한 광학시스템의 높이를 맞춘다(멈춤나사 (h)를 고정시킨다).

-간섭무늬의 밝기와 대비를 향상시키기 위해 플러그 타입의 받침대 안에 있는 붉은색 필터 혹은 전체 덮개를 들어 올릴 필요가 있다. 밝은 내부의 간섭무늬들은 관찰하기에 가장 좋다.

미세조정

망원경이 Lummer-Gehrcke plate의 뒷부분에 정확하게 정렬되었을 때, 간섭무늬가 위아래로 대칭된다.

- 접안렌즈를 빛을 향해 고정시키고, 십자선에 초점을 맞춘다.
- 망원경의 경통 내에 접안렌즈를 대체하고 접안렌즈를 이동시켜 간섭무늬의 초점을 맞춘다.

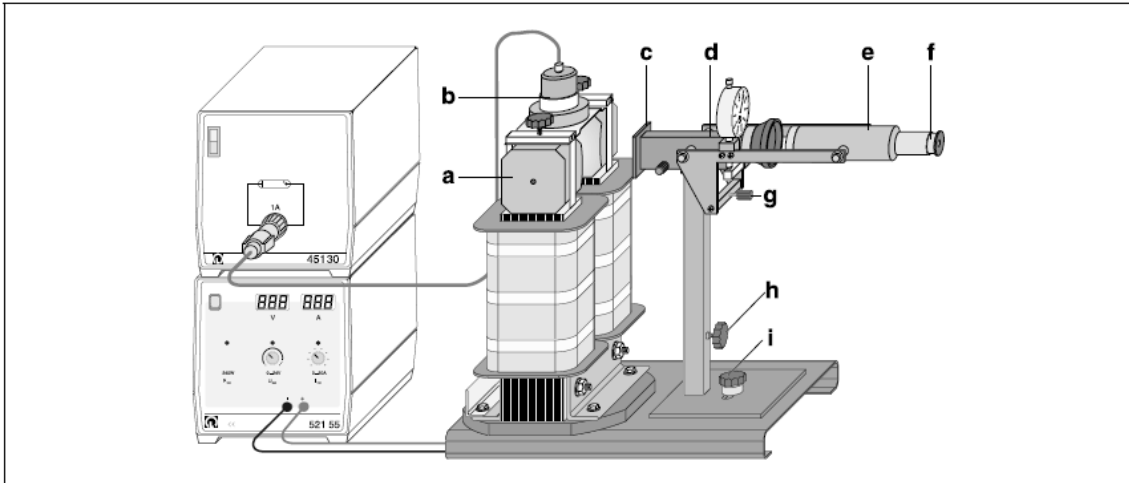


그림 5. Zeeman 효과 실험을 위한 실험설치의 측면그림.

(a) 전자석들, (b)받침대(holder)가 있는 카드뮴 램프(cadmium lamp), (c) 붉은색 filter를 위한 플러그 타입의 받침대, (d) 덮개, (e) 망원경, (f) 접안렌즈, (g) 망원경의 높이 조절나사, (h) 기둥의 멈춤나사, (i) 기둥받침의 멈춤나사

(5) 실험수행

참고: 편광 필터는 1/4 파장 알루미늄 박(quarter-wavelength foil)보다 다소 어둡다.

(a) 수평배치 관찰

- 먼저 자기장의 인가없이($I=10 A$) 간섭무늬를 관찰하고, 접안렌즈의 십자선이 간섭 무늬 위에 놓이도록 망원경을 조절한다.
- 자기전류 $I=10 A$ 가 될 때까지 천천히 증가시키면서, 간섭무늬가 분명히 갈라지는지 관찰한다.

σ^+ 와 σ^- 성분을 구별하기 위해:

- 1/4 파장 알루미늄박의 받침대 위에 외부 빛 차단 스크린을 설치한다.
- 1/4 파장 알루미늄박과 이것의 지지대를 설치하고, 망원경에 편광 필터를 설치한다.
- Doublet 성분 중 하나가 사라질 때까지 편광필터를 회전시킨다. 다른 한 성분까지 사라지도록 편광 필터를 90° 정도 회전시킨다.

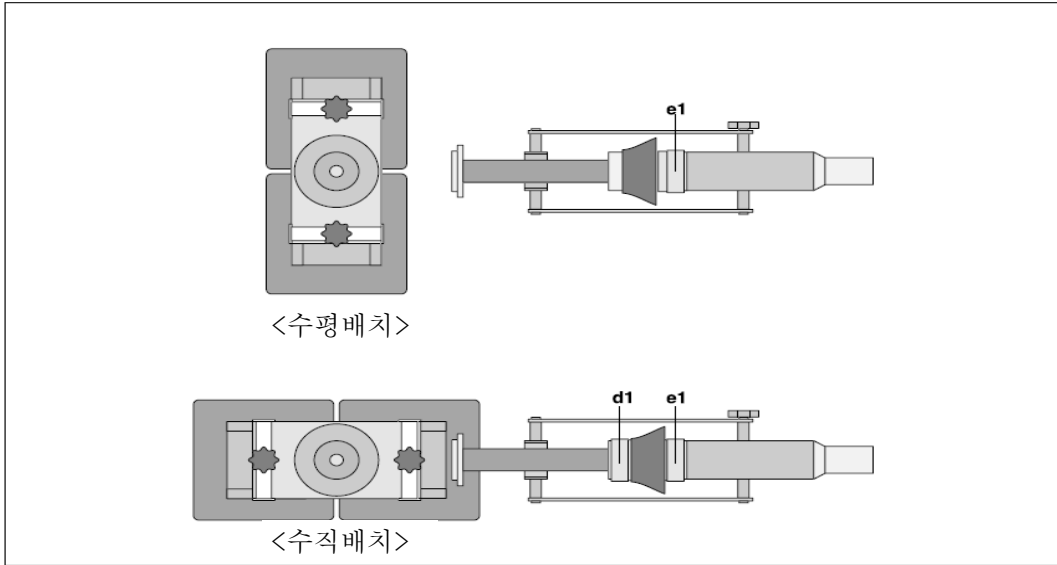


그림 6. 수평 배치의 평면도(위 그림)와 수직 배치의 평면도(아래 그림)
 (d1) 1/4 파장의 알루미늄 박이 있는 받침대
 (d2) 편광필터가 있는 받침대

(6) 측정 예와 수치 계산

a) 수평 배치 관찰

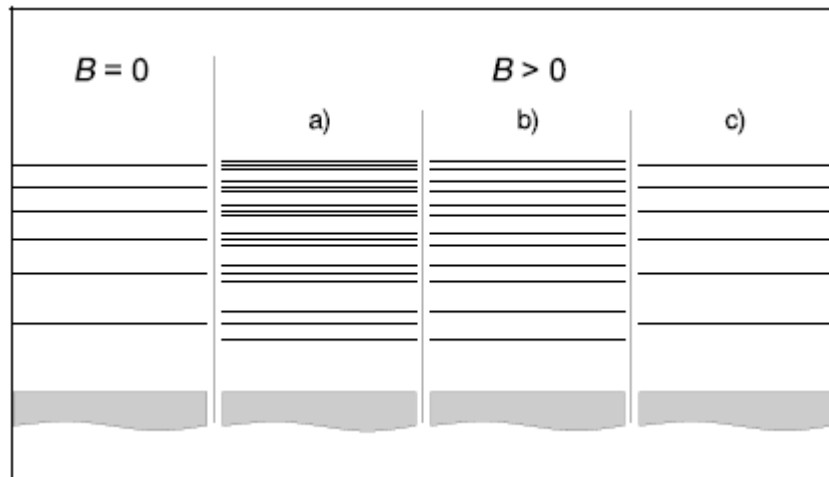


그림 7. 수평배치에서 Zeeman 효과의 간섭 무늬

- a) 편광필터 없이 관찰했을 때,
- b) 편광방향으로 관찰했을 때,
- c) 자기장에 평행한 필터의 편광방향에서 관찰했을 때

b) 수직 배치 관찰

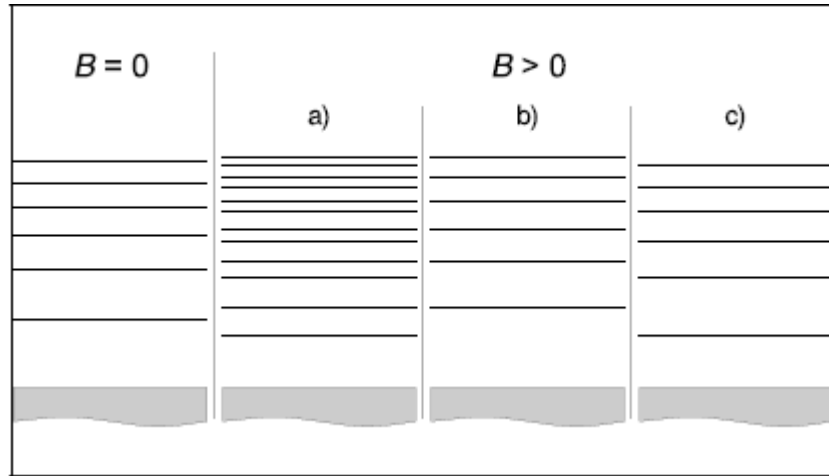


그림 8. 수직배치에서 Zeeman 효과의 간섭무늬

- a) 1/4 알루미늄 박과 편광필터없이 관찰했을 때,
- b)와 c) 시계방향과 반시계 방향 편광을 보이기 위한 편광 필터와 1/4 알루미늄 박을 사용하여 관찰했을 때

5. X-선 실험: Duane-Hunt의 법칙

(1) 실험목적

- X-선 튜브의 고전압 U 의 함수로서 연속 제동복사의 한계파장 λ_{\min} 측정
- Duane-Hunt 관계 확인
- Planck 상수 측정

(2) 기본원리

X-선 튜브의 방출 스펙트럼에서 연속 제동복사는 한계 파장 λ_{\min} 에 의해 결정되며(그림 1), 한계파장은 튜브의 고전압이 증가함에 따라 점점 작아진다. 1915년에 미국 물리학자 William Duane과 Franklin L. Hunt는 튜브의 고전압과 한계 파장 사이의 반비례관계를 발견했는데 그 관계는 아래와 같다:

$$\lambda_{\min} \sim \frac{1}{U} \quad (1)$$

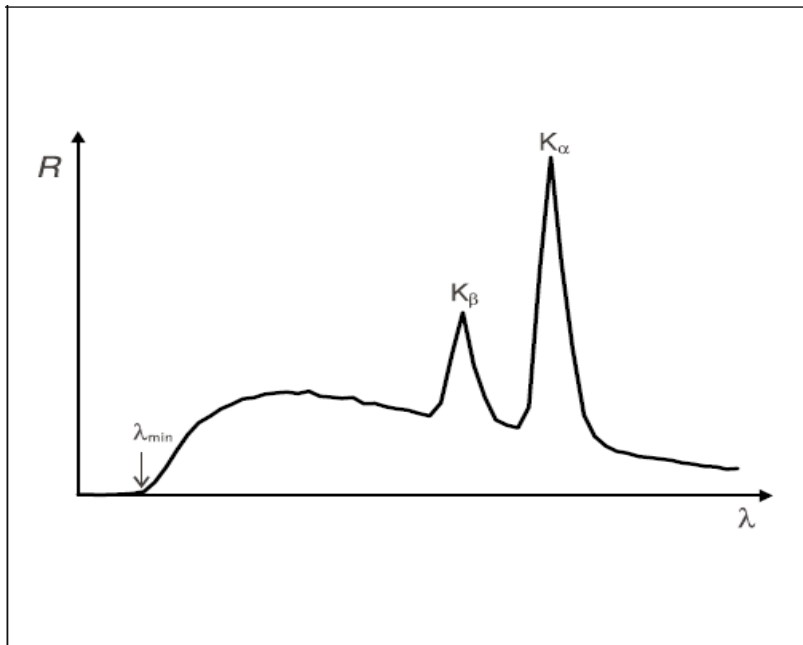


그림 1. 연속 제동복사의 한계파장 λ_{\min} 과 특성 K_{α} 와 K_{β} 선을 갖는 X-선 튜브의 방출 스펙트럼

이 Duane-Hunt 관계는 몇 가지 기본적인 양자역학적 고려로서 충분히 설명될 수 있다:
전자기 방사에 대한 파장 λ 와 주기 ν 가 아래와 같은 관계를 갖는다.

$$\lambda = \frac{c}{\nu} \quad (2)$$

($c : 2.9979 \cdot 10^8 \text{ m s}^{-1}$: 빛의 속도)

최소 파장 λ_{\min} 은 방출된 X-선 양자들의 최대 에너지는

$$E_{\max} = h \cdot \nu_{\max} \quad (3)$$

(h : Planck 상수)

로 최대 주기 ν_{\max} 에 해당한다. 그러나 X-선 양자는 양극에서 감속되는 전극의 총 운동에너지

$$E = -e \cdot U \quad (4)$$

($e = 1.6022 \cdot 10^{-19} \text{ As}$: 기본전하)

를 얻는 정확한 순간에 최대 에너지를 달성한다.

따라서, 이 때의 주기와 파장은 각각

$$\nu_{\max} = \frac{e}{h} \cdot U \quad (5)$$

$$\lambda_{\min} = \frac{h \cdot c}{e} \cdot \frac{1}{U} \quad (6)$$

과 같다.

식 (6)은 Duane-Hunt 법칙에 해당한다. 비례계수는

$$A = \frac{h \cdot c}{e} \quad (7)$$

c 와 e 의 값이 알려져 있어서 Planck 상수를 결정하는데 사용될 수 있다.

Bragg 실험배치에서 NaCl의 각조정기(Goniometer)와 Geiger-Muller 계수관은 이 실험에서 분광계를 구성한다. 결정이 입사 X-선에 대해서 θ 의 각도로 회전할 때, 계수관은 2θ 가 되도록 회전한다(그림 2를 참고).

Bragg 반사법칙에 따라서 1차 회절의 산란각 θ 는 파장

$$\lambda = 2 \cdot d \cdot \sin\theta \quad (8)$$

($d = 282.01 \text{ pm}$: NaCl의 격자 간격)

에 해당한다.

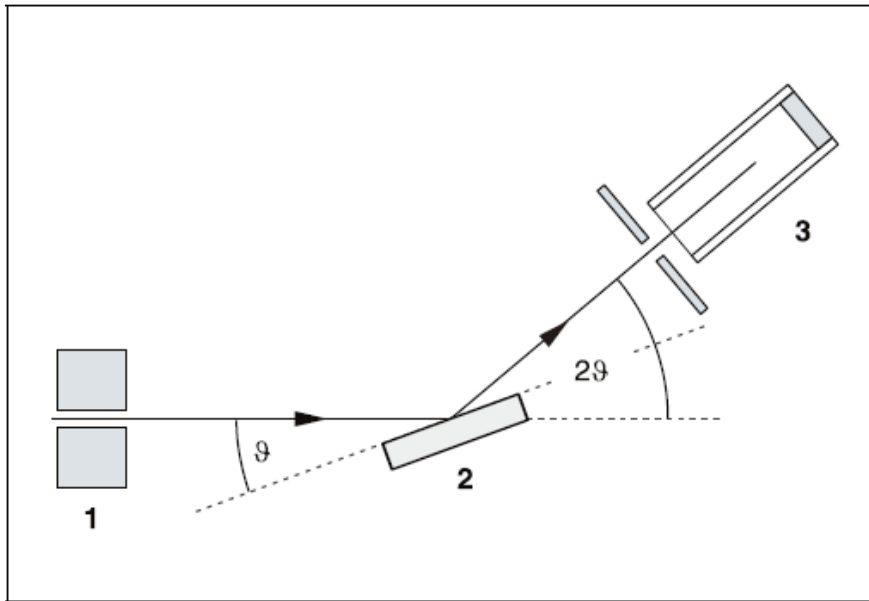


그림 2. 단결정에서 X-선 회절, 계수관 각도와 산란각(스침각) 사이의 2θ 결합의 개략도

1 집속기, 2 단결정, 3 계수관

(3) 실험기자재

①X-선 장치, ② α , β , γ 와 X-선 방사를 위한 End-window counter, ③PC

안전 주의사항

X-선 장치는 모든 관리규정을 만족해야 하고, 교육용으로 완전히 보호된 장비로 독일에서 교육용으로 보증되었다.

보호장치와 차폐가 내부에 설치되어 X-선 장치의 외부선량을 $1\mu Sv/h$ 이하인 자연방사선의 범위로 줄인다.

■ X-선 장치를 작동하기 전에 장치의 손상이 있는지, 미닫이 문이 열렸을 때 고전압의 전원이 내려가 있는지 반드시 확인한다.

■ X-선 장치는 권한이 없는 사람이 접촉하지 못하도록 한다.

X-선 튜브의 Mo 양극이 과열되지 않도록 한다.

■ X-선 장치의 스위치를 켰을 때, 튜브 챔버에 있는 환풍기가 돌아가는지 반드시 확인하라.

각조정기는 electric stepper motor에만 놓여 있다.

■ 각조정기의 표적부분과 센서 부분이 방해받지 않게 하고, 이것들을 강제로 움직여 사용해선 안된다.

(4) 설치

Bragg 실험 배치

그림 3은 실험 설치의 중요한 몇 가지 세부사항을 보여준다. 실험 설치를 위해 아래의 과정을 따른다.

-집속기 장착부 (a)에 집속기를 장착한다(안내 홈을 참조).

-집속기의 슬릿 칸막이와 표적부분 사이의 거리 s_1 이 대략 5 cm가 되도록 각조정기를 안내막대 (d)에 붙인다. 각조정기를 조절하기 위해 리본 케이블 (c)를 연결한다.

-End-window counter의 보호캡을 제거하고 센서 자리 (e)에 end-window counter를 놓고 계수관을 장착 표시된 GM TUBE에 연결한다.

-센서 고정대 (b)를 이동시킴으로서 표적부와 센서 수신기의 슬릿 칸막이 사이의 거리 s_2 가 대략 6 cm가 되도록 설정한다.

-표적부를 표적 고정대 (f)에 장착한다.

-표면에 홈이 있는 나사 (g)를 풀고, NaCl 결정을 표적부에 편평하게 놓고, 중지시키는 방법으로 단결정이 있는 표적부를 조심스럽게 들어 올리고, 홈이 있는 나사를 천천히 돌려 조인다(약간의 압력을 주어 결정이 비스듬히 움직이는 것을 막는다).

-필요하다면, 각조정기의 기계적인 영점 위치를 조절한다.

참고:

NaCl 결정은 축축해지기 쉽고 극히 깨지기 쉽다. 건조한 곳에 NaCl 결정을 보관한다; 결정이 기계적인 변형력을 받지 않게 한다; 작은 표면으로만 결정을 다룬다.

만약 수율이 너무 낮다면, 표적과 센서 사이의 거리 s_2 를 줄인다. 그러나 이 거리가 너무 짧아선 안되며, 거리가 너무 짧으면 각조정기는 더 이상 충분한 각(angular) 해상도를 갖지 못한다.

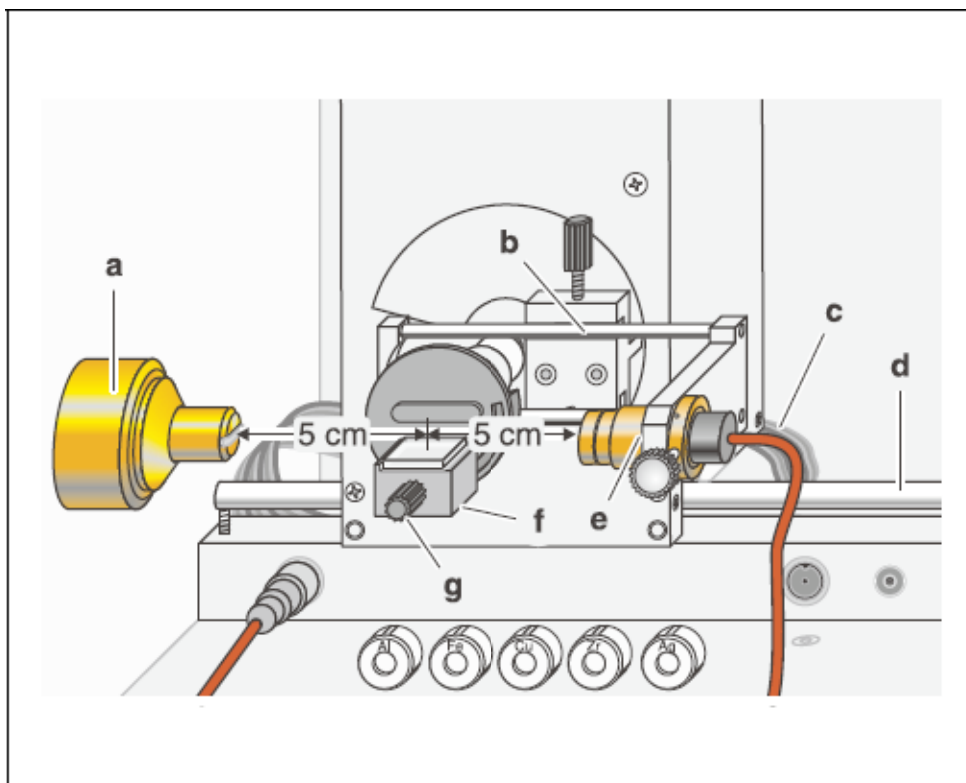



그림 3. Bragg 실험배치도

PC기반 측정 준비(MS-DOS 기반)

-본 실험장치는 GM 계수관으로부터 신호를 PC로 측정하도록 구성되어 있다.

-9핀 V.24 케이블을 사용하여(X-선 장치에 공급된) RS-232 출력과 컴퓨터(대개 COM1 혹은 COM2)의 직렬 인터페이스를 연결한다.

-PC를 켜 다음, 비번 “staff” 를 입력하여 Windows 95 운영체제를 실행한다. 바탕화

면에 있는 아이콘  을 더블클릭하여 DOS기반 X-선 실험 프로그램을 활성화

한다.






	
<p>① X-선 실험 더블클릭 하면, 위와 같은 첫 화면이 나타난다. 아무 키를 누르면 ②의 화면으로 넘어간다.</p>	<p>② 이 화면에서 Duane-Hunt 실험에서 사용되는 측정은 F3 Rate meter 이다.</p>
	
<p>③ 측정 전 실험조건(측정시간)을 설정한다. F3 Select meas. > Rate meas. > Free gate에서 측정시간을 설정한다.</p>	<p>④ 설정이 완료 되었으면, Enter를 누르고, 위의 그림과 같이 F1 Start new measurement를 누른다.</p>
	<p>참고:</p> <ul style="list-style-type: none"> *측정 이후 계수 N과 계수율 R은 저장되지 않으니, 반드시 측정결과를 기록해두어야 한다. *재측정을 원할 경우, F1을 한 번더 누르면 되며, 화면의 좌측 하단에 측정횟수가 표시된다.
<p>⑤ 준비완료된 상태에서 다시 F1을 누르면, 위의 그림과 같이 측정시간동안 N(계수)와 R(계수율;계수/측정시간)이 표시된다.</p>	

표 1. X-선 Duane-Hunt 실험을 위한 CASSY 프로그램 설정과정

(5) 실험방법

-스위치 (a)로 X-선 측정장치의 전원을 켜다.

(매뉴얼 영문원본 X-ray apparatus 42V p. 22쪽 필독.)

; 시간 (b)에서 작동시간을 "> 1h"로 선택한다 ; 검출기 (f)에 대한 다단계 설정 스위치 (e)의 setting 1에서 고전압 U_A ($U_A = \sqrt{2} \cdot 10^3 \cdot U$)를 켜다. 다단계 설정 스위치 (e)를 가지고 setting 8까지 올려 고전압을 설정해 본 뒤, lever를 사용하여 1mA까지 방출 전류 I_{EM} 를 설정하라.

-전압 U를 조절부(b)를 가지고 확인한다 ; 이것은 데모미터(demonstration meter)에서 고전압에 비례한다. 회전하는 결정의 배치를 "crystal angle" $\theta = 2.5^\circ$ (포인트 (h))와 "counter tube angle" $2\theta = 5^\circ$ 로 설정한다.

-100 초 이내에서 계수 n을 측정한다.(주어진 실험시간 내에서 실험수행이 가능하도록 시간을 정할 것.)

-각도 θ 는 0.5° 에서 6.5° 까지 증가시키고, 모든 측정은 100 초 내에서 계수 n을 측정한다.

-측정이 완료되면 voltage 값을 7로 바꾼다.

-측정 데이터 값을 그래프로 그려보고 θ_{\min} 을 구한다.

-시료의 격자상수와 θ_{\min} 을 이용하여 $\lambda_{\min} = 2d \sin\theta_{\min}$ 식에 대입하여 λ_{\min} 을 구한다.

- $h = \frac{e}{c} U_A \cdot \lambda_{\min}$ 에 위에서 구한 값을 대입하여 플랑크 상수 h를 구한다.

(6) 측정 예와 수치 계산

*영문매뉴얼의 측정 결과 참조(X-ray 6.3.2-7의 p.4-5)

튜브 고전압 U의 함수로서 한계파장 λ_{\min} 측정

Duane-Hunt 관계의 확인과 Plack 상수의 측정

측정예

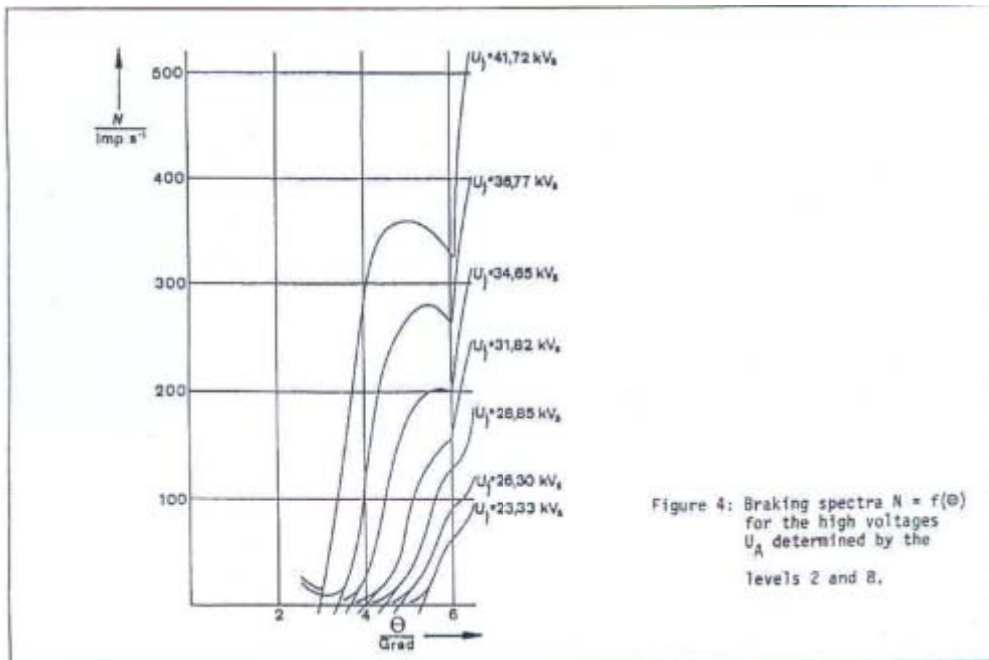


Figure 4: Braking spectra $N = f(\theta)$ for the high voltages U_A determined by the levels 2 and 8.

그림 4. 측정 결과의 그래프 예시

U_A level	.	8	7	6	5	4	3	2
U_A	kV_s	41,72	36,77	34,65	31,8	28,85	26,30	23,33
θ_{min}	Grad	2,95	3,35	3,60	3,92	4,42	4,77	5,30
λ_{min} from (7)	pm	29,0	32,9	35,4	38,6	43,5	46,9	52,7
$\frac{1}{U_A}$	kV_s^{-1}	0,0240	0,0272	0,0289	0,0314	0,0347	0,0380	0,0429
h from (6)	$10^{-34} J_s$	6,465	6,464	6,555	6,563	6,700	6,591	6,570

표 2. 측정 결과의 계산 예시

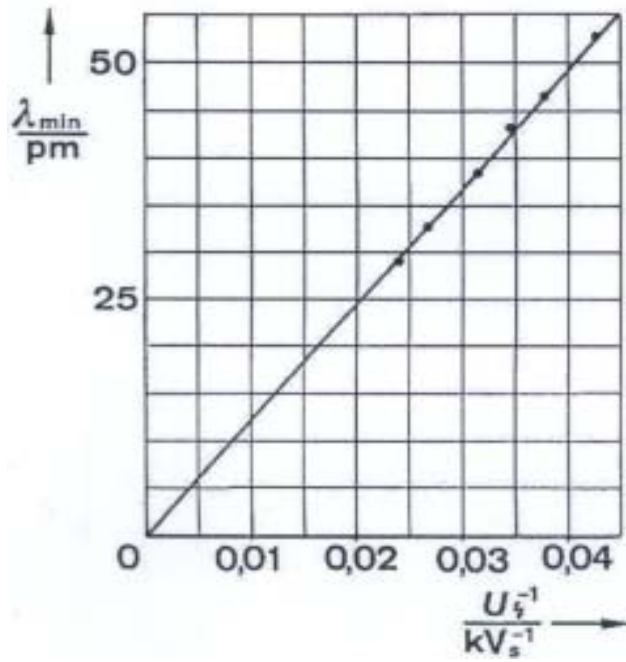


그림 5. $\lambda_{\min} = f(1/U)$

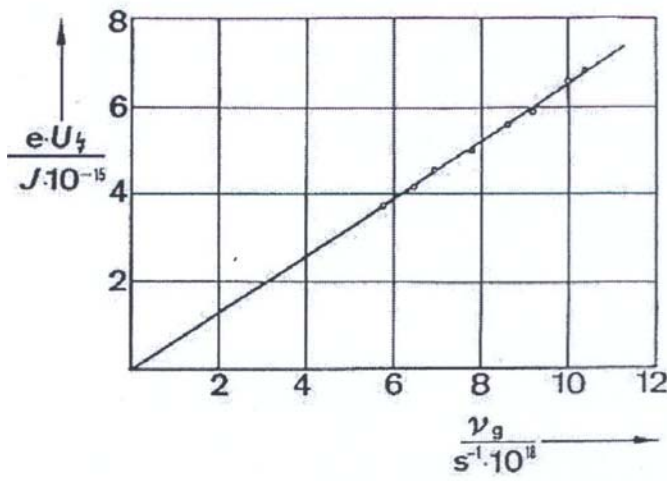


그림 6. $e \cdot U_A = f(\nu_g)$

6. Hall 계수 측정실험

(1) 실험목적

- Hall 계수와 자기선속밀도(Magnetic flux density)의 비례관계 확인하기
- 전하운반자(charge carriers)의 극성 결정하기
- Hall 계수와 전하운반자 농도 n 계산하기

(2) 기본원리

만약 전류가 흐르는 금속성 전도체(Metallic conductor) 스트립(strip)이 전류 I 에 수직인 자기장 B 에 놓여 있다면, 가로축 방향인 전기장 E_H 와 전위차(potential difference)가 발생하는데 이것을 Hall 효과라 한다.

아래의 식은 Hall 전압 U_H 에 관한 것이다.(그림 1을 참조)

$$U_H = \frac{1}{n \cdot e} \frac{B \cdot I}{d} \quad (1)$$

(B : 자기선속밀도, I : 금속 전도체를 통과하는 전류, d : 띠 모양 전도체의 두께,
 n : 전하운반자의 농도, $e = 1.602 \times 10^{-19} C$ 으로 기본전하)

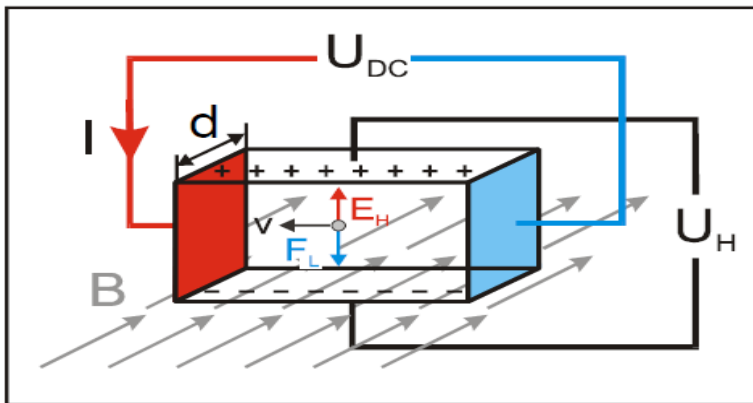


그림 1. Hall 효과의 그림. 자기장 B 에 놓인 전하를 운반하는 금속성 전도체 내부의 로렌츠 힘 F_L 은 전기장 E_H 의 원인이 되며, 그 결과 Hall 전압 U_H 가 발생.

Hall 전압 U_H 는 로렌츠 힘으로 인하여 자기장내에서 움직이고 있는 전하 운반자의

편향에 의해 야기되며, Hall 전압의 방향은 오른손 법칙에 의해 예측될 수 있다. $\frac{1}{ne}$ 인자는 Hall 계수 R_H 라고 한다.

$$R_H = \frac{1}{ne} \quad (2)$$

Hall 계수 R_H 의 부호는 전하 운반자의 극성에 의해 결정된다.

Hall 계수는 재료와 온도에 의존된다. 왜냐하면 금속의 R_H 는 매우 작지만, 반도체의 R_H 는 매우 커지기 때문이다.

전하 운반자의 극성은 Hall 전압의 방향으로부터 결정될 수 있다. 전하 운반자 n 의 농도는 다양한 전류 I 에 따른 자기장 B 의 함수인 Hall 전압 U_H 를 측정함으로써 실험적으로 결정될 수 있다.

(3) 실험기자재

Hall 효과 장치(은-Ag), 굴레가 있는 U자 형태의 코어, 한 쌍의 전자석, 250회 감긴 코일, 고전류 전원 공급장치, 가변 저전압 변압기, 멀티미터, 1m인 붉은색 및 파란색 (19Ω) 전선 4쌍, 1m인 검정색(32Ω)의 연결 전선 2쌍

안전 주의사항

- 가로 전류(transverse current)가 15 A 혹은 자기장에 의한 유도전류가 5 A 이상이 되면, 장치의 전원을 켜라(연결 전선이 과열되거나 코일이 과부하되는 것은 최대 부하가 5 A로 설계되었기 때문이다).
- 가로 전류(transverse current) 회로에서 최대부하 20 A로 정해진 전선을 사용하라(예를 들면, 검정색 연결전선은 32 A이며, 노란색 및 녹색 연결 전선은 최대 32 A이다).
- Hall 전압을 측정하는 동안에 임시보관대에서 실험 설정을 유지하라.

(4) 설치

*실험은 두 단계로 수행된다.

a) 자기장의 보정

굴레가 있는 U자 형태의 코어, 한 쌍의 전자석과 250회 감긴 코일을 그림 8.2와 같이 설치하라. 전자석들은 Hall 효과 장치(은-Ag)의 보조판 두께에 맞게 정확하게 놓는다. 설정을 위해 고정 장치를 느슨하게 하고, 전자석 사이에 있는 Hall 효과 장치(은-Ag)를 다른 한 곳에 두어라. 250회 감긴 코일을 저전압 변압기에 직렬로 연결하고 전자석 사이에 자기장 센서를 놓는다.

b) 자기장의 함수인 Hall 전압의 측정

보정 곡선을 기록한 뒤에 전자석 사이에 Hall 효과 장치(은-Ag)를 끼워라. 전자석의 극 간격은 하단의 지지대에 가능한 한 가깝게 한다.

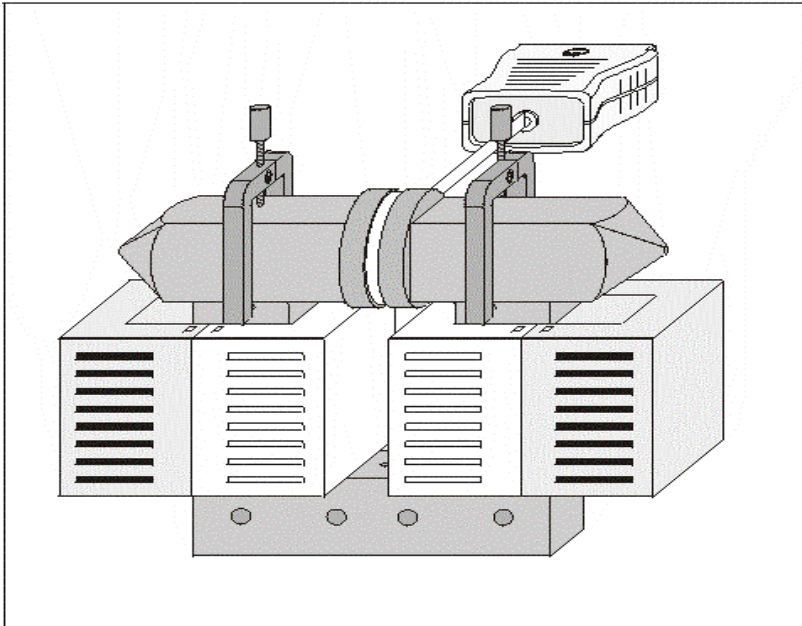


그림 2. 자기장 보정을 위한 개략도

Hall 전압을 측정하기 위해, Hall 효과 장치(은-Ag)의 보조판에 마이크로전압계를 연결한다.

그림 3과 같이 고전류 전원 공급장치에 Hall 효과 장치(은-Ag)를 연결한다. 자기장 B의 방향은 보조판에 인쇄된 것처럼 되어야 한다. 멀티미터를 사용하여 코일을 통과하는 전류 I를 측정한다.

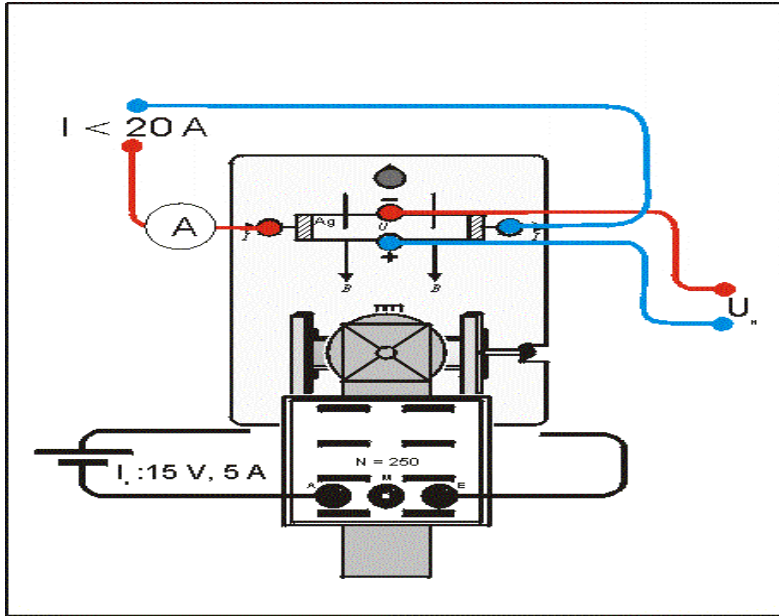


그림 3. Hall 효과 실험 설정(배선 도해)

(5) 실험수행

a) 자기장의 보정

-250회 감긴 코일을 통해 교류전류 $I=5A$ 에 의한 전류 I 의 함수로서 자기장을 기록하기 전에 전자석의 철에 의한 자기장을 짧은 시간 동안에 제거한다. 그런 뒤, 전류가 0이 될 때까지 점차적으로 줄인다.

-코일을 통해 흐르는 전류를 측정하기 위해 변압기의 (+) 극과 코일 사이에 전류계를 연결한다.

-직류전류를 0.5 A씩 증가시키면서 전류 I 의 함수로서 자기선속밀도 B 를 측정한다.

b) 자기장의 함수인 Hall 전압의 측정

-전자석 사이에 Hall 효과 장치(은-Ag)를 끼운다.(그림 3을 참조)

-Hall 효과 장치(은-Ag)를 자기장에 노출하기 전에, 영점을 조절한다.

: 예를 들어 10 A의 가로 전류 I 를 인가하고, Hall 효과 장치(은-Ag)의 조절 손잡이를 사용하여 Hall 전압 U_H 가 0에 이르도록 측정하는 동안 눈금 표시기를 놓는다. 전원을 끈 뒤에도 표시창의 눈금이 변한다면, 가로 전류를 다시 켜 뒤 영점 조절을 반복한다.

-Hall 효과 장치(은-Ag)에 가로 전류 $I=15A$ 를 인가하고 자기장 B 의 함수인 Hall 전압

U_H 를 측정한다(첫 번째 실험의 보정 곡선으로부터 효과적인 자기장의 눈금수치를 읽는다). Hall 전압 U_H 에 대한 평균값을 측정하기 위해 수 회의 측정을 수행한다.
-가로 전압 $I=2.0A$ 에 대한 측정을 반복한다.

(6) 측정 예

a) 자기장의 보정

$\frac{I}{A}$	$\frac{B}{T}$
0.0	0.000
0.5	0.118
1.0	0.200
1.5	0.295
2.0	0.374
2.5	0.455
3.0	0.520
3.5	0.585
4.0	0.630
4.5	0.665
5.0	0.695
5.5	0.715
6.0	0.735
6.5	0.748
7.0	0.760
7.5	0.780
8.0	0.790
8.5	0.800
9.0	0.810

표 1. 코일을 통과하는 전류 I 의 함수인 자기장 B

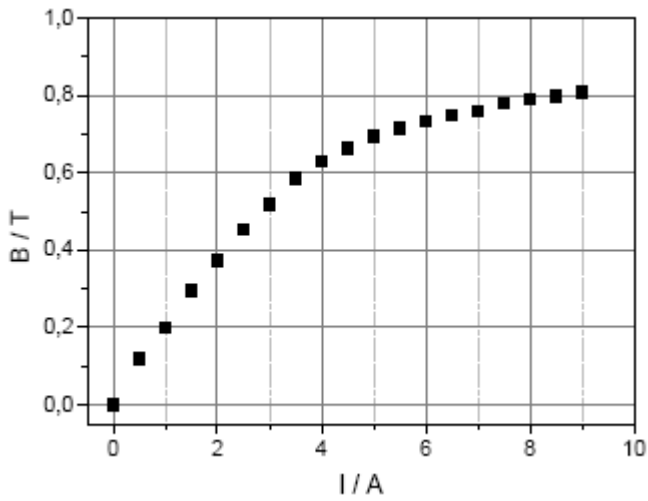


그림 4. 전류 I의 함수인 자기장 곡선의 보정

b) 자기장의 함수인 Hall 전압의 측정

$\frac{B}{T}$	$\frac{U_H}{\mu V} (I = 15 A)$	$\frac{B}{T}$	$\frac{U_H}{\mu V} (I = 20 A)$
0.20	4.6	0.20	6.25
0.35	8.2	0.38	11.7
0.51	12.0	0.50	15.0
0.62	14.1	0.61	18.1
0.70	16.1	0.68	20.5
0.73	17.0	0.70	21.0
0.76	17.7	0.72	21.6
0.78	18.1	0.76	22.7
0.80	18.6	0.80	24.0

표 2. 일정한 가로 전류 I에 대한 자기장의 함수인 Hall 전압 U_H

(7) 측정결과(예시)

b) 자기장의 함수인 Hall 전압의 측정

가로 전류(transverse current) $I=15A$ 와 $I=20A$ 에 대한 표 2의 기록된 데이터는 그림 5의 그래프와 같다.

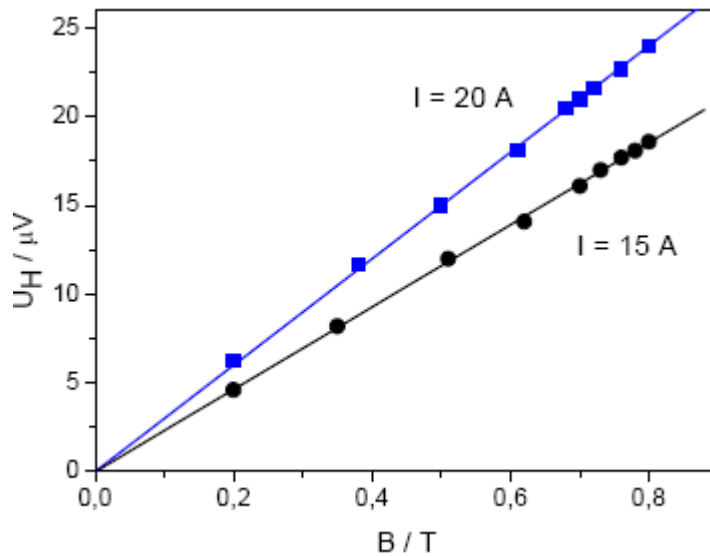


그림 5. 전류 I=15A(원형)과 전류 I=20A(사각형)에 대한 자기장 B의 함수인 Hall 전압 U_H . 사각형 연결선은 식(1)에 대응된다.

(8) 수치 계산

-그림 8.5로부터 Hall 전압 U_H 는 자기장 B에 비례하므로

$$U_H \sim B \quad (3)$$

위와 같은 식이 나온다.

-또한, 그림 5로부터 가로 전류 I가 증가할수록 Hall 전압 U_H 도 증가하므로

$$U_H \sim I \quad (4)$$

위와 같은 식이 나온다.

*참고: Hall 전압 U_H 와 가로 전류(transverse current) I 사이의 비례상수는 일정한 자기장 B에 대한 가로 전류 I의 함수인 Hall 전압 U_H 를 측정함으로써 실험적으로 결정될 수 있다.

-실험결과를 식(1)에 대입한 기울기의 결과는 아래와 같다.

$$A_H = \frac{1}{n \cdot e} \frac{I}{d}$$

$$A_H(I=15A) = 23.2 \frac{\mu V}{T}, \quad A_H(I=20A) = 30.4 \frac{\mu V}{T}$$

-두께 $d = 5 \cdot 10^{-5} m$ 인 Hall 계수는 아래와 같이 계산(절대값)될 수 있다.

$$R_H(I=15A) = 7.7 \cdot 10^{-11} \frac{m^3}{C}, \quad R_H(I=20A) = 7.6 \cdot 10^{-11} \frac{m^3}{C}$$

$$\text{문헌 수치: } R_H = 8.9 \cdot 10^{-11} \frac{m^3}{C}$$

-Hall 전압은 음의 부호로 결정된다. 이것은 은(Ag)내에서의 전도(conduction) 메커니즘이 주로 음의 전하 운반자(charge carrier)에 의한 것임을 보여준다.

-기본전하 $e = 1.602 \cdot 10^{-19} C$ 은 전하 운반자의 밀도를 따르는데 아래와 같다:

$$n(I=15A) = 8.1 \cdot 10^{28} \frac{1}{m^3}, \quad n(I=20A) = 8.2 \cdot 10^{28} \frac{1}{m^3}$$

$$\text{문헌 수치: } 6.6 \cdot 10^{28} \frac{1}{m^3} \quad (\text{원자들의 밀도: } 5.8 \cdot 10^{22} \frac{1}{m^3})$$

(9) 추가 정보

1916년에 Tolman은 전자가 금속내의 전하 운반자라는 확실한 증거를 얻었다.

참고자료

-매뉴얼 영문원본-

Determination of the Specific Charge of the Electron

Objects of the experiment

- Study of the deflection of electrons in a magnetic field into a circular orbit.
- Determination of the magnetic field B as a function of the acceleration potential U of the electrons at a constant radius r .
- Determination of the specific charge of the electron.

Principles

The mass m_e of the electron is hard to come by experimentally. It is easier to determine the specific charge of the electron

$$\varepsilon = \frac{e}{m_e} \quad (I),$$

from which the mass m_e can be calculated if the elementary charge e is known:

An electron moving at velocity v perpendicularly to a homogenous magnetic field B , is subject to the Lorentz force

$$F = e \cdot v \cdot B \quad (II)$$

which is perpendicular to the velocity and to the magnetic field. As a centripetal force

$$F = m_e \cdot \frac{v^2}{r} \quad (III)$$

it forces the electron into an orbit of radius r (see Fig. 1), thus

$$\frac{e}{m_e} = \frac{v}{r \cdot B} \quad (IV)$$

In the experiment, the electrons are accelerated in a fine beam tube by the potential U . The resulting kinetic energy is

$$e \cdot U = \frac{m_e}{2} \cdot v^2 \quad (V)$$

The specific charge of the electron thus is

$$\frac{e}{m_e} = \frac{2 \cdot U}{(r \cdot B)^2} \quad (VI).$$

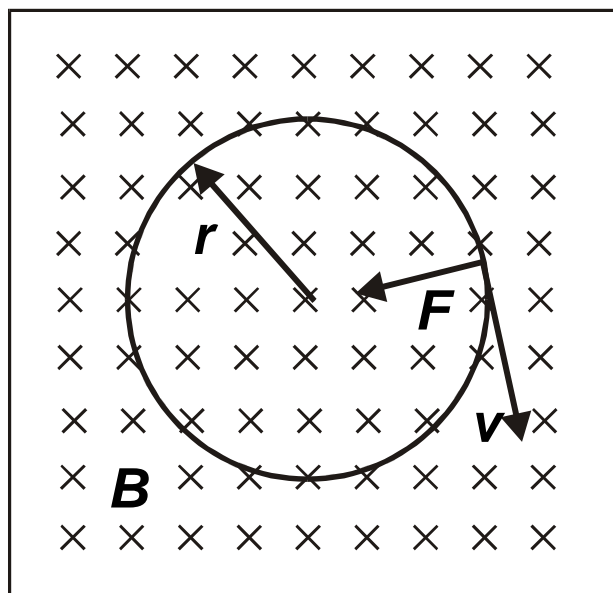


Fig. 1: Deflection of electrons in a magnetic field B by the Lorentz force F into a circular orbit of a given radius r .

Apparatus

1 Fine beam tube.....	555 571
1 Helmholtz coils with holder and measuring device	555 581
1 Tube power supply 0 to 500 V	521 65
1 DC Power Supply 0...16 V, 0...5 A	521 545
2 Multimeter LD analog 20.....	531 120
1 Steel tape measure, l = 2 m/78"	311 77
3 Safety connecting leads, 25 cm.....	500 614
3 Safety connecting leads, 50 cm.....	500 624
7 Safety connecting leads, 100 cm.....	500 644

Additionally recommended:

1 Universal Measuring Instrument Physics.....	531 835
1 Axial B-Sensor S.....	524 0382
1 Extension cable, 15-pole	501 11

The fine beam tube contains hydrogen molecules at low pressure, which through collisions with electrons are caused to emit light. This makes the orbit of the electrons indirectly visible, and their orbiting radius r can be directly measured with a ruler.

The magnetic field B is generated in a pair of Helmholtz coils and is proportional to the current I in the Helmholtz coils:

$$B = k \cdot I \quad (\text{VII})$$

The dependence on the accelerating potential U of the current I , in the magnetic field of which the orbiting radius of the electrons is kept to a constant value r , follows after recasting equations (VI) and (VII)

$$U = \frac{e}{m_e} \cdot \frac{1}{2} \cdot r^2 \cdot k^2 \cdot I^2 \quad (\text{VIII})$$

The proportionality factor

$$k = \mu_0 \cdot \left(\frac{4}{5}\right)^{\frac{3}{2}} \cdot \frac{n}{R} \quad (\text{IX})$$

$$\mu_0 = 4\pi \cdot 10^{-7} \frac{\text{Vs}}{\text{Am}} : \text{magnetic field constant}$$

can be calculated either from the coil radius $R = 150 \text{ mm}$ and the winding factor $n = 130$ per coil, or be determined by recording a calibration curve $B = f(I)$. All determining factors for the specific electron charge are now known.

Safety notes

The Attention: The fine beam tube requires dangerous contact voltages up to 300 V for accelerating the electrons. Other voltages that are connected with this dangerous contact voltage also present a contact hazard. Dangerous contact voltages are thus present at the connection panel of the holder and at the Helmholtz coils when the fine beam tube is in operation.

- Connect the connection panel only via safety connecting leads.
- Always be sure to switch off all power supplies before connecting and altering the experiment setup.
- Do not switch on the power supplies until you have finished assembling the circuit.
- Do not touch the experiment setup, particularly the Helmholtz coils, during operation.

Danger of implosions: The fine beam tube is a evacuated glass vessel with thin walls.

- Do not subject the fine beam tube to mechanical stresses.
- Operate the fine beam tube only in the holder (555 581).
- Connect the 6-pole plug of the holder carefully to the glass base.
- Read the instruction sheet supplied with the fine beam tube.

Setup

Note:

Perform measurements in a dark chamber.

Helmholtz coils may be charged with more than 2 A for short time only.

The experimental setup to determine the specific electron charge is shown in Fig. 2, the electric connections in Fig. 3.

- Disconnect the tube power supply and turn all rotary potentiometers to left catch position.
- Connect the 6.3-V input end of the fine beam tube to the 6.3-V outlet of the tube power supply.
- Short-circuit the positive pole of the 50-V outlet of the tube power supply with the negative pole of the 500-V outlet and connect with the socket “-” of the fine beam tube (cathode).
- Connect the socket “+” of the fine beam tube (anode) with the positive pole of the 500-V outlet, the socket W (Wehnelt-cylinder) with the negative pole of the 50-V outlet.
- In order to measure the acceleration potential U connect the voltmeter (measuring range 300 V₋) to the 500-V outlet.
- Short the deflection plates of the fine beam tube to the anode.
- Connect the DC power supply and ammeter (measuring range 3 A₋) in series with the Helmholtz coils.

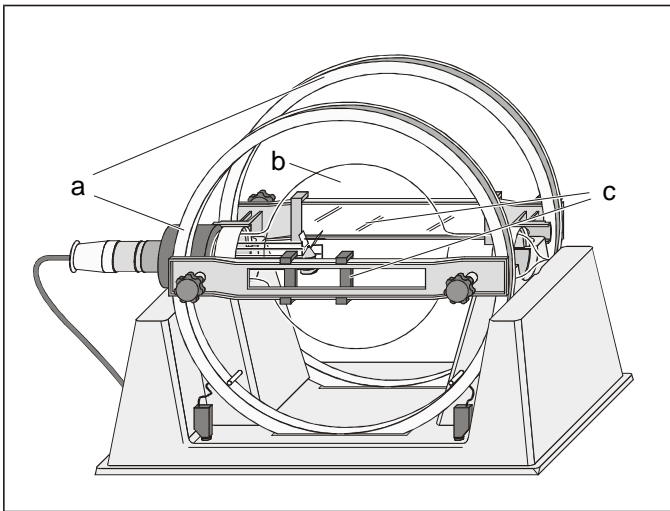
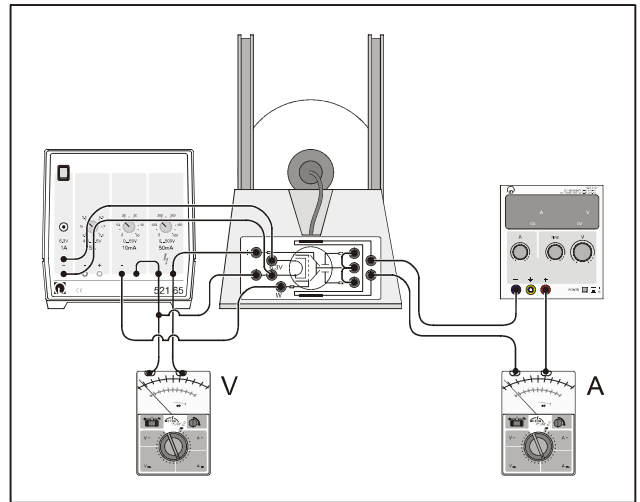


Fig. 2 Experiment setup for determining the specific electron charge

- a** Helmholtz coils
- b** Fine beam tubes
- c** Measuring device

Fig. 3 Electric connection



Carrying out the experiment

- Move the left slide of the measuring device so that its inner edge, mirror image and escape aperture of the electron beam come to lay on one line of sight.
- Set the right slide for both inside edges to have a distance of 8 cm.
- Sight the inside edge of the right slide, align it with its mirror image and adjust the coil current I until the electron beam runs tangentially along the slide edge covering the mirror image (see Fig. 4).
- Reduce the acceleration potential U in steps of 10 V to 200 V and choose the coil current I so that the orbit of the electron beam has a diameter of 8 cm.
- Record acceleration potential U and coil current I .

- Power up the tube power supply and set acceleration potential $U = 300$ V.

Thermionic emission starts after warming up for a few minutes.

- Optimize focussing of the electron beam by varying the voltage at the Wehnelt-cylinder from 0...10 V until it leads to a narrow, well defined beam with clear edge definition.
- Connect the DC power supply of the Helmholtz coils and look for current I , at which the electron beam is deflected into a closed orbit.

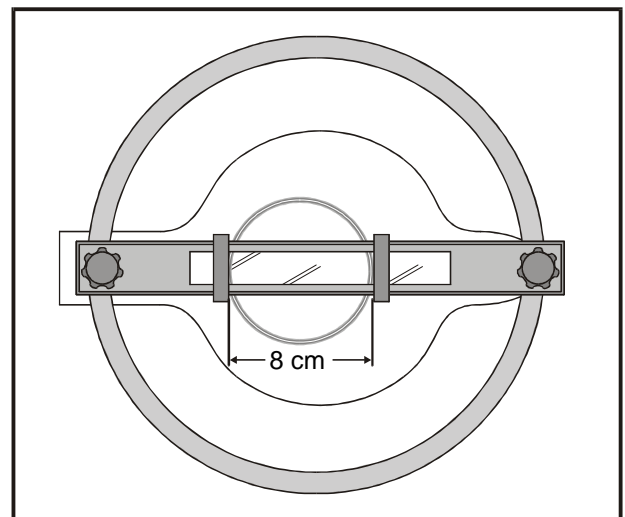
If the electron beam after leaving the anode is deflected to the wrong (left) side:

- disconnect both power supplies.
- exchange the connections at the DC power supply in order to change the polarization of the magnetic field.

If the electrons do not move on a closed orbit but on a helical curve line:

- Loosen the mounting bolts of both holding brackets (read the information manual for the fine beam tube).
- Carefully rotate the fine beam tube around its longitudinal axis, until the electron beam runs on a closed circular orbit.
- Fasten mounting bolts.

Fig. 4 Measurement of the orbit diameter with the measuring device



Calibration of the Helmholtz magnetic field (optional):

The setup for calibrating the magnetic field is shown in Fig. 5. The additionally recommended devices mentioned above are required for making measurements.

- If applicable disconnect all power supply units.
- Remove the measuring device and the Helmholtz coil at the front side, loosen the connection to the fine beam tube and the mounting bolts of the two holding brackets (read the instructions for the fine beam tube).
- Carefully remove the fine beam tube and place it e.g. in its original case.
- Re-assemble the Helmholtz at the front side coil and connect.
- Connect the axial B-probe to the Teslameter (measuring range 20 mT) and calibrate the zero-point (see Instruction Manual for Teslameter).
- Move the axial B-probe parallel to the magnetic field of the Helmholtz coils into the center of the pair of coils.
- Raise the coil current I from 0 to 3 A in steps of 0.5 A, measure the magnetic field B , and record the measured values.

After conclusion of the calibration:

- Reassemble the fine beam tube according to the instructions.

Measuring example

Table 1: The Coil current I as a function of the acceleration potential U at constant orbit radius $r = 0,04$ m.

$\frac{U}{V}$	$\frac{I}{A}$
300	2.15
290	2.10
280	2.07
270	2.03
260	2.00
250	1.97
240	1.91
230	1.88
220	1.83
210	1.79
200	1.75

Table 2: The Magnetic field B of the Helmholtz coils as a function of the coil current I (this measurement requires the above mentioned additionally recommended devices)

$\frac{I}{A}$	$\frac{B}{mT}$
0.5	0.35
1.0	0.65
1.5	0.98
2.0	1.34
2.5	1.62
3.0	2.05

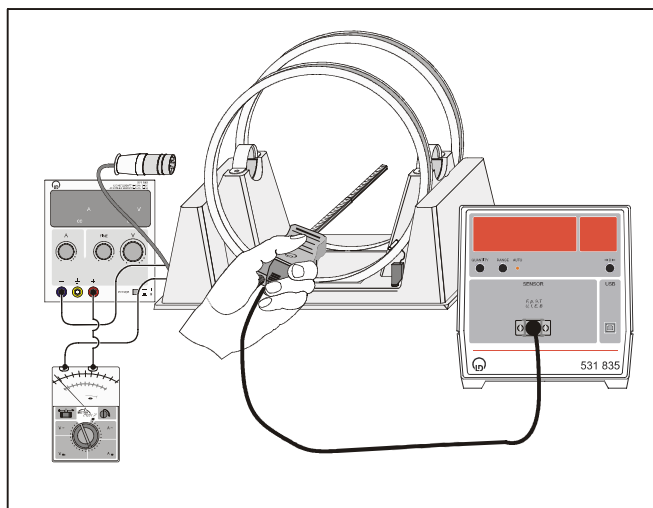


Fig. 5 Set-up for calibration of the Helmholtz magnetic field

Evaluation and results

In Fig. 6 the measured values from Tab. 1 are shown in their linear form $U = f(I^2)$ – according to (VIII). The slope of the resulting line through the origin is

$$\alpha = 65,3 \text{ V A}^{-2}.$$

According to equation (VIII), the specific electron charge is

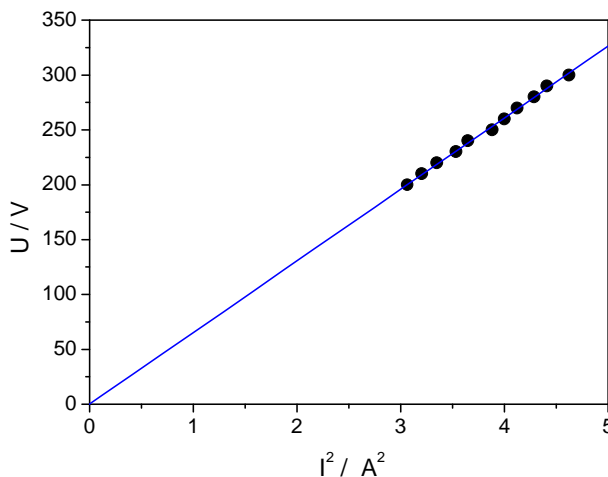
$$\frac{e}{m_e} = \frac{2 \cdot \alpha}{r^2 \cdot k^2}$$

Further evaluation thus requires the proportionality factor k .

If the light bundles impinge perpendicularly ($\alpha = \beta$) they are reflected back onto themselves.

If the light bundles impinge obliquely they are reflected into other directions, but remain parallel.

Fig. 6 Presentation of the measuring results from Table 1



Determination of the proportionality factor k from the calibration of the Helmholtz magnetic field:

Fitting of a straight line through the origin to the measuring values of Tab. 2, or of Fig. 7 leads to

$$k = 0,67 \text{ mT A}^{-1}$$

and further

$$\frac{e}{m_e} = 1,8 \cdot 10^{11} \frac{\text{As}}{\text{kg}}$$

Calculation of the proportionality factor k:

Using (IX) one calculates

$$k = 0,78 \text{ mT A}^{-1}$$

and further

$$\frac{e}{m_e} = 1,3 \cdot 10^{11} \frac{\text{As}}{\text{kg}}$$

Documented value:

$$\frac{e}{m_e} = 1,76 \cdot 10^{11} \frac{\text{As}}{\text{kg}}$$

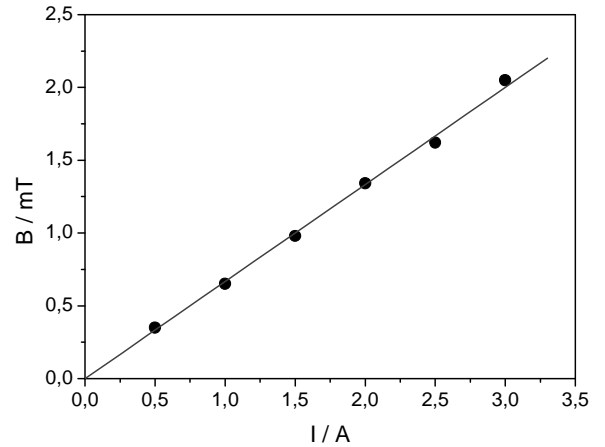


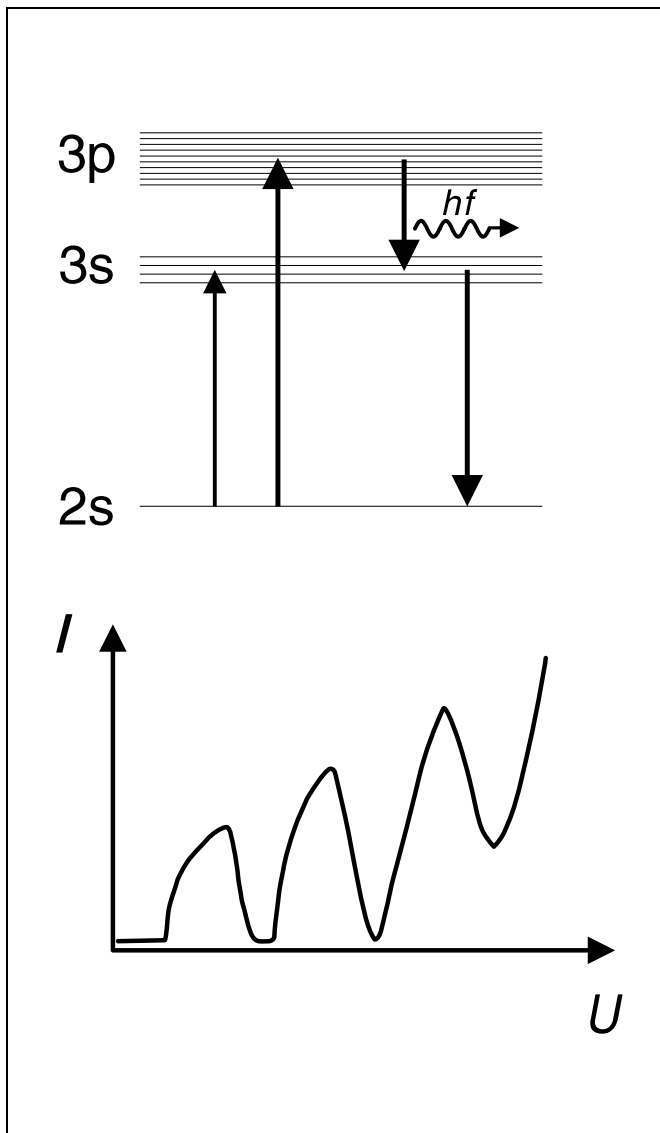
Fig. 7 Calibration curve for the magnetic field of the Helmholtz coils

Franck-Hertz experiment with neon

Recording with the oscilloscope, the XY-recorder and point by point

Objects of the experiment

- To record a Franck-Hertz curve for neon.
- To measure the discontinuous energy emission of free electrons for inelastic collision.
- To interpret the measurement results as representing discrete energy absorption by neon atoms.
- To observe the Ne-spectral lines resulting from the electron-collision excitation of neon atoms.
- To identify the luminance phenomenon as layers with a high probability of excitation.



Principles

As early as 1914, *James Frank* and *Gustav Hertz* discovered in the course of their investigations an “energy loss in distinct steps for electrons passing through mercury vapor”, and a corresponding emission at the ultraviolet line ($\lambda = 254 \text{ nm}$) of mercury. As it is not possible to observe the light emission directly, demonstrating this phenomenon requires extensive and cumbersome experiment apparatus.

For the inert gas neon, the situation is completely different. The most probable excitation through inelastic electron collision takes place from the ground state to the ten 3p-states, which are between 18.4 eV and 19.0 eV above the ground state. The four lower 3s-states in the range from 16.6 eV and 16.9 eV are excited with a lower probability. The de-excitation of the 3p-states to the ground state with emission of a photon is only possible via the 3s-states. The light emitted in this process lies in the visible range between red and green, and can thus be observed with the naked eye.

Top: Simplified term diagram for neon.
 Bottom: The electron current flowing to the collector as a function of the acceleration voltage in the Franck-Hertz experiment with neon

Apparatus

1 Franck-Hertz tube, Ne	555 870
1 Holder with socket and screen for 555 870	555 871
1 Connecting cable to Franck-Hertz tube, Ne	555 872
1 Franck-Hertz supply unit	555 88

Recommended for optimizing the Franck-Hertz curve:

1 Two-channel oscilloscope 303	575 211
2 Screened cables BNC/4 mm	575 24

Recommended for recording the Franck-Hertz curve:

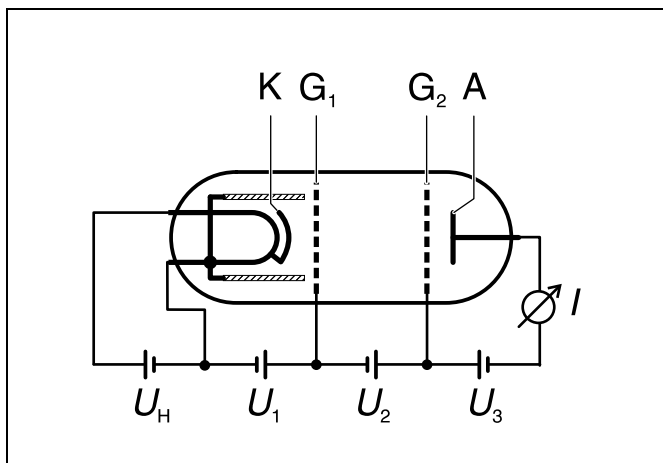
1 XY-Yt recorder SR 720	575 663
Connecting leads	

An evacuated glass tube is filled with neon at room temperature to a gas pressure of about 10 hPa. The glass tube contains a planar system of four electrodes (see Fig. 1). The grid-type control electrode G_1 is placed in close proximity to the cathode K; the acceleration grid G_2 is set up at a somewhat greater distance, and the collector electrode A is set up next to it. The cathode is heated indirectly, in order to prevent a potential differential along K.

Electrons are emitted by the hot electrode and form a charge cloud. These electrons are attracted by the driving potential U_1 between the cathode and grid G_1 . The emission current is practically independent of the acceleration voltage U_2 between grids G_1 and G_2 , if we ignore the inevitable punch-through. A braking voltage U_3 is present between grid G_2 and the collector A. Only electrons with sufficient kinetic energy can reach the collector electrode and contribute to the collector current.

In this experiment, the acceleration voltage U_2 is increased from 0 to 80 V while the driving potential U_1 and the braking voltage U_3 are held constant, and the corresponding collector current I_A is measured. This current initially increases, much as in a conventional tetrode, but reaches a maximum when the kinetic energy of the electrons closely in front of grid G_2 is just

Fig. 1: Schematic diagram of the Franck-Hertz tube, Ne



sufficient to transfer the energy required to excite the neon atoms through collisions. The collector current drops off dramatically, as after collision the electrons can no longer overcome the braking voltage U_3 .

As the acceleration voltage U_2 increases, the electrons attain the energy level required for exciting the neon atoms at ever greater distances from grid G_2 . After collision, they are accelerated once more and, when the acceleration voltage is sufficient, again absorb so much energy from the electrical field that they can excite a neon atom. The result is a second maximum, and at greater voltages U_2 further maxima of the collector currents I_A .

At higher acceleration voltages, we can observe discrete red luminance layers between grids G_1 and G_2 . A comparison with the Franck-Hertz curve shows them to be layers with a higher excitation density.

Preliminary remark

The complete Franck-Hertz curve can be recorded manually.

For a quick *survey*, e. g. for optimizing the experiment parameters, we recommend using a two-channel oscilloscope. However, note that at a frequency of the acceleration voltage U_2 such as is required for producing a stationary oscilloscope pattern, capacitances of the Franck-Hertz tube and the holder become significant. The current required to reverse the charge of the electrode causes a slight shift and distortion of the Franck-Hertz curve.

An XY-recorder is recommended for *recording* the Franck-Hertz curve.

a) Manual measurement:

- Set the operating-mode switch to MAN. and slowly increase U_2 by hand from 0 V to 80 V.
- Read voltage U_2 and current I_A from the display; use the selector switch to toggle between the two quantities for each voltage.

b) Representation on the oscilloscope:

- Connect output sockets $U_2/10$ to channel II (1 V/DIV) and output sockets U_A to channel I (2 V/DIV) of the oscilloscope. Operate the oscilloscope in XY-mode.
- Set the operating-mode switch on the Franck-Hertz supply unit to "Sawtooth".
- Set the Y-position so that the top section of the curve is displayed completely.

c) Recording with the XY-recorder:

- Connect output sockets $U_2/10$ to input X (0.5 V/cm) and output sockets U_A to input Y (1 V/cm) of the XY-recorder.
- Set the operating-mode switch on the Franck-Hertz supply unit to RESET.
- Adjust the zero-point of the recorder in the X and Y direction and mark this point by briefly lowering the recorder pen onto the paper.
- To record the curve, set operating-mode switch to "Ramp" and lower the recorder pen.
- When you have completed recording, raise the pen and switch to RESET.

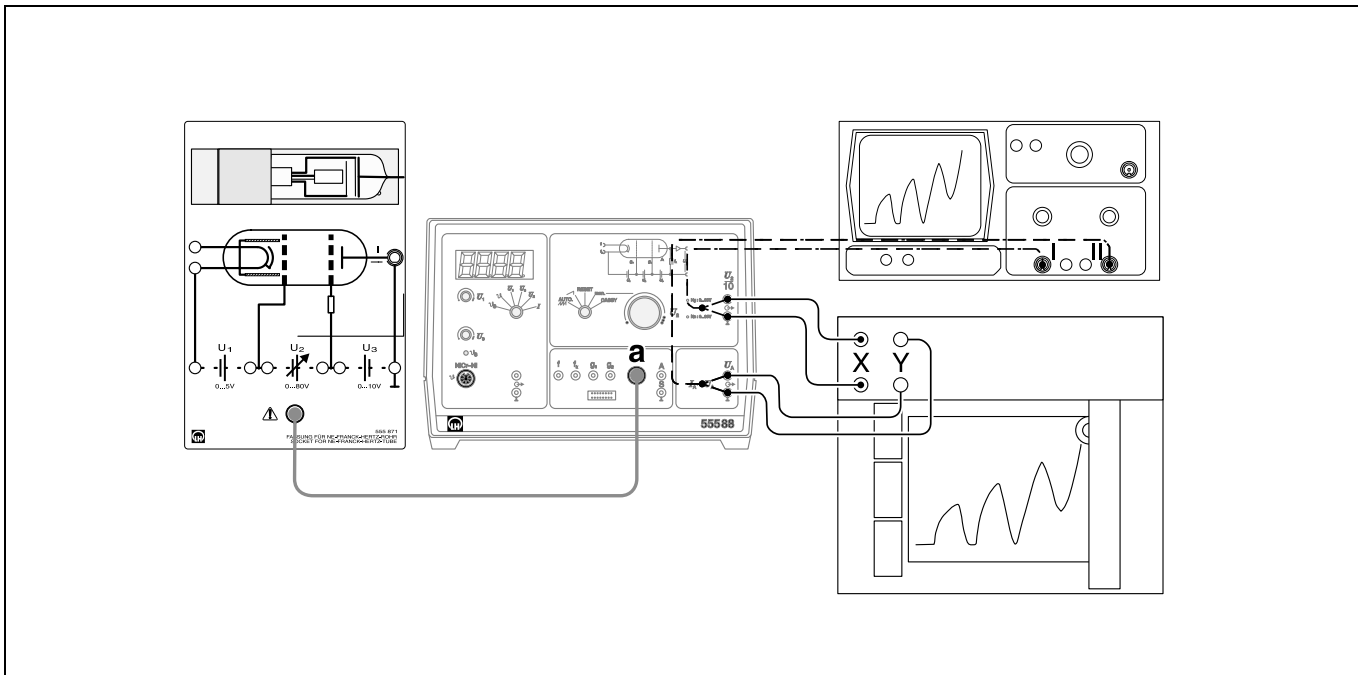


Fig. 2: Experiment setup for Franck-Hertz experiment with neon

Setup

Fig. 2 shows the experiment setup.

First:

- Insert and secure the Franck-Hertz tube in the holder and connect it to socket (a) on the Franck-Hertz supply unit via the connecting cable.

Optimizing the Franck-Hertz curve:

- Set the driving potential $U_1 = 1.5\text{ V}$ and the braking voltage $U_3 = 5\text{ V}$ and record the Franck-Hertz curve (see preliminary remark).

a) Optimizing U_1 :

A higher driving potential U_1 results in a greater electron emission current.

If the Franck-Hertz curve rises too steeply, i.e. the overdrive limit of the current measuring amplifier is reached at values below $U_2 = 80\text{ V}$ and the top of the Franck-Hertz curve is cut off (Fig. 3a):

- Reduce U_1 until the curve steepness corresponds to that shown in Fig. 3c.

If the Franck-Hertz curve is too flat, i.e. the collector current I_A remains below 5 nA in all areas (see Fig. 3b):

- Increase U_1 until the curve steepness corresponds to that shown in Fig. 3c.
- If necessary, optimize the cathode heating as described in the Instruction Sheet for the Franck-Hertz supply unit.

b) Optimizing U_3

A greater braking voltage U_3 causes better-defined maxima and minima of the Franck-Hertz curve; at the same time, however, the total collector current is reduced.

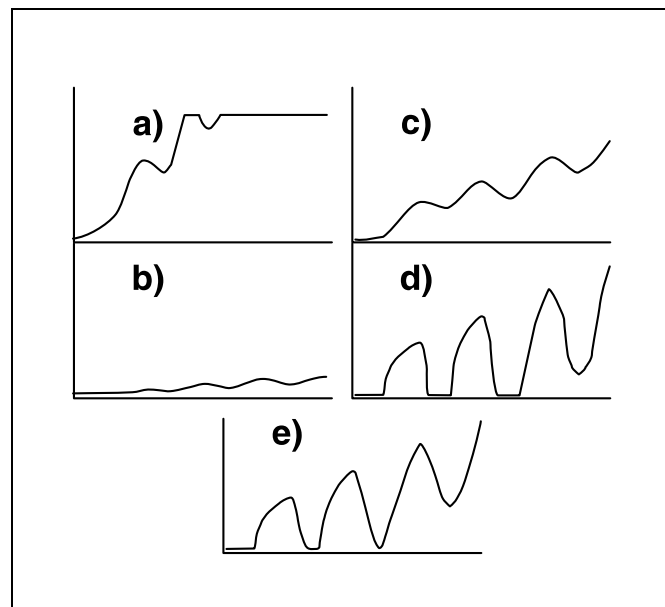
If the maxima and minima of the Franck-Hertz curve are insufficiently defined (see Fig. 3c):

- Alternately increase first the braking voltage U_3 (maximum 18 V) and then the driving potential U_1 until you obtain the curve form shown in Fig. 3e.

If the minima of the Franck-Hertz curve are cut off at the bottom (see Fig. 3d):

- Alternately reduce first the braking voltage U_3 (maximum 18 V) and then the driving potential U_1 until you obtain the curve form shown in Fig. 3e.

Fig. 3: Overview for optimizing the Franck-Hertz curves by selecting the correct parameters U_1 and U_3



Carrying out the experiment

a) Franck-Hertz curve:

- Record the Franck-Hertz curve (see preliminary remark).

b) Light emission:

- Set the operating mode switch to MAN.
- Optimize the acceleration voltage U_2 until you can clearly see a red-yellow luminance zone between grids G_1 and G_2 .
- Additionally, find the optimum acceleration voltages for two or three luminance zones and log these values.

b) Light emission:

$U_1 = 2.06 \text{ V}$

$U_3 = 7.94 \text{ V}$

The luminance layers are zones of high excitation density. They can be compared directly with the minima of the Franck-Hertz curve. Their spacing corresponds to an acceleration voltage $U_2 = 19 \text{ V}$. Therefore, an additional luminance layer is generated each time U_2 is increased by approx. 19 V (see table 1).

Table 1: Number n of the luminance zones in relation to the acceleration voltage U_2

n	U_2
1	30 V
2	48 V
3	68 V

Measuring example and evaluation

a) Franck-Hertz curve:

$U_1 = 2.06 \text{ V}$

$U_3 = 7.94 \text{ V}$

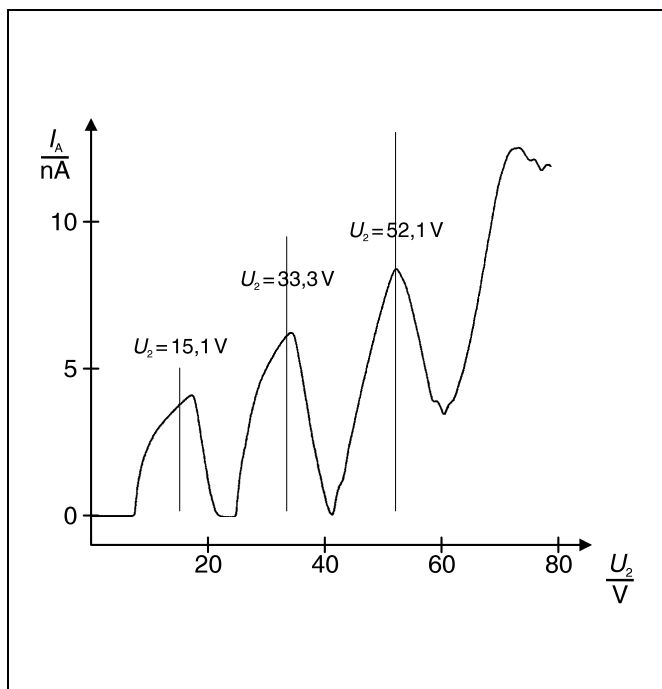
The distance between the vertical lines (these were placed by eye on the main points of the maxima) has an average value of $\Delta U_2 = 18.5 \text{ V}$. This value is much closer to the excitation energies for the 3p-levels of neon ($18.4 - 19.0 \text{ eV}$) than to the energies of the 3s-levels ($16.6 - 16.9 \text{ eV}$). Thus, the probability of excitation to the latter due to inelastic electron collision is significantly less.

The substructure in the measured curve shows that the excitation of the 3s-levels cannot be ignored altogether. Note that for double and multiple collisions, each combination of excitation of a 3s-level and a 3p-level occurs.

Supplementary information

The emitted neon spectral lines can be observed easily e.g. with the school spectroscope (467 112) when the acceleration voltage U_2 is set to the maximum value.

Fig. 4: Franck-Hertz curve for neon (recorded using an XY-recorder)



Electron spin resonance at DPPH

Determining the magnetic field as a function of the resonance frequency

Objects of the experiment

- Determining the resonance magnetic field B_0 as function of the selected frequency ν .
- Determining the g -factor of DPPH.
- Determining the line width δB_0 of the resonance signal

Principles

Since its discovery by *E. K. Zavoisky* (1945), electron spin resonance (ESR) has developed into an important method of investigating molecular and crystal structures, chemical reactions and other problems in physics, chemistry, biology and medicine. It is based on the absorption of high-frequency radiation by paramagnetic substances in an external magnetic field in which the spin states of the electrons split.

Electron spin resonance is limited to paramagnetic substances because in these the orbital angular momenta and spins of the electrons are coupled in a way that the total angular momentum is different from zero. Suitable compounds are, e.g., those which contain atoms whose inner shells are not complete (transition metals, rare earths), organic molecules (free radicals) which contain individual unpaired electrons or crystals with lattice vacancies in a paramagnetic state.

The magnetic moment associated with the total angular momentum \vec{J} is

$$\vec{\mu}_J = -g_J \cdot \frac{\mu_B}{\hbar} \cdot \vec{J} \quad (\text{I})$$

$$(\mu_B = \frac{\hbar \cdot e}{2 \cdot m_e}, \hbar = \frac{h}{2\pi}, \mu_B: \text{Bohr magneton},$$

h : Planck constant, g_J : Landé splitting factor, m_e : mass of the electron, e : electronic charge)

In a magnetic field \vec{B}_0 , the magnetic moment $\vec{\mu}_J$ gets the potential energy

$$E = -\vec{\mu}_J \cdot \vec{B}_0 \quad (\text{II})$$

E is quantized because the magnetic moment and the total angular momentum can only take discrete orientations relative to the magnetic field. Each orientation of the angular momentum corresponds to a state with a particular potential energy in the magnetic field. The component J_z of the total angular momentum, which is parallel to the magnetic field, is given by

$$J_z = \hbar \cdot m_J \text{ with } m_J = -J, -(J-1), \dots, J \quad (\text{III})$$

where the angular momentum quantum number is an integer or a half-integer, i.e. the potential energy splits into the discrete *Zeeman* levels

$$E = g_J \cdot \mu_B \cdot B_0 \cdot m_J \text{ with } m_J = -J, -(J-1), \dots, J \quad (\text{IV})$$

The energy splitting can be measured directly by means of electron spin resonance. For this a high-frequency alternating magnetic field

$$\vec{B}_1 = \vec{B}_{\text{HF}} \cdot \sin(2\pi\nu \cdot t)$$

which is perpendicular to the static magnetic field \vec{B}_0 is radiated into the sample. If the energy $h \cdot \nu$ of the alternating field is equal to the energy difference ΔE between two neighbouring energy levels, i.e., if the conditions

$$\Delta m_J = \pm 1 \quad (\text{V})$$

and

$$h \cdot \nu = \Delta E = g_J \cdot \mu_B \cdot B_0 \quad (\text{VI})$$

are fulfilled, the alternating field leads to a "flip" of the magnetic moments from one orientation in the magnetic field B_0 into the other one. In other words, transitions between neighbouring levels are induced and a resonance effect is observed which shows up in the absorption of energy from the alternating magnetic field radiated into the sample.

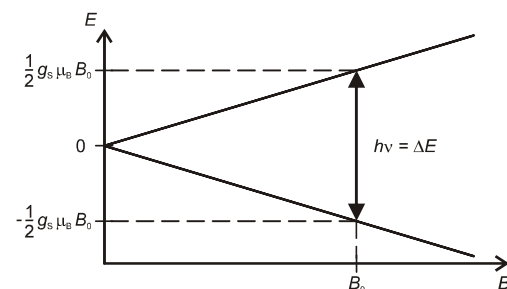


Fig. 1 Energy splitting of a free electron in a magnetic field and resonance condition for electron spin resonance.

In numerous compounds, orbital angular momentum is of little significance, and considerations can be limited to the spin of the electrons. To simplify matters, the situation is represented for a free electron in Fig. 1: here the total angular momentum is just the spin \vec{s} of the electron. The angular momentum quantum number is

$$J = s = \frac{1}{2}$$

and the Landé factor is

$$g_J = g_s \approx 2.0023.$$

In a magnetic field, the energy of the electron splits into the two levels

$$E = g_s \cdot \mu_B \cdot B_0 \cdot m_s \quad \text{with } m_s = -\frac{1}{2}, \frac{1}{2} \quad (\text{IVa}),$$

which correspond to an antiparallel and a parallel orientation of the electron spin with respect to the magnetic field. In a transition between the two levels, the selection rule (V) is automatically fulfilled: in analogy to Eq. (VI), the resonance condition reads

$$h \cdot \nu = g_s \cdot \mu_B \cdot B_0 \quad (\text{VIa}).$$

If now the energy which is absorbed from the alternating field is measured at a fixed frequency ν as a function of the magnetic field B_0 , an absorption line with a half-width δB_0 is obtained. In the simplest case, this line width in a homogeneous magnetic field is an expression of the uncertainty δE of the transition. The uncertainty principle applies in the form

$$\delta E \cdot T \geq \frac{\hbar}{2} \quad (\text{VII}),$$

where T is the lifetime of the level. Because of Eq. (V),

$$\delta E = g \cdot \mu_B \cdot \delta B_0 \quad (\text{VIII}).$$

Thus the relation

$$\delta B_0 = \frac{\hbar}{2 \cdot g_J \cdot \mu_B \cdot T} \quad (\text{IX}).$$

does not depend on the frequency ν . In this experiment, the position and width of the absorption lines in the ESR spectrum of the sample under consideration are evaluated.

From the position, the Landé factor g_J of the sample is determined according to Eq. (VI). In the case of a free atom or ion, the Landé factor lies between $g_J = 1$ if the magnetism is entirely due to orbital angular momentum and $g_J \approx 2,0023$ if only spins contribute to the magnetism. However, in actual fact the paramagnetic centres studied by means of electron spin resonance are not free. As they are inserted into crystal lattices or surrounded by a solvation sheath in a solution, they are subject to strong electric and magnetic fields, which are generated by the surrounding atoms. These fields lead to an energy shift and influence the *Zeeman* splitting of the electrons. Thereby the value of the g -factor is changed. It frequently becomes anisotropic, and a fine structure occurs in the ESR spectra. Therefore the g -factor allows conclusions to be drawn regarding electron binding and the chemical structure of the sample under consideration.

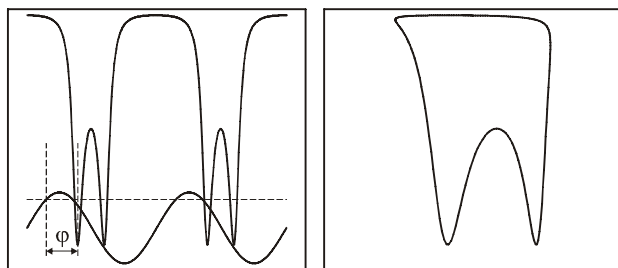
From the line width, dynamic properties can be inferred. If unresolved fine structures are neglected, the line width is determined by several processes which are opposed to an alignment of the magnetic moments. The interaction between aligned magnetic moments among each other is called spin-spin relaxation, and the interaction between the magnetic moments and fluctuating electric and magnetic fields, which are caused by lattice oscillations in solids and by thermal motion of the atoms in liquids, is called spin-lattice relaxation.

In some cases, the line width is influenced by so-called exchange interaction and is then much smaller than one would expect if there were pure dipole-dipole interaction of the spins.

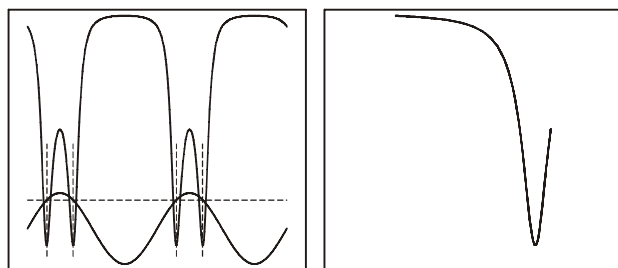
ESR spectrometers developed for practical applications usually work at frequencies of about 10 GHz (microwaves, X band). Correspondingly, the magnetic fields are of the order of magnitude of 0.1 to 1 T. In this experiment, the magnetic field B_0 is considerably weaker. It is generated by means of the Helmholtz coils and can be adjusted to values between 0 and 4 mT by appropriate choice of the coil current. A current which is modulated with 50 Hz is superimposed on the constant coil current. The magnetic field B , which is correspondingly modulated, is thus composed of an equidirectional field B_0 and a 50-Hz field B_{mod} . The sample is located in an HF coil which is part of a high-duty oscillating circuit. The oscillating circuit is excited by a variable frequency HF oscillator with frequencies between 15 and 130 MHz.

If the resonance condition (V) is fulfilled, the sample absorbs energy and the oscillating circuit is loaded. As a result, the impedance of the oscillating circuit changes and the voltage at the coil decreases. This voltage is converted into the measuring signal by rectification and amplification.

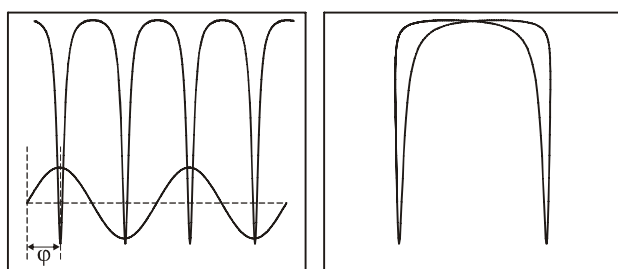
The measuring signal reaches the output of the control unit with a time delay relative to the modulated magnetic field. The time delay can be compensated as a phase shift in the control unit. A two-channel oscilloscope in X-Y operation displays the measuring signal together with a voltage that is proportional to the magnetic field as a resonance signal. The resonance signal is symmetric if the equidirectional field B_0 fulfils the resonance condition and if the phase shift φ between the measuring signal and the modulated magnetic field is compensated (see Fig. 2).



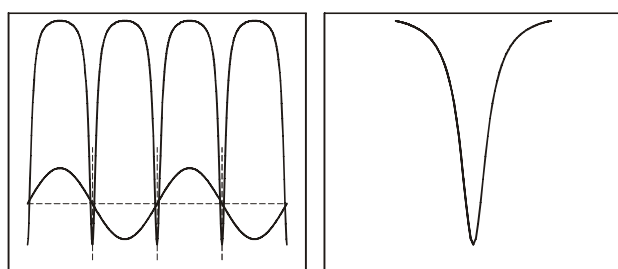
2a



2b



2c



2d

Fig. 2 Oscilloscope display of the measuring signal (Y or I, respectively) and the modulated magnetic field (X or II, respectively)

left: two-channel display with DC coupled channel II
right: XY display with AC coupled channel II

Fig. 2a phase shift φ not compensated, equidirectional field B_0 too weak

Fig. 2b phase shift φ compensated, equidirectional field B_0 too weak

Fig. 2c phase shift φ not compensated, appropriate equidirectional field B_0

Fig. 2d phase shift φ compensated, appropriate equidirectional field B_0

The sample substance used is 1,1-diphenyl-2-picryl-hydrazyl (DPPH). This organic compound is a relatively stable free radical which has an unpaired valence electron at one atom of the nitrogen bridge (see Fig. 3). The orbital motion of the electron is almost cancelled by the molecular structure. Therefore the g -factor of the electron is almost equal to that of a free electron. In its polycrystalline form the substance is very well suited for demonstrating electron spin resonance because it has an intense ESR line, which, due to exchange narrowing, has a small width.

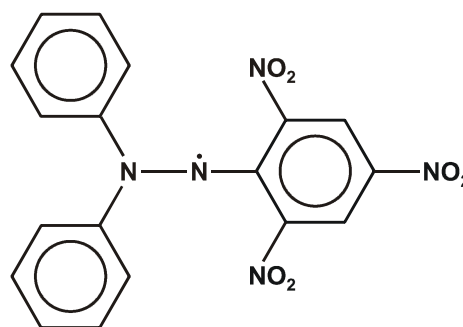


Fig. 3 Chemical structure of 1,1-diphenyl-2-picryl-hydrazyl (DPPH)

Apparatus

1 ESR basic unit	514 55
1 ESR control unit	514 571
1 pair of Helmholtz coils	555 604
1 two-channel oscilloscope 303	575 211
2 BNC cable 1m	501 02
3 saddle bases	300 11
1 connection lead 25 cm black	501 23
1 Connection lead 50 cm red	501 25
1 Connection lead 50 cm blue	501 26

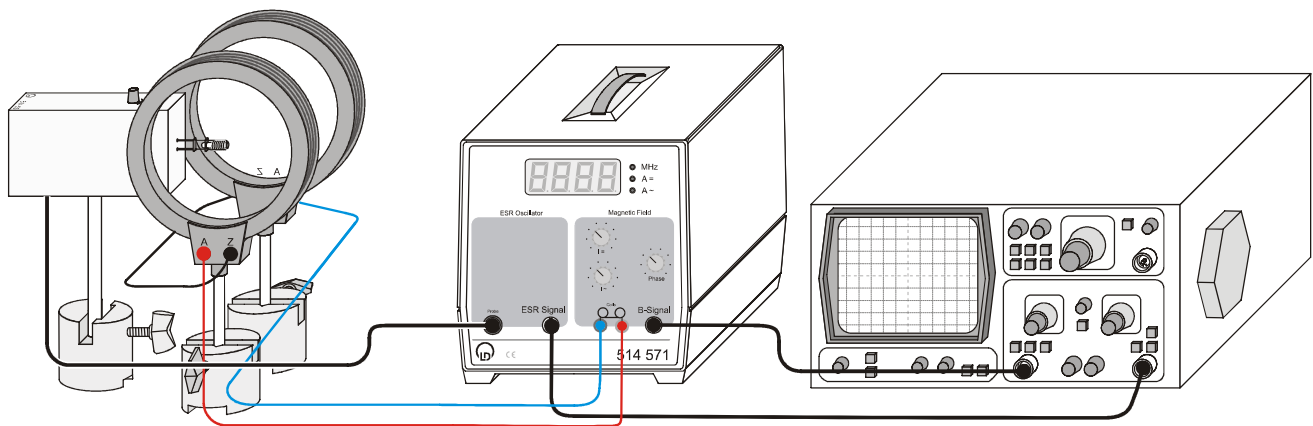


Fig. 4 Experimental setup for electron spin resonance at DPPH.

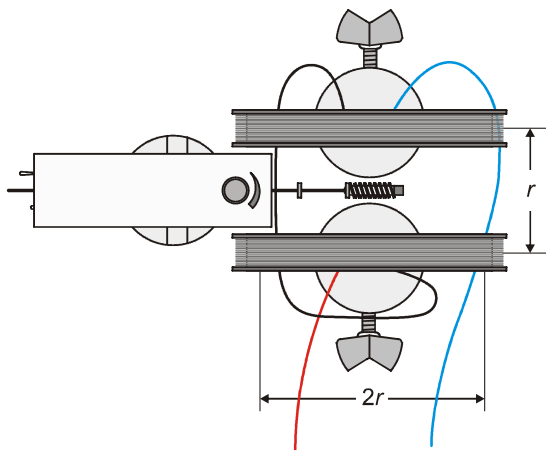


Fig. 5 Arrangement of the Helmholtz coils viewed from above.

Setup

The experimental setup is illustrated in Figs. 4 and 5.

- Set up the Helmholtz coils mechanically parallel to each other at an average distance of 6.8 cm (equal to the average radius r).
- Connect the Helmholtz coils electrically in series to each other and to the ESR control unit, note the details in Fig. 5.
- Connect the ESR basic unit to the ESR control unit via the 6-pole cable.
- Connect the output "ESR Signal" of the ESR control unit to channel II (y-Axis) of the two-channel oscilloscope and the output "B-Signal" to channel I (x-Axis) via BNC cables.

Carrying out the experiment

Determining the resonance magnetic field B_0 :

- Put on the plug-in coil 15-30 MHz (the biggest one of the three coils) and insert the DPPH sample so that it is in the centre.
- Switch the ESR basic unit on and set it up so that the plug-in coil with the DPPH sample is located in the centre of the pair of Helmholtz coils (see Fig. 5).
- Set the resonance frequency $\nu = 15$ MHz (potentiometer on top of the basic unit).

- Set the modulation amplitude I_{\sim} to the middle.
- Set the phase shift to the right (potentiometer Phase).
- Select two-channel operation at the oscilloscope.

Dual	on	
time base	2	ms/cm
Amplitude I and II	0.5 V/cm AC	

- Use the button on the control unit to switch the display of the control unit to "A=", showing the value of I_{\sim} . Slowly enhance the equidirectional field of the Helmholtz coils with the current I_{\sim} until the resonance signals are equally spaced (see Fig. 3). At a frequency of 15 MHz this will be at an approximate current of 0.13 A.
- Switch the oscilloscope to XY operation, and set the phase shift so that the two resonance signals coincide (see Fig. 2).
- Vary the direct current I_{\sim} until the resonance signal is symmetric. Select a modulation current I_{\sim} as small as possible.
- Read the direct current I_{\sim} through the pair of Helmholtz coils, and take it down together with the resonance frequency ν , creating Table 1.
- Increase the resonance frequency ν by 5 MHz, and adjust the new resonance condition by increasing the direct current I_{\sim} .
- Again measure the current I_{\sim} and take it down.
- Continue increasing the high frequency in steps of 5 MHz (use the plug-in coil 30-75 MHz for frequencies greater than 30 MHz and the plug-in coil 75-130 MHz (the smallest one) for frequencies greater than 75 MHz) and repeat the measurements.

Determining the half-width δB_0 :

- Select XY operation at the oscilloscope.
- | | |
|--------------|-------------|
| Amplitude II | 0.5 V/cm AC |
|--------------|-------------|
- Adjust the resonance condition for $\nu = 50$ MHz (medium plug-in coil) once more.
 - Extend the resonance signal in the X direction exactly over the total width of the screen (10 cm) by varying the modulation current I_{\sim} .
 - Switch the control unit display to I_{\sim} and read the RMS (!) value of the modulation current I_{mod} , for example 0.282 A.
 - Spread the X deflection (changing to 0.2 V/cm), read the width ΔU of the resonance signal at half the height of the

oscilloscope screen, and take it down, for example 1.5 cm.

Measuring example

Determining the resonance magnetic field B_0

In Table 1, the current through the series-connected Helmholtz coils I_0 in the case of resonance is listed as a function of the frequency ν of the alternating high frequency field.

Table 1: the current I_0 as a function of the frequency ν of the alternating field

$\frac{\nu}{\text{MHz}}$	$\frac{I}{\text{A}}$	Plug-in coil
15	0.13	big
20	0.17	big
25	0.21	big
30	0.26	big
30	0.26	medium
35	0.30	medium
40	0.34	medium
45	0.38	medium
50	0.43	medium
55	0.47	medium
60	0.51	medium
65	0.55	medium
70	0.60	medium
75	0.64	medium
75	0.64	small
80	0.68	small
85	0.72	small
90	0.77	small
95	0.81	small
100	0.85	small
105	0.89	small
110	0.94	small
115	0.98	small
120	1.02	small
125	1.06	small
130	1.11	small

Determining the half-width δB_0 :

half-width read from the oscilloscope, 1.5 cm corresponding

$$\text{to: } \delta U = 1.5 \text{ cm} \cdot 0.2 \frac{\text{V}}{\text{cm}} = 0.3 \text{ V}$$

Calibration of the full modulation voltage U_{mod} :

$$U_{\text{mod}} = 10 \text{ cm} \cdot 0.5 \frac{\text{V}}{\text{cm}} = 5 \text{ V}$$

corresponds to $I_{\text{mod}} = 0.28 \text{ A}$ (RMS of AC).

Peak-to-peak Amplitude is $2\sqrt{2}$ of RMS.

Evaluation

The magnetic field B of the Helmholtz coils can be calculated from the current I through each coil:

$$B = \mu_0 \cdot \left(\frac{4}{5}\right)^2 \cdot \frac{n}{r} \cdot I \quad \text{with } \mu_0 = 4\pi \cdot 10^{-7} \frac{\text{Vs}}{\text{Am}}$$

(n : number of turns per coil, r : radius of the coils)

With $n = 320$ and $r = 6.8 \text{ cm}$ $B = 4.23 \text{ mT} \cdot \frac{I}{\text{A}}$ is obtained.

Determining the resonance magnetic field B_0 :

In Table 2 the values calculated for the magnetic field are compiled.

Table 2: The magnetic field B_0 as a function of the frequency ν of the alternating field.

$\frac{\nu}{\text{MHz}}$	$\frac{B_0}{\text{mT}}$
15	0.55
20	0.74
25	0.93
30	1.08
35	1.27
40	1.46
45	1.63
50	1.82
55	1.99
60	2.12
65	2.33
70	2.54
75	2.75
80	2.86
85	3.07
90	3.28
95	3.38
100	3.60
105	3.81
110	4.02
115	4.12
120	4.23
125	4.44
130	4.65

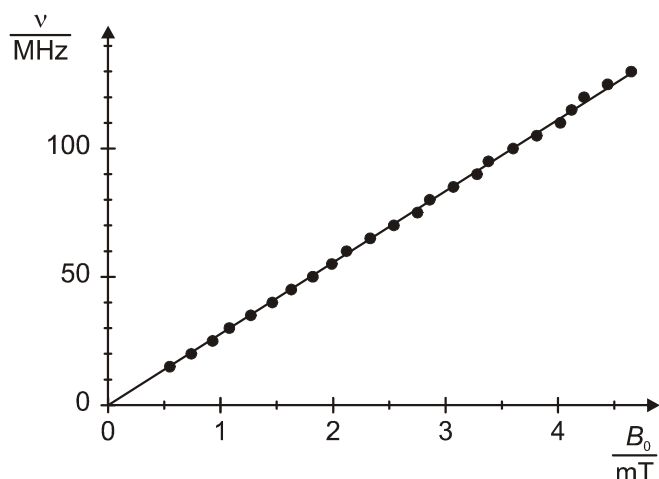


Fig. 6 the resonance frequency as a function of the magnetic field for DPPH

Fig. 6 shows a plot of the measured values. The slope of the straight line through the origin drawn in the plot is

$$\frac{\nu}{B_0} = 27.8 \frac{\text{MHz}}{\text{mT}}.$$

From this the g -factor follows:

$$g = \frac{h \cdot \nu}{\mu_B \cdot B_0} = \frac{6.625 \cdot 10^{-34} \text{Ws}^2}{9.273 \cdot 10^{-24} \text{Am}^2} \cdot 27.8 \frac{\text{MHz}}{\text{mT}} = 1.99$$

Value quoted in the literature: $g(\text{DPPH}) = 2.0036$.

Determining the half-width δB_0 :

$$\delta I = \frac{\delta U}{U_{\text{mod}}} \cdot I_{\text{mod}} = \frac{0.3 \text{ V}}{5 \text{ V}} \cdot 0.28 \text{ A} \cdot 2 \cdot \sqrt{2} = 0.049 \text{ A}$$

From this

$$\delta B_0 = 4.23 \text{ mT} \cdot \frac{\delta I}{\text{A}} = 0.21 \text{ mT}$$

is obtained.

Value quoted in the literature:

$$\delta B_0 (\text{DPPH}) = 0.15\text{-}0.81 \text{ mT}$$

The line width strongly depends on the solvent in which the substance has recrystallized. The smallest value quoted in the literature is obtained with CS_2 as solvent.



KLINGER
EDUCATIONAL
PRODUCTS CORP.

112-19 14TH ROAD
COLLEGE POINT, NEW YORK 11356
(718) 461-1822

Electron spin resonance; magnetic field dependence of the resonance frequency, determination of the g-factor

The absorption of alternating field energy of a sample in the magnetic field of a pair of Helmholtz coils, on which a high frequency alternating field has been superimposed, is measured with ESR equipment and an oscilloscope in xy-mode. From the relationship between resonance frequency and resonance field strength B of the electromagnet, the g-factor for the spin of the electron g_s is calculated.

A paramagnetic electron spin system - a sample of DIPHENYL-PICRYL-HYDRAZYL (DPPH) - in the coil of the high frequency resonance circuit absorbs high frequency energy in a DC field during resonance. This leads to a measurable change in the resonance circuit's impedance.

With this resonance method, we can discover something about the intrinsic angular momentum of the electron (spin); the magnetic torque, the quantized adjustment possibilities of the spin in outer magnetic field and the energy level connected with it. To do this, bridges between energy levels are induced in high frequency alternating current fields, corresponding to two possible stable spin adjustments in the outer magnetic field.

The organic compound Diphenyl-picryl-hydrazyl (DPPH) is a radical, in which an unpaired electron appears on one of the nitrogen atoms (see Fig. 1).

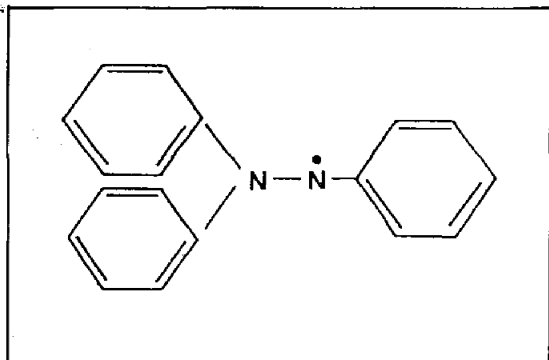


Fig. 1: DPPH

The electrons of a DPPH sample, which do not possess any orbital angular momentum ($l = 0$), are well suited for electron spin resonance experiments.

The sample is placed into a magnetic DC field, which is superimposed by a high frequency magnetic AC field (in the coil of a resonance circuit).

During resonance (the energy of the irradiated photons is equal to the energy difference between two possible stable spin positions; transitions are induced) high frequency energy is absorbed, which is reflected in an alteration of the resonance circuit's impedance.

During electron spin resonance measurement, due to experimental reasons, the frequency of the irradiated microwaves is not adapted, but the strength of the outer magnetic field is varied.

Through modulation of the magnetic DC field, a change in resistance during resonance can periodically be brought about and therefore can be displayed on the oscilloscope.

Vertical deflection plates: voltage proportional to the amplitude of the high frequency field.

Horizontal deflection plates: voltage proportional to the field of the Helmholtz coils.

The resonance frequency f is a function of the resonance field strength B . The dependence is determined experimentally, is then compared with the theoretical result derived below and is then evaluated.

Electron spin resonance formula

A magnetic moment is linked with electron spin. It can be clearly understood by considering the electron as a rotating electric charge and by virtue of the fact that a circular current possesses a magnetic moment. Because of the negative charge of the electron, the magnetic moment acts in the opposite direction to the spin. This clear notion of a rotating electron cannot be taken too literally, because no quantitatively correct results can be derived from it. In particular it does not follow that the electron spin has only half numbers.

The relationship between the electron spin \vec{s} and the magnetic moment $\vec{\mu}_s$ of the electron is expressed in the form

$$\vec{\mu}_s = \frac{g_s \mu_B}{\hbar} \vec{s}$$

μ_B is Bohr's magneton, depicting the structural unit for atomic magnetic moment; and \hbar (read 'h-cross'; $\hbar = h/2\pi$) Planck's action quantum

which in a similar way is the structural unit for atomic angular momentum. The constant g_s is a

value characteristic for the electron, which is designated as the g-factor for the spin of the electron.

It shows the ratio of the values of the magnetic moment to that of the angular momentum in the corresponding atomic units:

$$g_s = \frac{\mu_s}{s} \frac{\mu_B}{\hbar}$$

If the corresponding ratio of magnetic moment and orbital angular momentum is formed, then the experimentally correct value $g=1$ is obtained and for Bohr's magneton one finds $\mu_B = e \cdot \hbar / (2m_0 \cdot c)$; m_0 is the calculation $\mu_B = e \cdot \hbar / (2m_0 \cdot c)$; m_0 is the resting mass of the electron. The g-factor for the spin of an electron cannot be understood with classical physics (see note at end). It can only be understood by means of relativistic quantum mechanics. It has a value of $g_s = 2$ with a

correction factor of 0.1%, which is in agreement with the experiment.

To derive the resonance formula, the results of quantum mechanics are used, with which the orbital angular momentum \vec{l} can be calculated with the formula $\vec{l} = \sqrt{l(l+1)} \cdot \hbar$. l is the angular momentum quantum number. Also, the observable components of the angular momentum are quantized in one privileged direction according to the

formula $l_z = m \cdot \hbar$. m is the magnetic quantum number. The z-direction is defined here by the magnetic field. For the orbital angular momentum with an orbital quantum number l , m must have integral values, $m = 0, +1, +2 \dots +l$. In total, an odd number of $2l + 1$ values and the same number of energy levels are obtained (Z-direction corresponds to the direction of the outer field).

The angular momentum vector \vec{s} follows the same rules as those of the orbital angular momentum.

$$s = \sqrt{s(s+1)} \cdot \hbar$$

$$s_z = m_s \cdot \hbar; \quad m_s = -s, \dots, +s$$

When splitting up the S-basic state ($l = 0$), into two components (even number), we can conclude that the electron has a spin. On the other hand, the spin quantum number must have the value $s = \frac{1}{2}$, so that for all possible values of the magnetic spin quantum number m_s :

$$2 \cdot s + 1 = 2.$$

The magnetic spin quantum number can only take on the value $m_s = +\frac{1}{2}$, this being able to explain the splitting into two levels.

With only two spin sets possible, the magnetic moment of the electron which is coupled with the intrinsic angular momentum has also only two setting possibilities. From

$$\vec{\mu} = -g_s \frac{\mu_B}{\hbar} \vec{s} \text{ and } s_z = \pm \hbar/2$$

it follows that the z-component of the magnetic moment is

$$\mu_z = \pm \frac{1}{2} g_s \mu_B.$$

The potential energy E_m of a magnetic moment $\vec{\mu}$, which is in a magnetic field with the force flux density \vec{B} , is:

$$E_m = \vec{\mu} \cdot \vec{B} = \mu_z B.$$

Accordingly, the energy E_0 , which has an electron without a magnetic field, divided up into the two following levels (compare Fig. 2):

$$E_m = E_0 \pm \frac{1}{2} g_s \mu_B B.$$

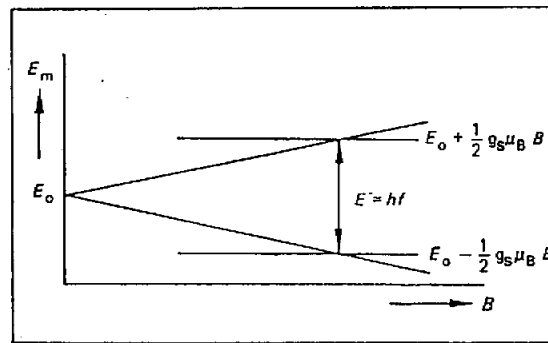


Fig. 2: Splitting up of an energy level in a magnetic field (total impulse $j = s + l = s$) with resonance conditions.

Resonance absorption takes place when the energy of the irradiation photon $E = hf$ is equal to the magnetic splitting up of energy. Here f is the frequency of the beam. As the resonance formula we obtain

$$hf = g_s \mu_B B$$

In general, we must take into consideration the fact that the total angular momentum J is the sum of the orbital angular momentum and the spin.

Apparatus:

1 ESR-basic unit (sample head)	514 55
1 Pair of Helmholtz coils	555 06
3 Saddle bases	300 11
1 Oscilloscope, two-channel	e.g. 575 20
2 Cable, screened, BNC, 4 mm socket	575 24

For power supply:

1 ESR-control unit	514 57
and	
1 Measuring instrument D, measuring range	
3 A, e.g. E measuring instrument D	531 88
3 Connecting leads, 50 cm	501 28
2 Connecting leads, 25 cm	501 23

Setting up:

Connect the Helmholtz coils in parallel, choose a distance for the coils equal to the coil radius r ($r = 6.8 \text{ cm}$).

Important!
Below the current in each coil will be designated I . Because of the parallel connection of both coils, the ammeter displays $2 I$.

Oscilloscope setting
HOR, EXT.

Y_1 : AC; $0,5 \frac{V}{cm}$

X : AC; $2 \frac{V}{cm}$

Point of origin: The middle of the uppermost screen line.

Carrying out the experiment:

- Choose one of the following plug-in coils corresponding to the frequency range of the high frequency alternating current field:

Plug-in coil (E) (f approx. 13 - 30 MHz),
Plug-in coil (F) (f approx. 30 - 75 MHz),
Plug-in coil (G) (f approx. 75 - 130 MHz)

Insert the DPPH-sample.

- If the amplitude of the AC field superimposed with the magnetic DC field is too small, slowly increase the magnetic DC field until impulses can be seen on the screen.

Note:

In general two resonance impulses can be seen. This is because the magnetic AC field goes through the resonance position twice per phase and because there is a phase offset between the voltages shown on the oscilloscope (verify with a two channel oscilloscope: instead of X-input (HOR.EXT.):

Y_{II} -input, TIMEBASE $1 \frac{ms}{cm}$).

- Coincide resonance impulses with the phase shifter and by varying the direct current field, set it symmetrically to the center of the screen ($x = 0$) (example: oscillogram Figure 4).

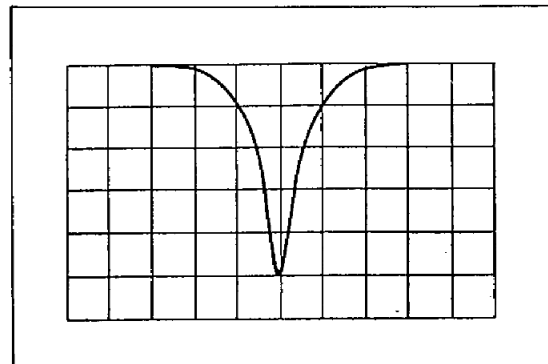


Fig. 4: Oscillogram

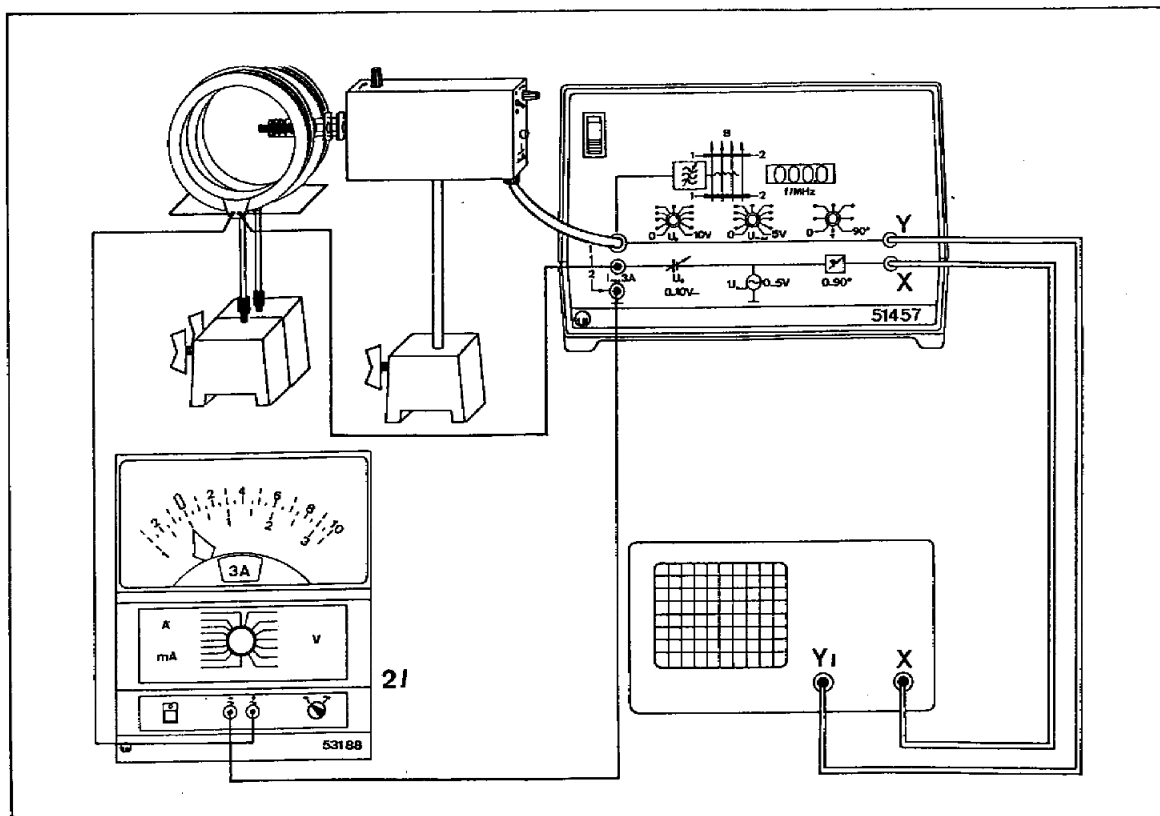


Fig. 3: Experiment setup

- Increase the frequency f of the HF oscillator, so that the resonance line displaces itself to the right on the oscilloscope screen, because resonance only occurs when there is a large magnetic force flux density B .
- By increasing the magnetic direct current field, reset the resonance line back to its original position (middle of the screen) (symmetrical to $X = 0$).
- Measure the frequency f and the direct current amplitude I which is proportional to B . For an exact measurement of I , choose a low ESR signal by decreasing the modulation amplitude of the outer field, and adjust the remaining ESR signal so that it is symmetrical to the middle of the screen ($x = 0$) with the direct current field (see Fig. 5).
- Determine the pair of values f and I according to the methods described (see diagram Fig. 6).

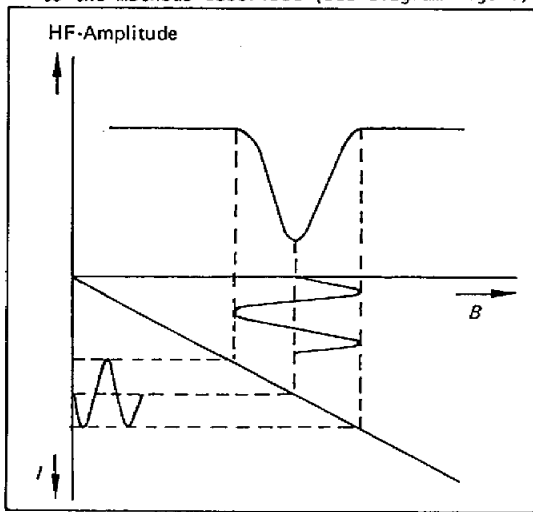


Fig. 5: In the case of a symmetrical resonance impulse its maximum marks the amplitude of the magnetic DC-field with the force flux density B proportional to I .

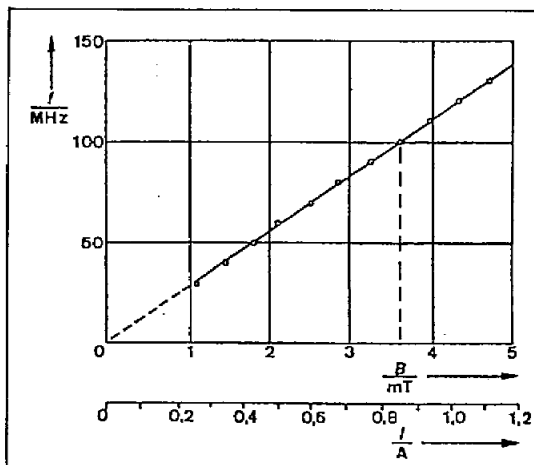


Fig. 6: Resonance frequency f as a function of the magnetic resonance field strength B , proportional to the current measured on the Helmholtz coils.

Deducing B by measuring I:

If the amount of the current in the coil I is known, then the force flux density B of the almost homogenous magnetic field in the pair of Helmholtz coils (distance between the coils = coil radius) can be calculated with Biot-Savart's law.

$$B = \mu_0 \left(\frac{4}{5}\right)^{\frac{3}{2}} \cdot \frac{n}{r} \cdot I$$

n = Number of turns in the coil
 r = Coil radius
 I = Current in each coil

With the magnetic field constant

$$\mu_0 = 1,2566 \cdot 10^{-6} \frac{Vs}{Am}$$

$$n = 320 \text{ und}$$

$$r = 6,8 \text{ cm}$$

we get $\frac{B}{mT} = 4,23 \frac{I}{A}$

Recalibrate the I -abscissa in Fig. 6 according to this relationship.

Measuring example:

The slope of the line is taken from diagram Fig. 6

$$\frac{f}{B} = \frac{100 \text{ MHz}}{3,57 \text{ mT}}$$

Evaluation and result:

The resonance frequency is proportional to the magnetic resonance force flux density B .

From the resonance condition

$$h \cdot f = g_s \cdot \mu_B \cdot B$$

it follows that $\frac{f}{B} = \frac{g_s \cdot \mu_B}{h}$

$$h = 6,625 \cdot 10^{-34} \text{ Js}^2 \text{ (Planck's action quantum)}$$

$$\mu_B = 9,273 \cdot 10^{-24} \text{ Am}^2 \text{ (Bohr's magneton).}$$

The g -factor can be calculated with the help of the experimentally determined slope $\frac{f}{B}$:

$$g_s = \frac{h \cdot f}{\mu_B \cdot B} = \frac{6,625 \cdot 10^{-34} \text{ Js}^2 \cdot 100 \text{ MHz}}{9,273 \cdot 10^{-24} \text{ Am}^2 \cdot 3,57 \text{ mT}} = 2,0$$

The g -factor ($g_s = \frac{h \cdot f}{\mu_B \cdot B}$) which was calculated

with the help of the proportionality constant $\frac{f}{B}$, has the value 2.0.

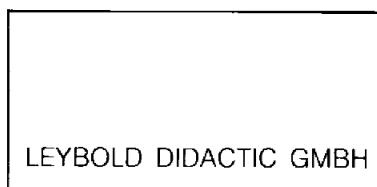
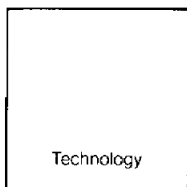
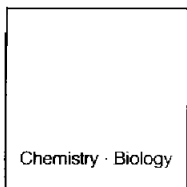
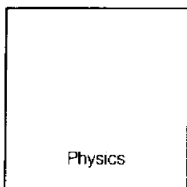
Note:

The g-factor $g_s = 2$ cannot be understood in classical physics.

$g_s = 2$ means that the spin generates at twice as large a magnetic moment as a classical rotating charge with the angular momentum $1/2 h$.

Literature on electron spin resonance

- (1) Elektronenspin-Resonanz
F. Schneider and M. Plato
Thiemig-Taschenbücher, Band 40
Verlag Karl Thiemig KG, München
- (2) Paramagnetic resonance in solids
W. Low
Academic Press 1960, New York and London
- (3) Principles of Magnetic Resonance
C. P. Slichter
Harper and Row 1963
- (4) Paramagnetic Resonance
G.E. Pake
W. A. Benjamin 1962, New York



5/89 -Kr-Brs-

Instruction Sheet

514 55/56/57



KLINGER EDUCATIONAL PRODUCTS CORP.

112-19 14TH ROAD COLLEGE POINT, NEW YORK 11356 (718) 461-1822

ESR Basic Unit
ESR Adapter
ESR Control Unit

The ESR basic unit is used in experiments on electron spin resonance, the ESR control unit provides all the required voltages and also digitally indicates the frequency of the oscillatory circuit

The ESR adapter is used in those cases where other power supply units and frequency indicators are used instead of the ESR control unit.

Measuring Principle:

A paramagnetic electron spin system - probe consisting of DIPHENYL-PICRYL-HYDRAZYL (DPPH) - placed between the coils of an r-f oscillatory circuit and applying a constant field, will absorb r-f energy thus measurably changing the impedance of the oscillatory circuit. The impedance change of the constant magnetic field as produced by the modulation can be displayed on an oscilloscope.

Examples of experiments:

- Verification of electron spin resonance
• Magnetic field as a function of resonant frequency (linearity of Zeeman interaction)
• Measurement of the gyromagnetic ratio and factor of g
• ESR line width
• Signal amplitude as a function of resonant frequency

A monograph describing experiments on electron spin resonance is in preparation.

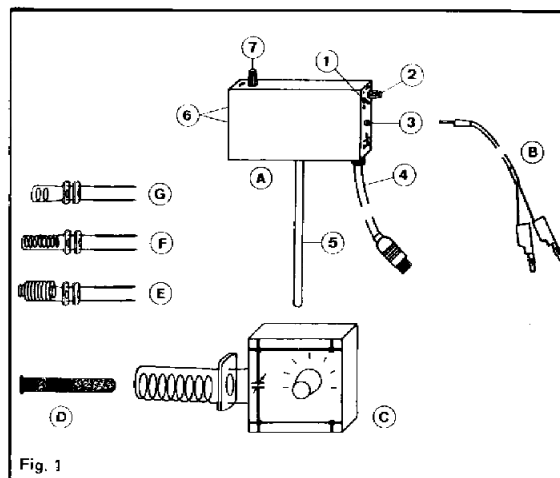


Fig. 1

Control elements:

- 1 On/off switch
2 Potentiometer for r-f amplitude adjustment
3 Socket for measuring cable B
4 Multi-core lead for supply and signal voltages
5 Stand rod
6 Sockets for connecting the r-f plug-in coils
7 Variable capacitor for frequency adjustment

Technical Data:

Supply voltage and current: ±12 V/175 mA
Frequency ranges: with plug-in coil G: 13 to 30 MHz approx. with plug-in coil F: 30 to 75 MHz approx. with plug-in coil E: 75 to 130 MHz approx.
Voltage across the r-f coil: 6 Vpp approx. at 13 MHz amplitude adjusted to maximum
ESR signal: 1 to 6 V approx. (depending on frequency)
Frequency divider: 1000:1
Frequency output for digital counter: TTL
D. C. current (at output 3): 100 µA approx.
Test substance: Diphenyl-Picryl-Hydrazyl (DPPH)
Frequency range of the passive resonant circuit C: 10 to 50 MHz
Dimensions of the probe holder: 130 mm x 70 mm x 40 mm
Length of stand rod: 185 mm
Weight: 0.7 kg approx.

1 Safety

- The ESR control unit can be converted for mains voltages other than 220 V a. c. (see Section 4.2).
□ Output 3 of the ESR control unit (magnet supply)

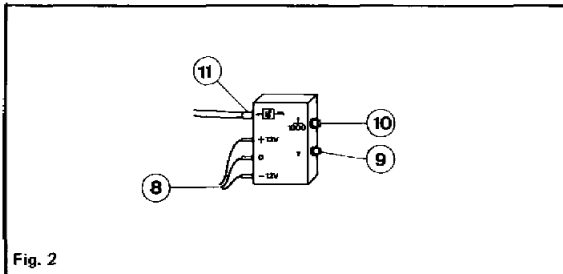
2 Parts, Description, Technical Data

2.1 514 55 ESR basic unit

The basic unit consists of the following parts:

- A ESR probe holder with frequency divider 1000:1 and signal amplifier
B Measuring lead to use the apparatus as a resonance meter
C Electric resonant circuit, passive (for investigating the relationship between resonant frequency and magnetic field)
D DPPH probe
E, F, G Plug-in coils for different frequency ranges

2.2 514 56 ESR adapter



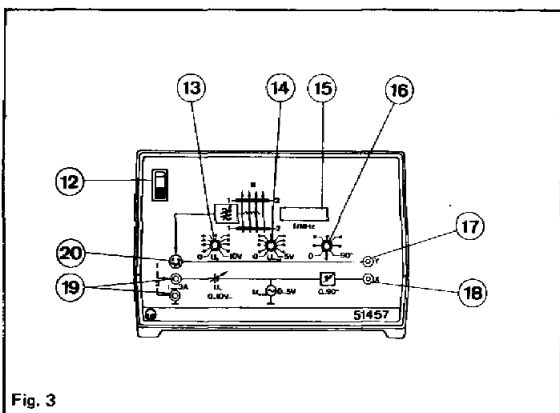
Control elements:

- ⑧ Supply voltage connection
- ⑨ Signal output Y
- ⑩ Frequency output
- ⑪ Connection for the ESR basic unit (probe holder)

Technical Data:

Signal output Y:	BNC socket
Frequency output $\frac{f}{1000}$:	BNC socket
Supply voltage input +12 V, 0, -12 V:	4-mm sockets
Socket for ESR basic unit:	for 5-pin connector
Dimensions:	95 mm x 75 mm x 25 mm
Weight:	0.2 kg

2.3 514 57 ESR control unit



Control elements:

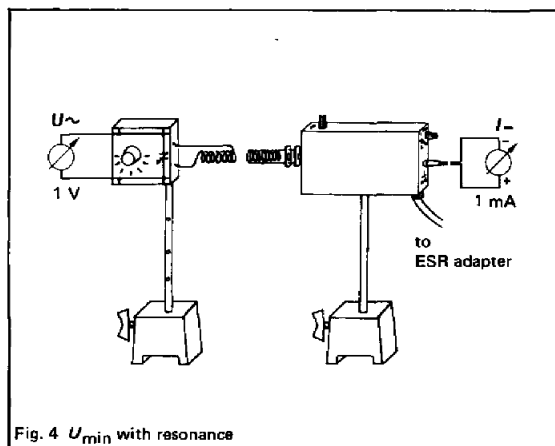
- ⑫ On/off switch
- ⑬ D. C. voltage adjusting potentiometer
- ⑭ Modulation voltage adjusting potentiometer
- ⑮ Digital frequency indication
- ⑯ Phase shifter
- ⑰ Signal output
- ⑱ Modulation output
- ⑲ Output magnet supply
- ⑳ Socket for connection to the ESR basic unit (probe holder)

Technical Data:

Mains connection:	110/130/220/240 V a. c., 50/60 Hz
Primary fuse:	0.8 A (slow blow) for 220 V and 240 V (Spare Part No. 69 814) 1.6 A (slow blow) for 110 V and 130 V (Spare Part No. 69 817)
Magnetic field supply:	0 to 10 V d. c. 0 to 5 V a. c. max. current 3 A (no overload protection!)
Phase shifter:	0 to 90°
Digital frequency indication:	4 digits
Signal output:	BNC socket
Modulation output:	BNC socket
Magnet supply output:	pair of 4-mm sockets
Dimensions:	30 cm x 21 cm x 23 cm
Weight:	6.2 kg approx.

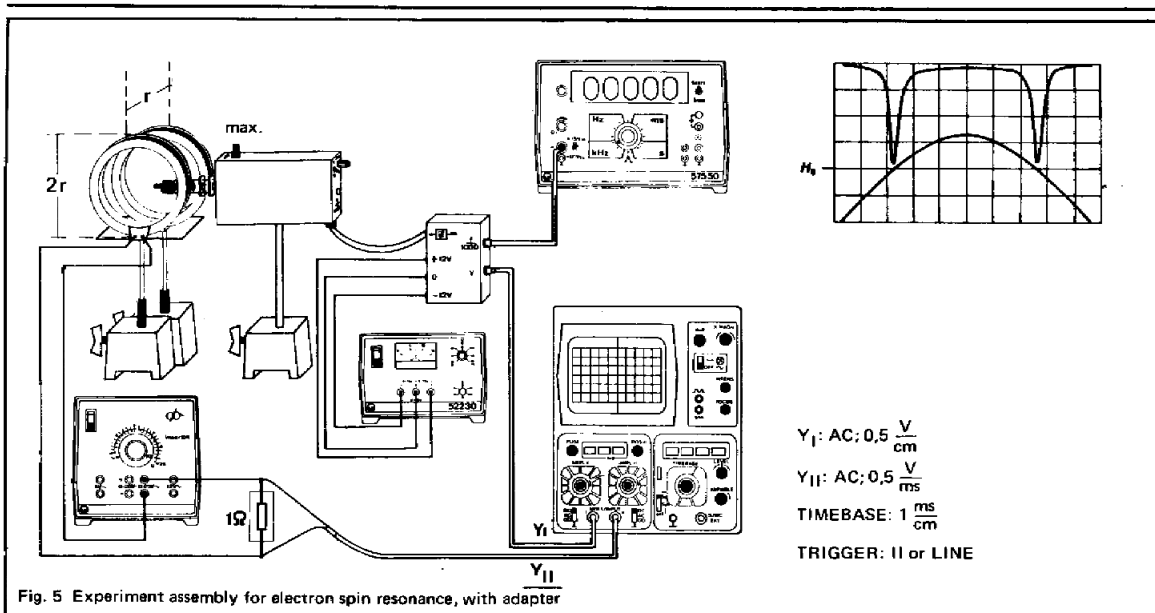
3 Experiment Assemblies, Operation

3.1 Assembly for demonstrating the operating principle of the ESR basic unit (514 55)



Equipment:

Equipment:	Cat. No.
1 ESR basic unit (probe holder)	514 55
1 Perforated stand rod	590 13
2 Saddle bases	300 11
1 D. C. power supply, stabilized	522 30
1 ESR adapter	514 56
or instead of (522 20) and (514 56):	
1 ESR control unit	514 57
1 Voltmeter, range 1 V a. c.	
1 Ammeter, range: 1 mA d. c.	
e. g. E measuring instruments D.	531 88



3.2 Assembly for demonstrating electron spin resonance

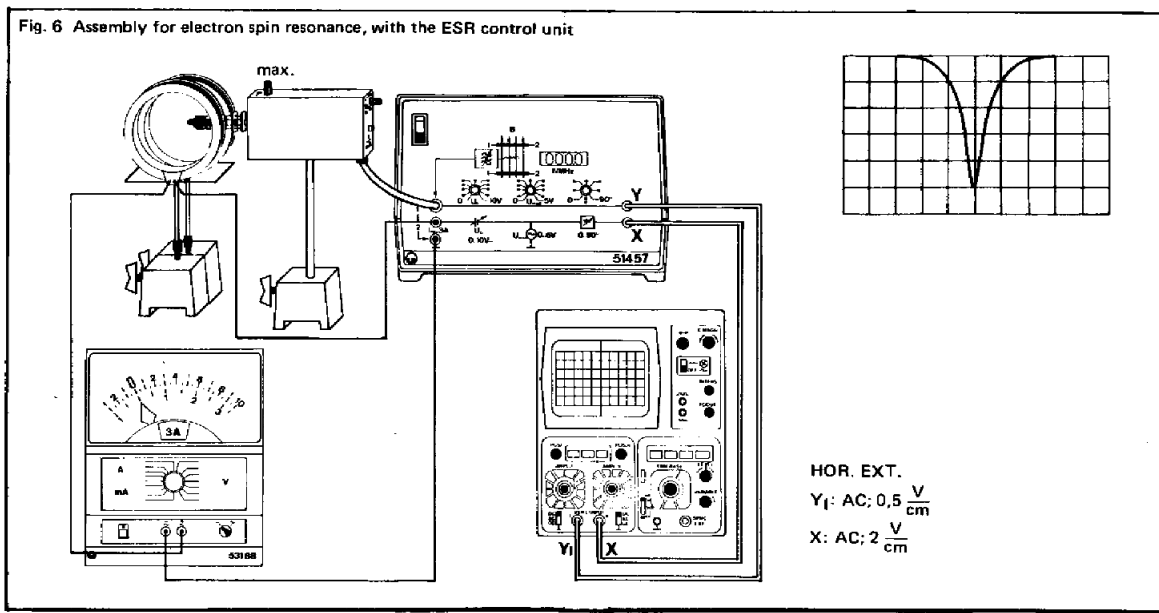
Equipment:

1 ESR basic unit (probe holder)	Cat. No.	514 55
1 Pair of Helmholtz coils		555 06
3 Saddle bases		300 11
1 Two-channel oscilloscope, e. g.		575 20

Power supply options:

a) 1 ESR control unit	514 57
and	
1 Ammeter, range: 3 A, e. g.	
E measuring instrument D	531 88

or	
b) 1 ESR adapter	514 56
1 Measuring resistor, 1Ω	536 10
1 D. C. power supply unit, regulated	522 30
1 Low-voltage transformer SE	522 20
or	
Low-voltage transformer S	591 09
1 Digital counter	575 50
or	
Counter P	575 45
and stop-clock, e. g.	313 05



Observing the normal Zeeman effect in transverse and longitudinal configuration

Objects of the experiment

- Observing the line triplet for the normal transverse Zeeman effect.
- Determining the polarization state of the triplet components.
- Observing the line doublet for the normal longitudinal Zeeman effect.
- Determining the polarization state of the doublet components

Principles

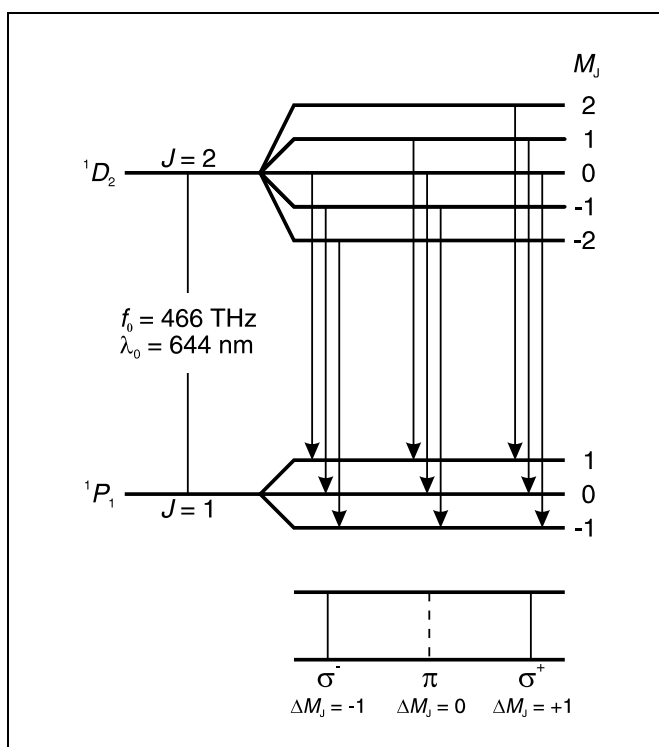
Normal Zeeman effect

The *Zeeman* effect is the name for the splitting of atomic energy levels or spectral lines due to the action of an external magnetic field. The effect was first predicted by *H. A. Lorentz* in 1895 as part of his classic theory of the electron, and experimentally confirmed some years later by *P. Zeeman*. Zeeman observed a line triplet instead of a single spectral line at right angles to a magnetic field, and a line doublet parallel to the magnetic field. Later, more complex splittings of spectral lines were

observed, which became known as the anomalous Zeeman effect. To explain this phenomenon, *Goudsmit* and *Uhlenbeck* first introduced the hypothesis of electron spin in 1925. Ultimately, it became apparent that the anomalous Zeeman effect was actually the rule and the "normal" Zeeman effect the exception.

The normal Zeeman effect only occurs at the transitions between atomic states with the total spin $S = 0$. The total angular momentum $J = L + S$ of a state is then a pure orbital angular momentum ($J = L$). For the corresponding magnetic moment, we can simply say that:

Fig. 1: Level splitting and transitions of the normal Zeeman effect in cadmium



$$\mu = \frac{\mu_B}{\hbar} J \quad (I)$$

where

$$\mu_B = \frac{\hbar e}{2m_e} \quad (II)$$

$\mu_B = \text{Bohr's magneton}$, $m_e = \text{mass of electron}$, $e = \text{elementary charge}$, $\hbar = \text{Planck's constant}$

In an external magnetic field B , the magnetic moment has the energy

$$E = -\mu \cdot B \quad (III)$$

The angular-momentum component in the direction of the magnetic field can have the values

$$J_z = M_J \cdot \hbar \quad \text{mit } M_J = J, J-1, \dots, -J \quad (IV)$$

Therefore, the term with the angular momentum J is split into $2J + 1$ equidistant Zeeman components which differ by the value of M_J . The energy interval of the adjacent components M_J, M_{J+1} is

$$\Delta E = \mu_B \cdot B \quad (V)$$

We can observe the normal Zeeman effect e.g. in the red spectral line of cadmium ($\lambda_0 = 643.8 \text{ nm}$, $f_0 = 465.7 \text{ THz}$). It corresponds to the transition ${}^1D_2 (J = 2, S = 0) \rightarrow {}^1P_1 (J = 1, S = 0)$ of an electron of the fifth shell (see Fig. 1).

Apparatus

1 Cadmium lamp for Zeeman effect	451 12
1 Optical system for observing the Zeeman effect	471 20
1 Lummer-Gehrcke plate	471 21
1 Electromagnet for Zeeman effect	514 50
1 Universal choke for 451 12	451 30
1 High current power supply	521 55
Connecting leads with conductor cross-section 2.5 mm ²	

In the magnetic field, the ¹D₂ level splits into five Zeeman components, and the level ¹P₁ splits into three Zeeman components having the spacing calculated using equation (V).

Optical transitions between these levels are only possible in the form of electrical dipole radiation. The following selection rules apply for the magnetic quantum numbers *M_J* of the states involved:

$$\Delta M_J \begin{cases} = \pm 1 & \text{für } \sigma\text{-Components} \\ = 0 & \text{für } \pi\text{-Components} \end{cases} \quad (VI)$$

Thus, we observe a total of three spectral lines (see Fig. 1); the π component is not shifted and the two σ components are shifted by

$$\Delta f = \pm \frac{\Delta E}{h} \quad (VII)$$

with respect to the original frequency. In this equation, ΔE is the equidistant energy split calculated in (V).

Safety notes

The electrical leads on the cadmium lamp and the resistors of the starting electrodes are open and easily accessible:

- Do not touch any current-carrying (live!) parts.
- The Lummer-Gehrcke plate has been manufactured with great precision with regard to the parallelism and flatness of its surfaces.
- Do not mechanically stress the Lummer-Gehrcke plate by bending or in any other manner.
- Pick up the Lummer-Gehrcke plate only by the edges.
- When mounting the Lummer-Gehrcke plate, make sure that the plate is supported evenly in its holder over its entire length.
- Before transporting the apparatus, remove the Lummer-Gehrcke plate from its holder and store it in a safe place.

Loose ferromagnetic objects can be strongly attracted by the electromagnet and can damage the quartz bulb of the cadmium lamp.

- Check to make sure that the pole pieces are screwed tight before switching on the magnet current.
- When the magnet current is switched on, do not handle ferromagnetic objects in the vicinity of the cadmium lamp.

Deposits of skin secretions can destroy the quartz bulb of the cadmium lamp when it becomes hot.

- Never handle the quartz bulb of the cadmium lamp with your bare hands.

Angular distribution and polarization

Depending on the angular momentum component ΔM_J in the direction of the magnetic field, the emitted photons demonstrate different angular distributions. Fig. 2 shows the angular distributions in the form of two-dimensional polar diagrams. They can be observed experimentally, as the magnetic field is characterized by a common axis for all cadmium atoms.

In classical terms, the case $\Delta M_J = 0$ corresponds to an infinitesimal dipole oscillating parallel to the magnetic field. No quanta are emitted in the direction of the magnetic field, i.e. the π component cannot be observed parallel to the magnetic field. The light emitted perpendicular to the magnetic field is linearly polarized, whereby the *E*-vector oscillates in the direction of the dipole and parallel to the magnetic field (see Fig. 3)

Conversely, in the case $\Delta M_J = \pm 1$, most of the quanta travel in the direction of the magnetic field. In classical terms, this case corresponds to two parallel dipoles oscillating with a phase difference of 90°. The superposition of the two dipoles produces a circulating current. Thus, in the direction of the magnetic field, circularly polarized light is emitted; in the positive direction, it is clockwise-circular for $\Delta M_J = +1$ and counterclockwise-circular for $\Delta M_J = -1$ (see Fig. 3).

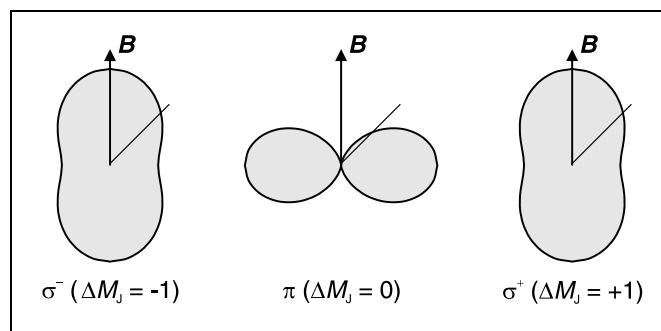


Fig. 2: Angular distributions of the electrical dipole radiation (ΔM_J : angular-momentum components of the emitted photons in the direction of the magnetic field)

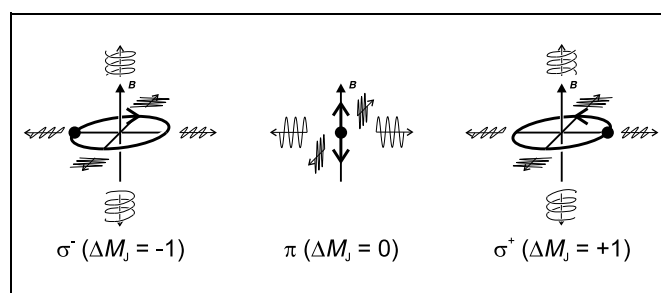
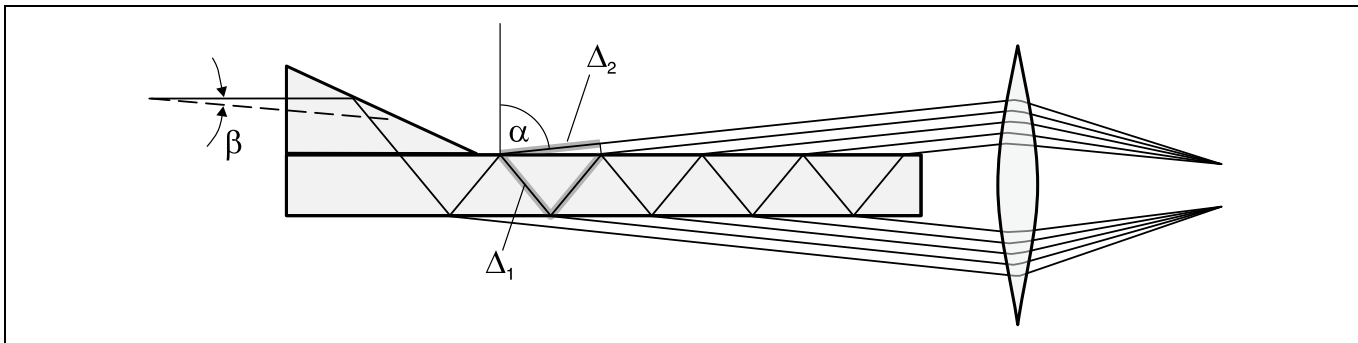


Fig. 3: Schematic representation of the polarization of the Zeeman components

Spectroscopy of the Zeeman components

The Zeeman effect enables spectroscopic separation of the differently polarized components. To demonstrate the shift, however, we require a spectral apparatus with extremely high resolution, as the two σ components of the red cadmium line are shifted e.g. at a magnetic flux density $B = 1$ T by only $\Delta f = 14$ GHz, respectively $\Delta \lambda = 0.02$ nm.

A Lummer-Gehrcke plate is used for this experiment. This component has been manufactured with great precision with respect to the parallelism and flatness of its surfaces. The light, which is divergent in the vertical direction, passes through a



horizontal slit via an attached prism into a long, plane-parallel glass plate (see Fig. 4). Inside this plate, the light is reflected back and forth repeatedly, with some part of it emerging each time. When observed at an angle of $\alpha \approx 90^\circ$, the reflection within the plate occurs almost completely within the limit angle of total reflection. The result is a high reflection coefficient, i. e. many of the rays can interfere with each other when the plate is long enough. The emerging waves are observed from behind the plate using a telescope focused on infinity. For a given wavelength λ , two mirror-image identical systems of horizontal lines can be observed above and below the plate. Each interference line can be assigned to one emerging angle α of the component rays from the Lummer-Gehrcke plate and an angle of incidence β at the prism.

The rays emerging at an angle of α_k interfere constructively with each other when two adjacent rays fulfill the condition for "curves of equal inclination" (see Fig. 4):

$$\Delta = 2d \cdot \sqrt{n^2 - \sin^2 \alpha_k} = k \cdot \lambda \quad \text{mit } k = 1, 2, 3, \dots \quad \text{(VIII)}$$

(Δ = optical path difference, d = thickness of plate, n = refractive index of the glass, k = order of interference)

A change in the wavelength by $\delta\lambda$ appears as a shift in the interference lines by the angle $\delta\alpha$. If a spectral line contains multiple components with a distance $\delta\lambda$, each interference line is split into a corresponding number of components with the spacing $\delta\alpha$. It thus becomes possible to recognize a spectral-line doublet in a doublet structure and a spectral-line triplet in a triplet structure in the interference lines.

Fig. 4: Lummer-Gehrcke plate as an interference spectrometer (the beam path for the angle of incidence $\beta = 0^\circ$ is drawn as a series of unbroken lines). The optical path difference between two adjacent emerging rays is $\Delta = n \Delta_1 - \Delta_2$

Setup

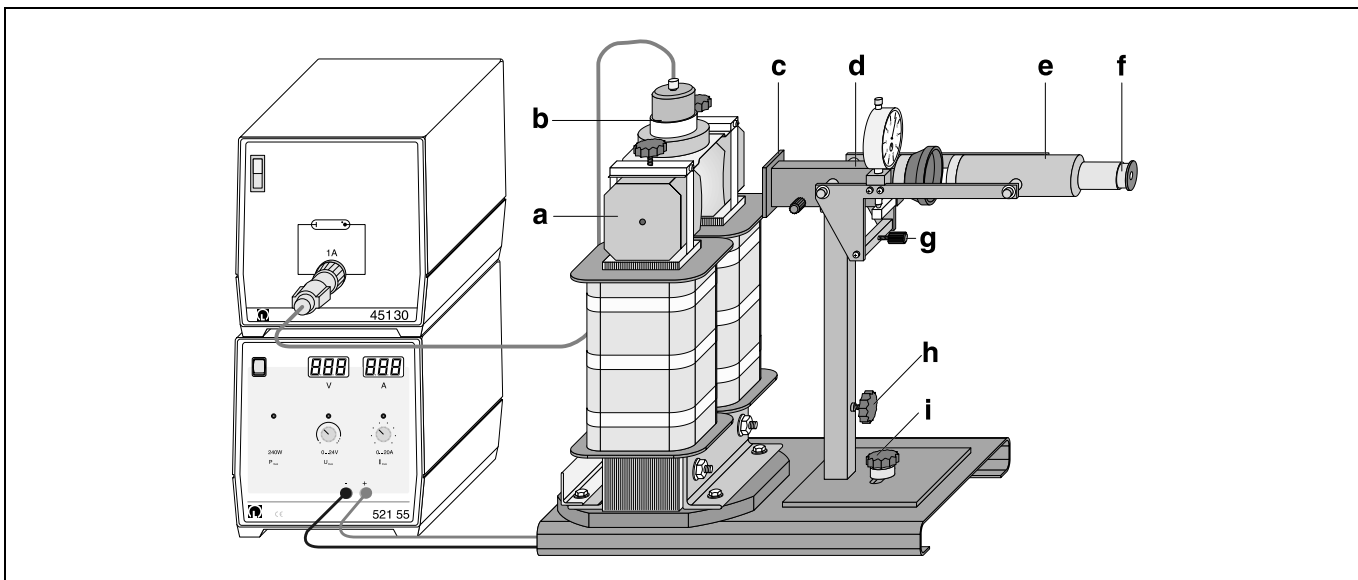
First-time setup:

Fig. 5 shows the complete setup in the transverse configuration.

- Mount the electromagnet for the Zeeman effect on the base plate of the optical system. When tightening the hex screw (size 27) beneath the base plate, make sure that you can still turn the electromagnet on the base plate when you really try.
- Mount the pole pieces of the electromagnet (a) at a spacing of 10 mm.

Fig. 5: Experiment setup for the Zeeman effect in the transverse configuration

- (a) pole pieces
- (b) cadmium lamp with holder
- (c) plug-in holder for red filter
- (d) cover
- (e) telescope
- (f) ocular
- (g) height adjustment for telescope
- (h) arresting screw for column
- (i) arresting screw for column base



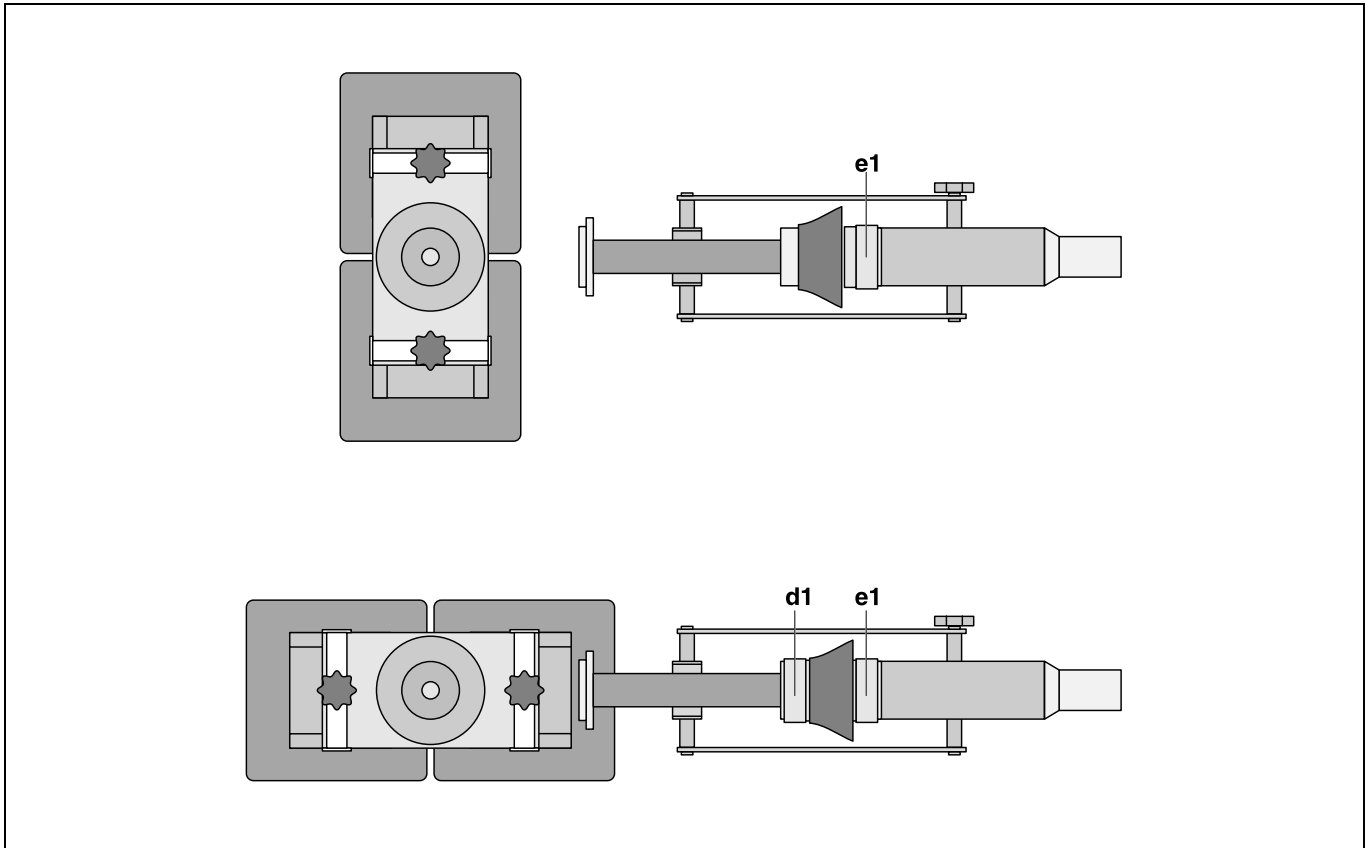


Fig. 6: Top view of setup in the transverse configuration (top) and the longitudinal configuration (bottom)
(d1) holder with quarter-wavelength foil
(e1) holder with polarization filter

- Screw in the holder for the cadmium lamp **(b)** with the opening facing the electrical connections of the electromagnet.
- Secure the pole pieces and the holder of the cadmium lamp using arresting screws and retaining straps.
- Turn the fused point on spectral lamp toward the side with the electrical connections so that the electrical leads do not obstruct the beam path.
- Screw in the column of the optical system so that the column base is as far as possible from the electromagnet.
- Remove the cover **(d)** and carefully place the Lummer-Gehrcke plate on the velour-lined base. Make sure the plate is aligned horizontally and is evenly supported over its entire length. Slide the prism as close as possible to the illuminated side.
- Turn the cover together with the cylindrical attachment toward the telescope **(e)** and rest it carefully against the telescope without disturbing the Lummer-Gehrcke plate. Then tighten the arresting screws.
- Slide the red filter with collecting lens into the plug-in holder **(c)**.
- To prevent interference from ambient light, slide the flexible light screen onto the cylindrical attachment of the cover, and slide the foam rubber ring over the telescope.

Switching from transverse to longitudinal observation:

- Loosen arresting screw **(i)** on the column base and move the column of the optical system as far as possible from the electromagnet.
- Remove the red filter with collecting lens from the plug-in holder.
- Swivel the electromagnet with cadmium lamp into the desired position (see Fig. 6) and align it so that the edge of the base plate of the electromagnet is parallel to the rear edge of the base plate of the optical system.
- Slide the red filter with collecting lens into the plug-in holder.
- Bring the column of the optical system and the electromagnet as close together as possible.

Electrical connection:

- Connect the cadmium lamp to the universal choke. After switching on, wait five minutes until a sufficiently strong light intensity is obtained.
- Connect the coils of the electromagnet in parallel (connect socket 1 to socket 3 and socket 2 to socket 4) and connect this assembly to the high current power supply.

Adjusting the optical system for observing the Zeeman effect:

Adjust the height of the optical system in the longitudinal configuration, and do not change it when swiveling to the transverse configuration.

The optical system is optimally adjusted when the red horizontal interference patterns above and below the Lummer-Gehrcke plate show maximum brightness and contrast.

- Remove the ocular of the telescope **(f)**; to optimize brightness and contrast, alternately

- a) shift and swivel the entire optical system left and right on the base plate (fix with arresting screw **(i)**);
- b) set the height of the complete optical system in relation to the cadmium lamp and the hole in the pole pieces (fix with arresting screw **(h)**).
- To improve brightness and contrast of the lines, you may need to raise the entire cover or the red filter with collecting lens in the plug-in holder.

Fine adjustment:

When the telescope is aimed precisely at the rear of the Lummer-Gehrcke plate, the interference lines appear symmetrically distributed between the top and the bottom. The bright inner lines are best suited for observation.

- Hold the ocular up to the light and focus the cross-hairs.
- Replace the ocular in the tube of the telescope and focus the interference lines by shifting the ocular.

Carrying out the experiment

Note: the polarization filter is somewhat darker than the quarter-wavelength foil.

a) Observing in the transverse configuration:

- First observe the pattern of interference lines without the magnetic field ($I = 0 \text{ A}$) and align the telescope so that the cross-hairs of the ocular rest on an interference line.
- Slowly increase the magnet current to about $I = 10 \text{ A}$, until the split lines are clearly separated from each other.

To distinguish between the π and the σ -components:

- Slide the foam rubber ring over the holder of the polarization filter.
- Place the holder with polarization filter **(e1)** over the telescope (see Fig. 6) and turn it around the axis of observation until the middle component of the line triplet disappears.
- Turn the holder with polarization filter 90° further until the outer components of the line triplet disappear.

b) Observing in the longitudinal configuration:

- First observe the pattern of interference lines without the magnetic field ($I = 0 \text{ A}$) and align the telescope so that the cross-hairs of the ocular rest on an interference line.
- Slowly increase the magnet current to about $I = 10 \text{ A}$, until the split lines are clearly separated from each other.

To distinguish between the σ^+ and the σ^- components:

- Slide the flexible light screen onto the holder for the quarter-wavelength foil.
- Mount the holder with quarter-wavelength foil **(d1)** on the cylindrical attachment of the cover, and the holder with polarization filter **(e1)** on the telescope (see Fig. 6).
- Turn the holder with polarization filter around the axis of observation until one of the two doublet components disappears, and turn it 90° further until the other component disappears.

Measuring example and evaluation

a) Observing in the transverse configuration:

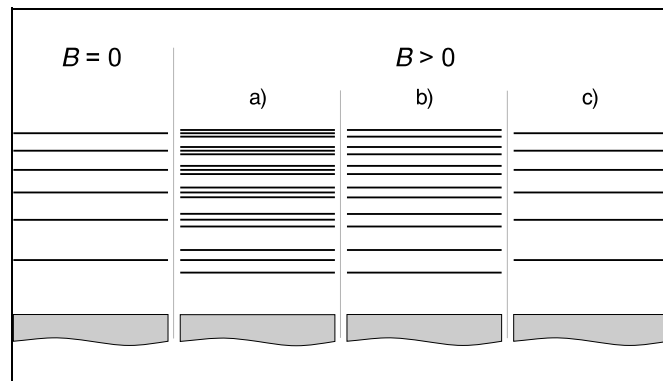


Fig. 7: Interference pattern for the Zeeman effect in the transverse configuration

- a) observed without polarization filter
- b) observed with polarization direction of the filter perpendicular to the magnetic field
- c) observed with polarization direction of the filter parallel to the magnetic field

b) Observing in the longitudinal configuration:

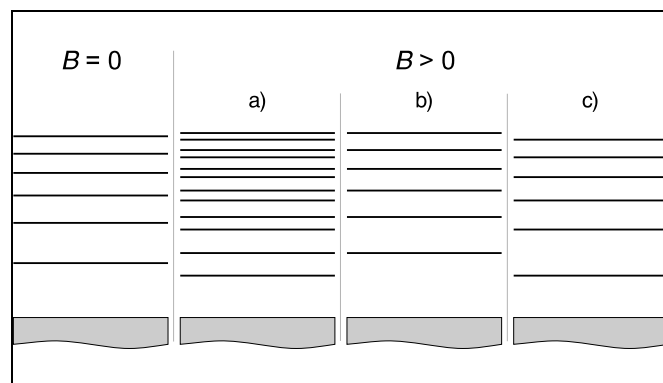


Fig. 8: Interference pattern for the Zeeman effect in the longitudinal configuration

- a) observed without quarter-wavelength foil and polarization filter
- b), c) observed with quarter-wavelength foil and polarization filter to demonstrate counterclockwise and clockwise-circular polarization

Additional information

The total intensity of all Zeeman components is the same in all spatial directions. In transverse observation, the intensity of the π component is equal to the total intensity of the two σ components.

Duane-Hunt relation and determination of Planck's constant

Objects of the experiment

- To determine the limit wavelength λ_{\min} of the bremsstrahlung continuum as a function of the high voltage U of the x-ray tube.
- To confirm the Duane-Hunt relation.
- To determine Planck's constant.

Principles

The bremsstrahlung continuum in the emission spectrum of an x-ray tube is characterized by the limit wavelength λ_{\min} (see Fig. 1), which becomes smaller as the tube high voltage increases (see experiment P6.3.3.2). In 1915, the American physicists *William Duane* and *Franklin L. Hunt* discovered an inverse proportionality between the limit wavelength and the tube high voltage:

$$\lambda_{\min} \sim \frac{1}{U} \quad (I).$$

This Duane-Hunt relationship can be sufficiently explained by examining some basic quantum mechanical considerations: As the wavelength λ and the frequency ν for any electromagnetic radiation are related in the manner

$$\lambda = \frac{c}{\nu} \quad (II)$$

$c = 2.9979 \cdot 10^8 \text{ m s}^{-1}$: velocity of light

the minimum wavelength λ_{\min} corresponds to a maximum frequency ν_{\max} respectively a maximum energy

$$E_{\max} = h \cdot \nu_{\max} \quad (III)$$

h : Planck's constant

of the emitted x-ray quanta. However, an x-ray quantum attains maximum energy at precisely the moment in which it acquires the total kinetic energy

$$E = e \cdot U \quad (IV)$$

$e = 1.6022 \cdot 10^{-19} \text{ A s}$: elementary charge

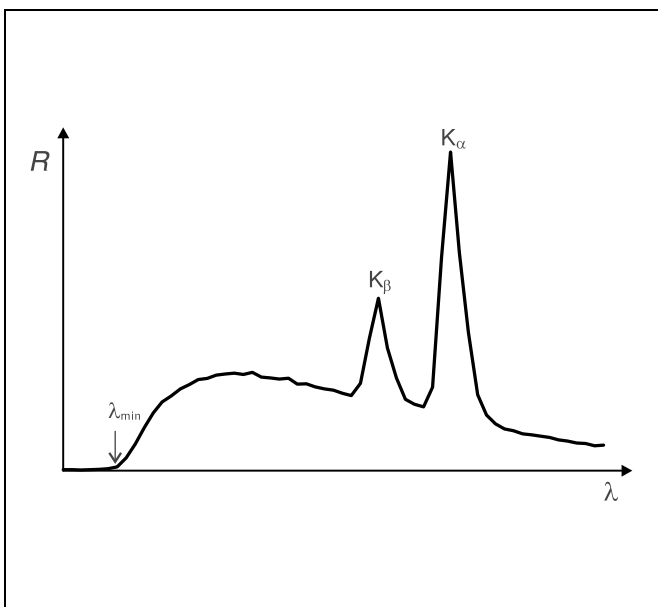
of an electrode decelerated in the anode. It thus follows that

$$\nu_{\max} = \frac{e}{h} \cdot U \quad (V)$$

respectively

$$\lambda_{\min} = \frac{h \cdot c}{e} \cdot \frac{1}{U} \quad (VI)$$

Fig. 1 Emission spectrum of an x-ray tube with the limit wavelength λ_{\min} of the bremsstrahlung continuum and the characteristic K_{α} and K_{β} lines.



Apparatus

- 1 X-ray apparatus 554 811
 - 1 End-window counter
for α , β , γ and x-ray radiation 559 01
- additionally required:*
- 1 PC with Windows 95/98/NT

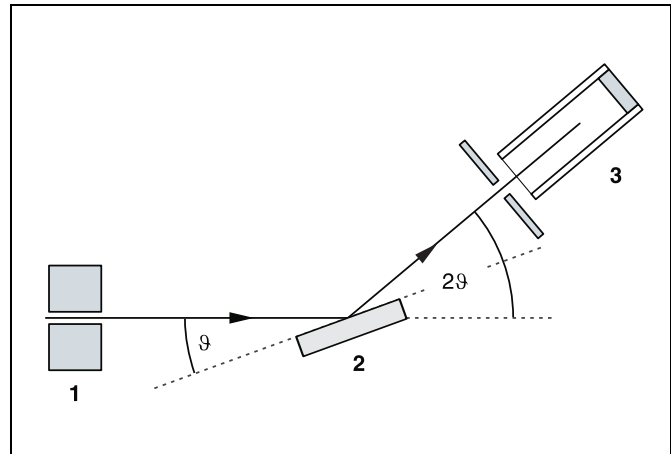


Fig. 2 Schematic diagram of diffraction of x-rays at a monocrystal and 2ϑ coupling between counter-tube angle and scattering angle (glancing angle)
1 collimator, 2 monocrystal, 3 counter tube

Equation (VI) corresponds to Duane and Hunt's law. The proportionality factor

$$A = \frac{h \cdot c}{e} \quad \text{(VII)}$$

can be used to determine Planck's constant h when the quantities c and e are known.

A goniometer with NaCl crystal and a Geiger-Müller counter tube in the Bragg configuration together comprise the spectrometer in this experiment. The crystal and counter tube are pivoted with respect to the incident x-ray beam in 2ϑ coupling (cf. Fig. 2).

In accordance with Bragg's law of reflection, the scattering angle ϑ in the first order of diffraction corresponds to the wavelength

$$\lambda = 2 \cdot d \cdot \sin \vartheta \quad \text{(VIII)}$$

$d = 282.01$ pm: lattice plane spacing of NaCl

Safety notes

The x-ray apparatus fulfills all regulations governing an x-ray apparatus and fully protected device for instructional use and is type approved for school use in Germany (NW 807/97 Rö).

The built-in protection and screening measures reduce the local dose rate outside of the x-ray apparatus to less than $1 \mu\text{Sv/h}$, a value which is on the order of magnitude of the natural background radiation.

- Before putting the x-ray apparatus into operation inspect it for damage and to make sure that the high voltage is shut off when the sliding doors are opened (see Instruction Sheet for x-ray apparatus).
- Keep the x-ray apparatus secure from access by unauthorized persons.

Do not allow the anode of the x-ray tube Mo to overheat.

- When switching on the x-ray apparatus, check to make sure that the ventilator in the tube chamber is turning.

The goniometer is positioned solely by electric stepper motors.

- Do not block the target arm and sensor arm of the goniometer and do not use force to move them.

Setup

Setup in Bragg configuration:

Fig. 3 shows some important details of the experiment setup. To set up the experiment, proceed as follows (see also the Instruction Sheet for the x-ray apparatus):

- Mount the collimator in the collimator mount (a) (note the guide groove).
- Attach the goniometer to guide rods (d) so that the distance s_1 between the slit diaphragm of the collimator and the target arm is approx. 5 cm. Connect ribbon cable (c) for controlling the goniometer.
- Remove the protective cap of the end-window counter, place the end-window counter in sensor seat (e) and connect the counter tube cable to the socket marked GM TUBE.
- By moving the sensor holder (b), set the distance s_2 between the target arm and the slit diaphragm of the sensor receptor to approx. 6 cm.
- Mount the target holder (f) with target stage.
- Loosen knurled screw (g), place the NaCl crystal flat on the target stage, carefully raise the target stage with crystal all

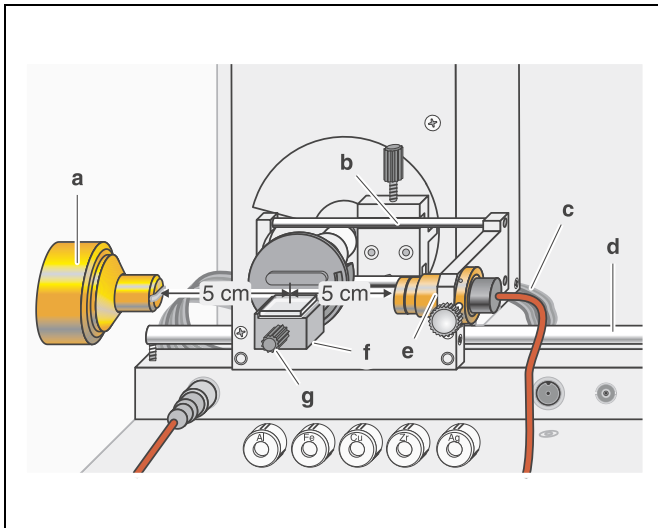


Fig. 3 Experiment setup in Bragg configuration

the way to the stop and gently tighten the knurled screw (prevent skewing of the crystal by applying a slight pressure).

- If necessary, adjust the mechanical zero position of the goniometer (see Instruction Sheet for x-ray apparatus).

Notes:

NaCl crystals are hygroscopic and extremely fragile. Store the crystals in a dry place; avoid mechanical stresses on the crystal; handle the crystal by the short faces only.

If the counting rate is too low, you can reduce the distance s_2 between the target and the sensor somewhat. However, the distance should not be too small, as otherwise the angular resolution of the goniometer is no longer sufficient.

Preparing the PC-based measurement:

- Connect the RS-232 output and the serial interface on your PC (usually COM1 or COM2) using the 9-pin V.24 cable (supplied with x-ray apparatus).
- If necessary, install the software "X-ray Apparatus" under Windows 95/98/NT (see Instruction Sheet for x-ray apparatus) and select the desired language.

Carrying out the experiment

- Start the software "X-ray Apparatus", check to make sure that the apparatus is connected correctly, and clear any existing measurement data using the button or the F4 key.
- Set the tube high voltage $U = 22$ kV, the emission current $I = 1.00$ mA, the measuring time per angular step $\Delta t = 30$ s and the angular step width $\Delta\beta = 0.1^\circ$.
- Press the COUPLED key to activate 2θ coupling of target and sensor and set the lower limit of the target angle to 5.2° and the upper limit to 6.2° .
- Start measurement and data transfer to the PC by pressing the SCAN key.

Tab. 1: Recommended parameters for recording the measurement series

$\frac{U}{\text{kV}}$	$\frac{I}{\text{mA}}$	$\frac{\Delta t}{\text{s}}$	$\frac{\beta_{\min}}{\text{grd}}$	$\frac{\beta_{\max}}{\text{grd}}$	$\frac{\Delta\beta}{\text{grd}}$
22	1.00	30	5.2	6.2	0.1
24	1.00	30	5.0	6.2	0.1
26	1.00	20	4.5	6.2	0.1
28	1.00	20	3.8	6.0	0.1
30	1.00	10	3.2	6.0	0.1
32	1.00	10	2.5	6.0	0.1
34	1.00	10	2.5	6.0	0.1
35	1.00	10	2.5	6.0	0.1

- Additionally record measurement series with the tube high voltages $U = 24$ kV, 26 kV, 28 kV, 30 kV, 32 kV, 34 kV and 35 kV; to save measuring time, use the parameters from table 1 for each series.
- To show the wavelength-dependency, open the "Settings" dialog with the button or F5 and enter the lattice plane spacing for NaCl.
- When you have finished measuring, save the measurement series under an appropriate name by pressing the button or the F2 key.

Measuring example and evaluation

Determining the limit wavelength λ_{\min} as a function of the tube high voltage U :

For each recorded diffraction spectrum (see Fig. 4):

- In the diagram, click the right mouse button to access the evaluation functions of the software "X-ray Apparatus" and select the command "Best-fit Straight Line".
- Mark the curve range to which you want to fit a straight line to determine the limit wavelength λ_{\min} using the left mouse button.
- Save the evaluations under a suitable name using the button or by pressing F2.

Confirming the Duane-Hunt relation and determining Planck's constant

- For further evaluation of the limit wavelengths λ_{\min} determined in this experiment, click on the register "Planck".
- Position the pointer over the diagram, click the right mouse button, fit a straight line through the origin to the curve $\lambda_{\min} = f(1/U)$ and read the slope A from the bottom left corner of the evaluation window (see Fig. 5).

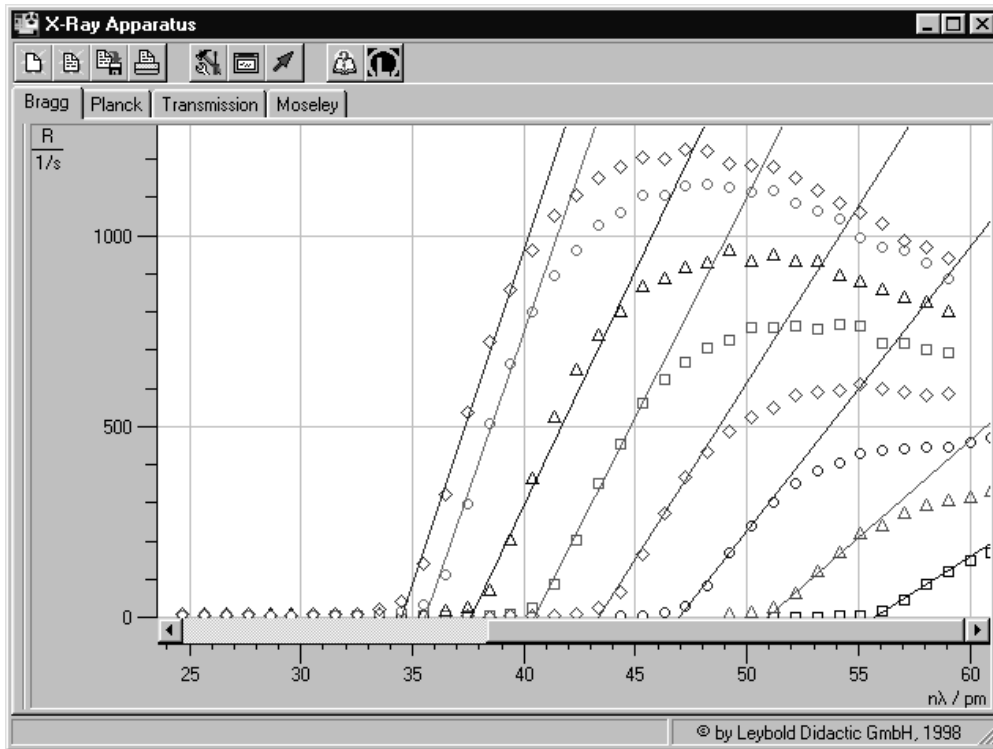


Fig. 4 Sections from the diffraction spectra of x-radiation for the tube high voltages $U = 22, 24, 26, 28, 30, 32, 34$ and 35 kV (from right to left) with best-fit straight line for determining the limit

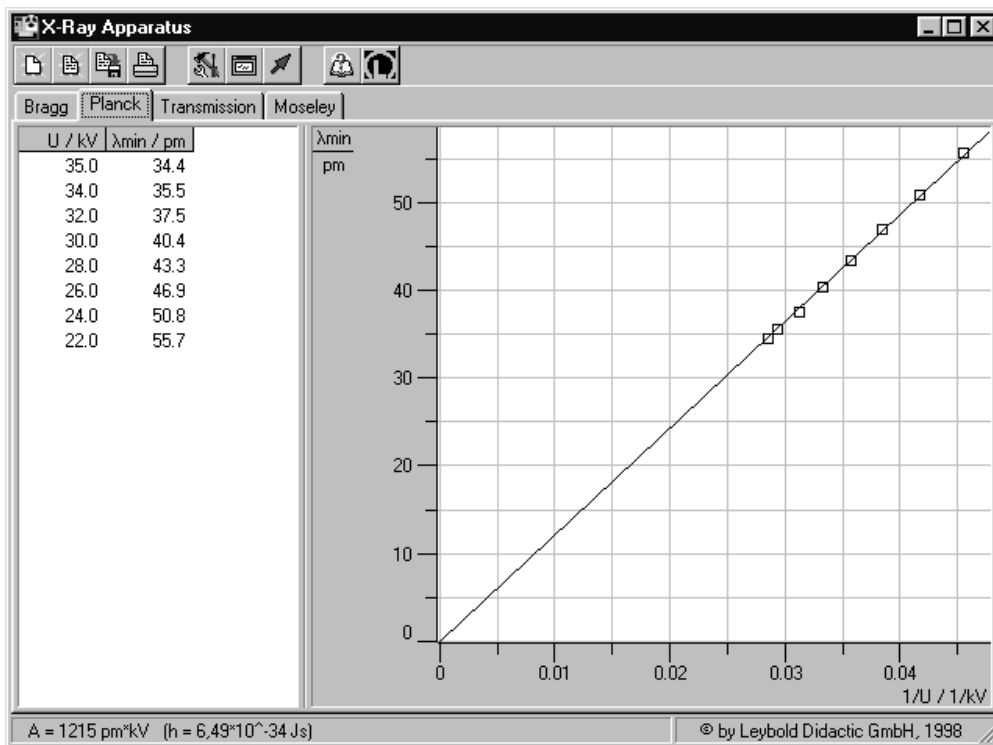


Fig. 5 Evaluation of the data $\lambda_{\min} = f(1/U)$ for confirming the Duane-Hunt relation and determining Planck's constant

The best-fit straight line gives us

$$A = 1215 \text{ pm kV}$$

When we insert this value in equation (VII), we can calculate Planck's constant as:

$$h = 6.49 \cdot 10^{-34} \text{ J s}$$

Literature value:

$$h = 6.626 \cdot 10^{-34} \text{ J s}$$

Duane-Hunt's displacement law; h - to be determined

- Recording the braking spectrum $N = f(\Theta)$ of the X-rays of a molybdenum anode for various high voltages U_A according to Bragg's rotating crystal method with a counter tube goniometer.
 N : Counting rate
 Θ : Angle between the primary beam and the grating plate of a monocrystal; Bragg angle.
- Determination of the angle Θ_{\min} from the graph of the measured curves $N(U_A) = f(\Theta)$ (Θ_{\min} : angle at which the braking spectrums first occur).
- Determination of the corresponding critical wavelength λ_{\min} from Bragg's reflection condition
 $\lambda_{\min} = 2 d \sin \Theta_{\min}$
 d : Lattice plane distance.
- Exploring the dependency $U_A = f(\lambda_{\min})$
- Determining Planck's action quantum

$$h = \frac{e}{c} U_A \cdot \lambda_{\min}$$
 e = Elementary charge
 c = Speed of light

With decreasingly high voltages, the braking spectrum of the X-rays displaces itself towards larger wavelengths. Duane and Hunt found the proportionality between the voltage U_A and the frequency of the short wave boundary ν_g in 1915:

$$U_A \sim \nu_g \text{ bzw. } \lambda_{\min} \sim \frac{1}{U_A} \quad (1)$$

This proportionality can be explained only by the quantum theory with Einstein's equation

$$h \cdot \nu = e \cdot U_A \quad (2)$$

The energy $h \cdot \nu$ of the emitted X-ray quantum can maximally be equal to the kinetic energy of the fastest electrons in the X-ray tube, which is

$$W_{\max} = e \cdot U_A \quad (3)$$

From $h \cdot \nu = e \cdot U_A$, it follows that:

$$\lambda_{\min} = \frac{h \cdot c}{e} \cdot \frac{1}{U_A} \quad (4)$$

When $h = 6.6256 \cdot 10^{-34} \text{ Js}$
 $c = 2.9979 \cdot 10^8 \text{ m s}^{-1}$
 and $e = 1.6021 \cdot 10^{-19} \text{ C}$

we calculate the wavelength λ_{\min} of the shortwave boundary of the braking spectrum as:

$$\lambda_{\min} = 1,2398 \cdot 10^{-6} \text{ V} \cdot \text{m} \cdot \frac{1}{U_A} \quad (5)$$

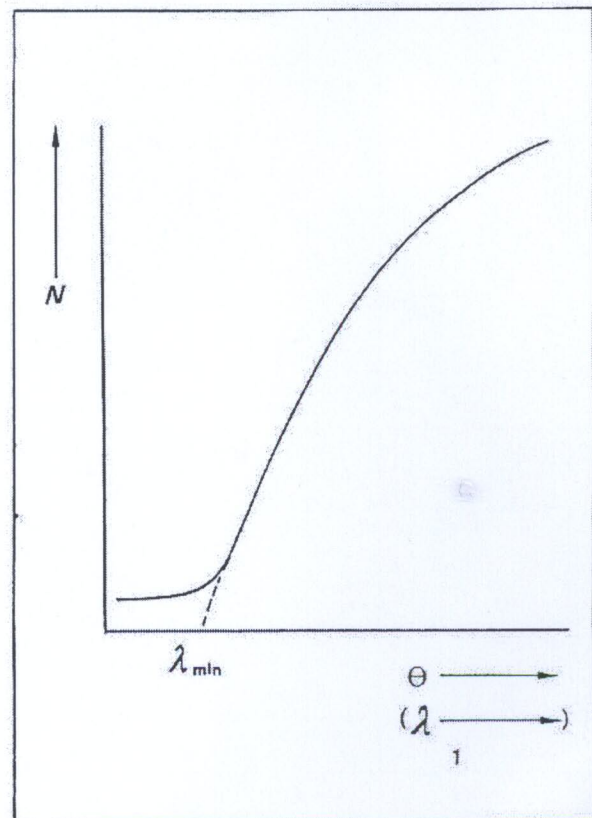


Fig. 1: Graphic determination of the shortwave boundary Θ_{\min} (or λ_{\min}) by extrapolating the measured curve $N = f(\Theta)$.

The Duane-Hunt law is proven by the experimental determination of λ_{\min} . Also Planck's action

quantum can be determined with the same measuring values according to the equation

$$h = \frac{e}{c} \cdot U_A \cdot \lambda_{\min} \quad (6)$$

In the experiment, the critical wavelength λ_{\min} is determined as a function of U_A . X-ray spectra at various high voltages U_A are recorded with Bragg's configuration. The corresponding boundary angle is determined at which radiation starts.

The braking spectrum suddenly stops at θ_{\min} ; but this is concealed during measurement by apparatus influences. Therefore the short wave boundary must be found by extrapolating the edge of the graph spectra as shown in Fig.1. The boundary wavelength λ_{\min} then results from Bragg's reflection condition

$$\lambda_{\min} = 2 d \sin \theta_{\min} \quad (7)$$

Apparatus:

- 1 X-ray apparatus, 42 kV, with counter, angle graduation, aperture slot collimator and holder for samples with table 554 90
- 1 X-ray tube 554 94
- 1 Sodium flouride monocrystal 554 78
- alternatively
- 1 Lithium fluoride monocrystal 554 77
- 1 End-window counter for β , γ and X-rays 559 05
- 1 Cable for counter tube, 1 m length ... 559 07

- 1 Digital counter 575 50
- 1 Ratemeter 575 52
- 1 Interchangeable scale demonstration meter, basic unit, measuring range 30 V \sim 530 50
- Power supply unit, plug-in 9.2 V 530 88
- module, pass scale 30 V/100 V 530 58
- 2 Connecting leads, 50 cm, black 501 28

Setting up:

Pay attention to the information given in the operating instructions of the X-ray apparatus (554 90 ff).

Set up as shown in Fig. 2 and Fig. 3 (take the sequence 3.1 - 3.5 into consideration).

Release the couplings by turning the knurled screws (d) between the hinge pins for the crystal table and the holder for the counter. Set both pointers of the counter goniometer so that the tips of the pointers are exactly on top of the zero and the angle graduation (pay attention to the parallax); couple the two pins by tightening the knurled screws (d).

Important: You will only obtain satisfactory results if the setup is adjusted exactly.

Voltage on the counter: approx. 460 V (control (k))

Adjustments on the digital counter:
 Frequency measurement: measuring time 100 s
 Sensitivity: >1.5 V_{pp}

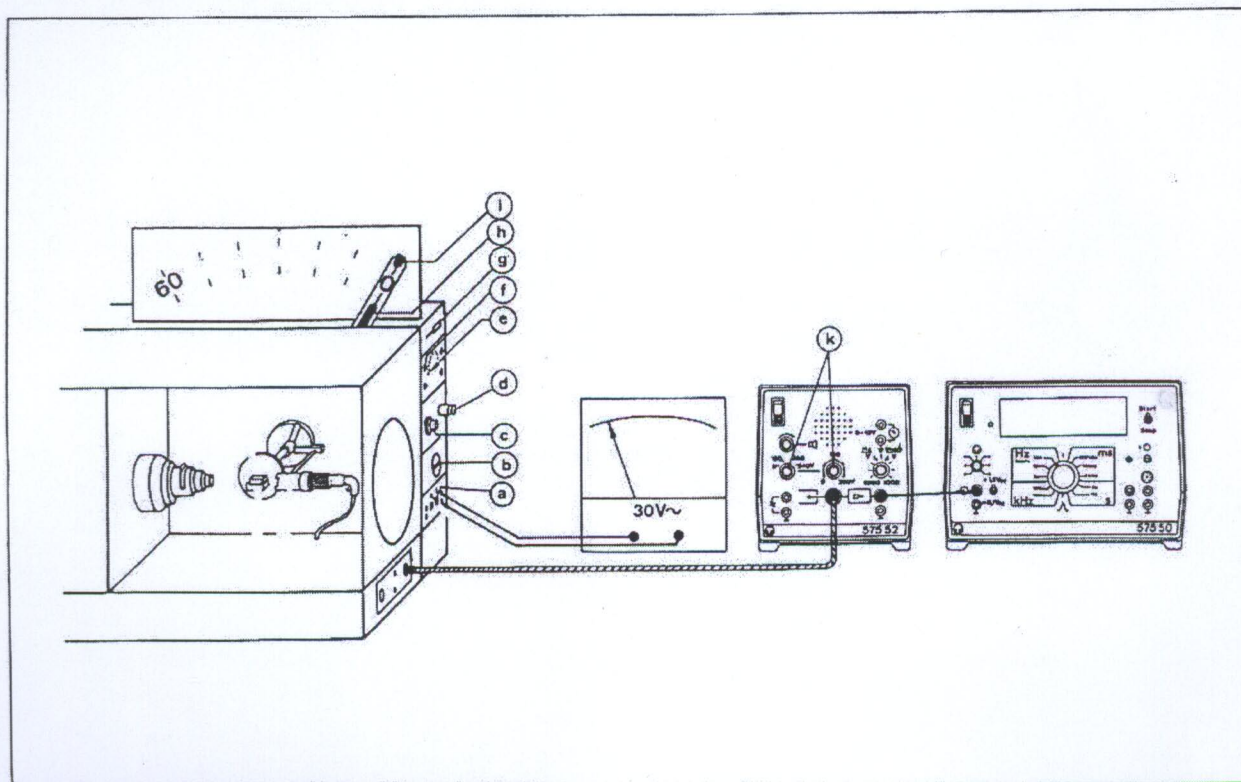


Fig. 2: Setup to record the braking spectrum as a function of high voltage

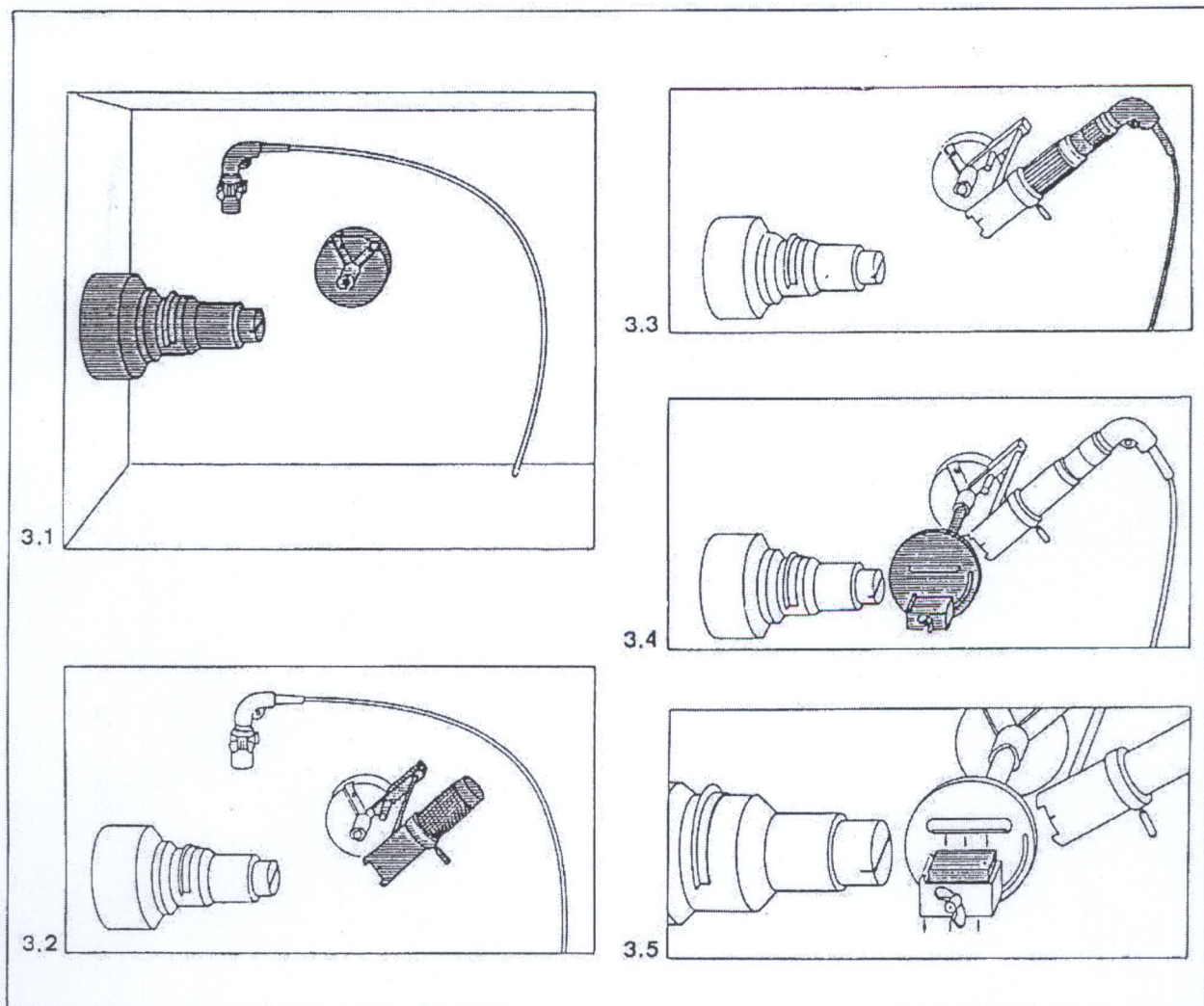


Fig. 3.1.3.5.: Installing the apparatus for Bragg's method, with the counter (559 05) in the experimentation chamber of the X-ray apparatus.

Carrying out the experiment:

1. Turn on the X-ray apparatus with switch (a); choose an operating time of > 1 h on the clock (b); turn on the high voltage U_A at setting 1 of

the multiple step switch (e) on the probe (f). Set the high voltage to position 8 with the multiple step switch (e) and then set the emission current I_{EM} to 1 mA with the lever (g).

2. Read the voltage U , which is proportional to the high voltage U_A , on the demonstration meter

$$(U_A = \sqrt{2} \cdot 10^3 \cdot U).$$

With adjusting knob (c), set the rotating crystal arrangement to the "crystal angle" $\Theta = 2.5^\circ$ (pointer (h)) and the "counter tube angle" $2\Theta = 5^\circ$ (pointer (i)) coupled to it.

Measure the number n of impulses in 100 s.

3. Increase the angle Θ step by step from 0.5° to 6.5° , and measure the number n of impulses in 100 s every time.

4. With the switch (e), lower the high voltage step by step until it reaches position 2. Determine each time, as described in experiment parts 2 and 3, the high voltage U_A and record the braking spectrum $n = f(\Theta)$.

Measuring example:

Crystal: NaCl: 2 d = 563.94 mpm

$I_{EM} = 1 \text{ mA}$

Angle Θ in degrees	2,5	3,0	3,5	4,0	4,5	5,0	5,5	6,0	6,5
Counting rate $U_A = 41.72 \text{ kV}_S$	25,21	15,70	133,2	285,1	348,87	358,96	352,14	325,05	524,95
N in $U_A = 36.77 \text{ kV}_S$	24,37	8,49	15,46	117,02	224,82	264,89	279,62	264,48	402,21
Imp. s^{-1} $U_A = 34.65 \text{ kV}_S$	20,1	5,20	5,56	26,1	111,99	170,32	200,23	200,73	313,15

Table 1

The measured values $N = f(\Theta)$ for the high voltage levels 5, 4, 3, and 2 (Fig. 4), used for further evaluation, are not reproduced here.

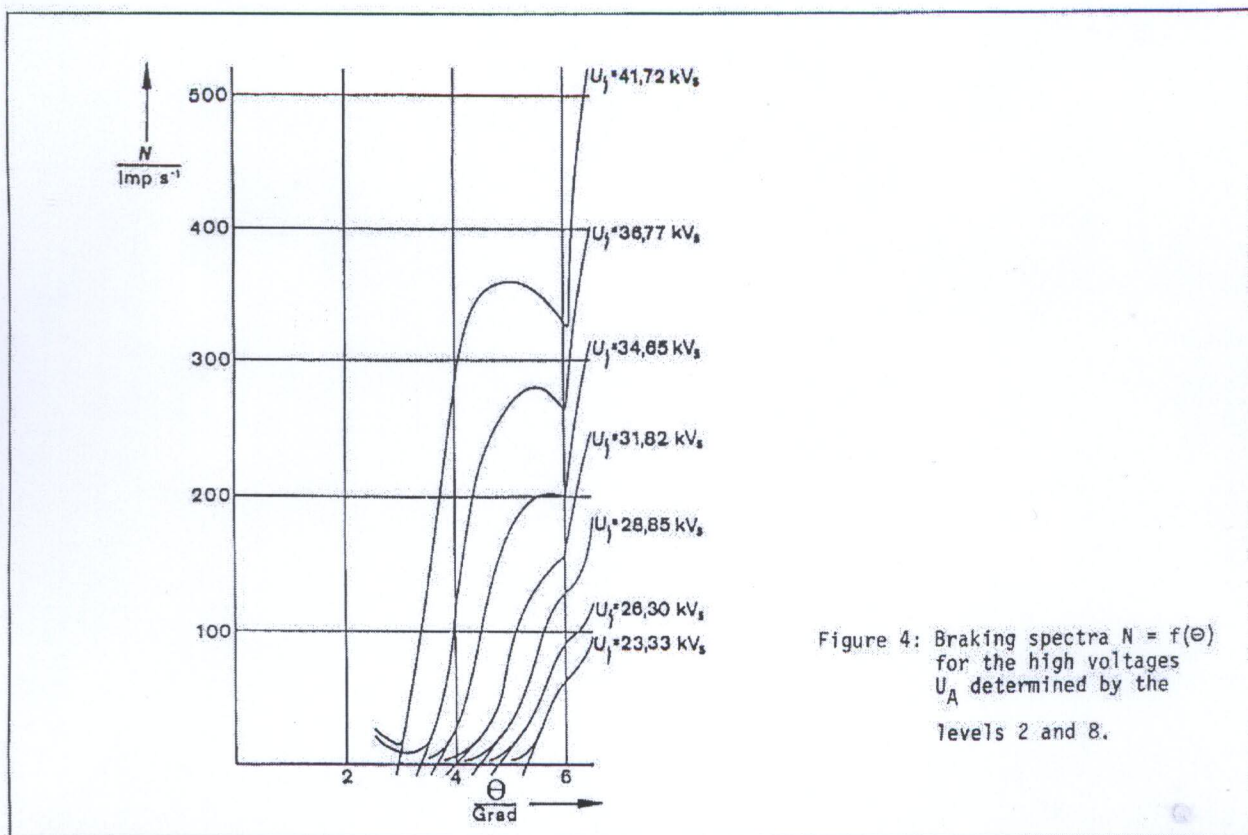


Figure 4: Braking spectra $N = f(\Theta)$ for the high voltages U_A determined by the levels 2 and 8.

Evaluation and results:

Table 2

U_A level	./.	8	7	6	5	4	3	2
U_A	kV_S	41,72	36,77	34,65	31,8	28,85	26,30	23,33
Θ_{\min}	Grad	2,95	3,35	3,60	3,92	4,42	4,77	5,30
λ_{\min} from (7)	pm	29,0	32,9	35,4	38,6	43,5	46,9	52,7
$\frac{1}{U_A}$	kV_S^{-1}	0,0240	0,0272	0,0289	0,0314	0,0347	0,0380	0,0429
h from (6)	10^{-34} Js	6,465	6,464	6,555	6,563	6,700	6,591	6,570

1. The displacement of the braking spectrum and the shortwave boundary with decreasing high voltages can be recognized in Fig. 4.

Graphical extrapolation gives us the values for the critical wavelength and from this λ_{\min} is calculated according to Bragg's equation

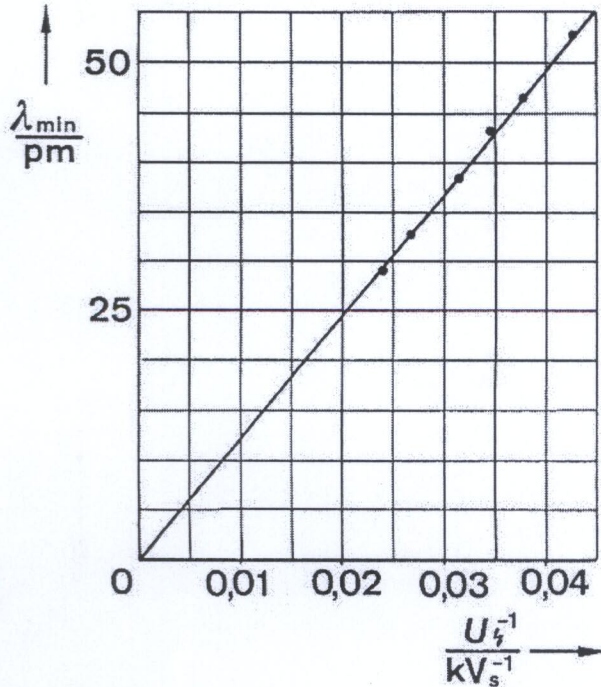
$$\lambda = 2 d \sin \theta \quad (7)$$


Fig. 5: $\lambda_{\min} = f\left(\frac{1}{U_A}\right)$.

2. The graphical representation of the wavelength, λ_{\min} plotted against the reciprocal value of the voltage U_A , gives us a straight line through the origin of the coordinate system (Fig. 5).

Thus, the Duane-Hunt law is confirmed:

$$\lambda_{\min} \sim \frac{1}{U_A} \quad (1)$$

3. Additionally, the slope of the straight line, calculated from the values $\lambda_{\min} = 55 \text{ pm}$ and $U_A^{-1} = 0,045 \text{ kV}_s^{-1}$, gives us a proportionality factor $k = 1,22 \cdot 10^{-6} \text{ Vm}$. This is in agreement with the theoretically calculated value of $1,2398 \cdot 10^{-6} \text{ Vm}$ (from (5)).

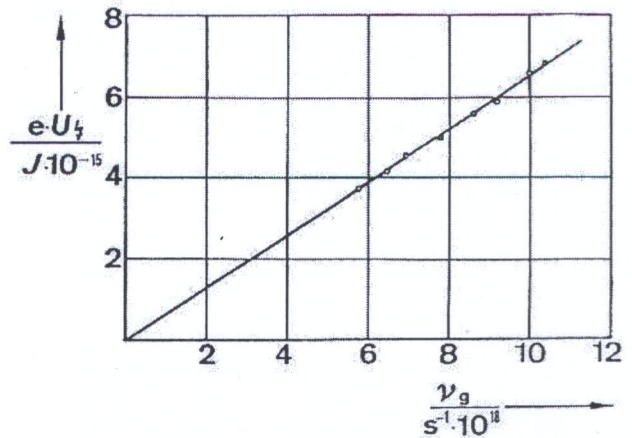


Fig. 6: $e \cdot U_A = f(\nu_g)$.

4. In Fig. 6, the energy value $e U_A$ calculated from U_A plotted against the boundary frequencies ν_g in a graph.

Planck's action quantum can be determined both by calculation and also graphically.

a) From the equation

$$h = \frac{e \cdot \lambda_{\min} \cdot U_A}{c} \quad (6)$$

we obtain the average $h = 6,56 \cdot 10^{-34} \text{ Js}$ from the values given in table 2 of the measuring example.

b) From the slope of the line in Fig. 6, we find

$$h = 6,5 \cdot 10^{-34} \text{ Js with the set } h \text{ of the line } e \cdot U_A = h \cdot \nu_g.$$

Table 3

λ_{\min}	pm	29,0	32,9	35,4	38,6	43,5	46,9	52,7
$\nu_g = \frac{c}{\lambda_{\min}}$	10^{18} s^{-1}	10,34	9,12	8,47	7,77	6,90	6,40	5,69
$e \cdot U_A$	10^{-15} J	6,72	5,91	5,57	5,11	4,63	4,22	3,75



Description

2.1 Scope of delivery and brief description of the "X-ray apparatus 42 kV," equipment (Refer to Figure 1-5 on the folding page at the end of the book)

2.1.1 42 kV X-ray apparatus (554 90)

Apart from the basic apparatus (Figure 1), the scope of delivery of the 42 kV X-ray apparatus (554 90) comprises:

Slit diaphragm collimator (A), which is inserted in the beam outlet aperture and which permits stopping down of a slim bundle of X-rays with an aperture of approximately 0.5° .

Plug-on angular scale (B) with 0.5 degree divisions $0^\circ \dots 60^\circ$.

Counter tube holder (C) for the end-window counter (559 05 or 01) for securing to the retaining disk (27), coupled with the long pointer (15).

Shaft with sample holder (D) for insertion into the hollow shaft of the goniometer mechanism; secured with a captive knurled screw (16); coupled to the short pointer (14); on the sample holder, securing attachments for the absorber holder (from 554 92) and for the rotating table (28) for placing monocrystals (554 77/78) and scattering elements (L), for instance.

In conjunction with a pulse-counting apparatus (e.g. rate meter, 575 52, with digital counter 575 50), the basic apparatus equipped with the slit diaphragm collimator (A), the angular scale (B), counter tube holder (C) with end-window counter (559 05 or 01), sample holder (D) and rotating table (28) forms a counter tube goniometer which can be swivelled with respect to the horizontal axis.

Experimenting rail (E), for insertion into the sockets (30) of the experimenting chamber, provided with a millimeter scale with a zero mark located at distance of approximately 110 mm from the cathode spot of the X-ray tube (measured horizontally!).

Experimenting table (F), which can be attached to the experimenting rail (E), for instance, for placing X-ray examination samples.

Magnetical adhesive suspension attachment (G), e.g. for fixing X-ray examination samples.

Stepped cuvette (H) after filling with chalk powder, for instance, suitable for verification of attenuation as a function of the material thickness.

Zircon sheet (I), 0.05 mm thick; predominately allows X-radiation of the MoK_α -line to pass, attenuates the shorter-wave Bremsstrahlung and almost completely suppresses the MoK_β -line; suitable for investigation of the wavelength dependence of attenuation (K-edge) and for coarse monochromatization.

Copper foil (K), 0.07 mm thick, mainly for verification of the Compton effect and for investigation of the wavelength dependence of attenuation.

Aluminium scatter element (L), especially for verification of the Compton effect.

2 x 1.50 m stranded steel wire as hook-up cable for connection of the basic apparatus to the TY recorder (575 60).

2 cutter fuses each: 0.63 A slow-blow, 1.25 A slow-blow and 2 A slow-blow.

Dust cover for the basic apparatus.

2.1.2 Accessories for the 42 kV X-ray apparatus (554 90) with separate catalog numbers

Plate capacitors (M) (554 91), see Figure 2, for insertion in the experimentation chamber of the basic apparatus.

The 3 plug-in feet comprise the electrical connections which can be externally wired through the sockets (31), (32) of the control panel. A low voltage of 0...25 V AC, is routed in through (32) and is converted to a DC voltage of 0...250 V DC by a transformer incorporated into the capacitor (see 5.2). When emitting radiation through air, the ionization current generated between the capacitor plates can be routed to a measuring amplifier through (31).

(Refer to 1.17 and the group of experiments 4.4 for dimensions, the current/voltage characteristics and dose rate).

Absorption accessory (N) (554 92), see Figure 3, consisting of 2 cylindrical jacket segments with 7 slits each and a two-sided scale for attachment to the basic apparatus.

On one segment, 6 of the 7 slits are covered with aluminium layers having thicknesses of 0.5; 1.0; 1.5; 2.0; 2.5; 3.0 mm; this is used for quantitative



X-ray apparatus 42 kV

Investigation of the dependence of attenuation on thickness of the material (refer to experiment 4.7.2). On the second segment, 6 of the 7 slits are provided with 0.5 mm thick layers of polystyrene, aluminium, iron, copper, zircon and silver with the atomic numbers 6; 13; 26; 29; 40; and 47; this serves to investigate the dependence of attenuation of the atomic number of the absorber (refer to experiment 4.7.3).

Both segments each contain one open slit for measuring the intensity of the unattenuated bundle of rays. The segments are inserted in the sample holder (D). With the rotary knob (6), the segments can be swivelled out of the control panel of the basic apparatus. The short pointer (14) of the basic apparatus indicates on the scale which sample is in the path of the beam.

Film holder (P) and aperture (O) (554 93), see Figure 4.

Aperture (\varnothing 1 mm) which can be fitted onto the slit diaphragm collimator (A) for stopping out a fine bundle of X-rays (for instance, required for Laue and Debye Scherrer photographs; refer to experiments 4.6.1 and 4.6.4).

Film holder of transparent acrylic glass plate (38 mm x 165 mm) with base foot for attachment to the experimenting rail (E).

Singly packed flat X-ray films in a maximum format of 9 cm x 12 cm are held on the film holder by means of two included spring clips. A register mark for the center of the film and the layouts of two different, commercially available single-packing formats of the 9 cm x 12 cm X-ray film (OSRAY from AGFA-GEVAERT, commercially available) and the layout of the 38 mm x 35 mm film for immediate daylight development from Filmpack 2 (554 892) are printed on the film holder as aids to correct positioning.

2.2 Description of the 42 kV X-ray apparatus (554 90)

The X-ray apparatus is functionally subdivided into the following parts (see Figure 6):

- Safety circuit (see Section 2.2.1)
- Radiation generation chamber (see Section 2.2.2)
- Experimentation chamber (see Section 2.2.3)
- Control panel (see Section 2.2.4)
- Goniometer (2-fold swivel attachment with angular scale (see Section 2.2.5))
- Electrical power supply (not accessible to the user; not described).

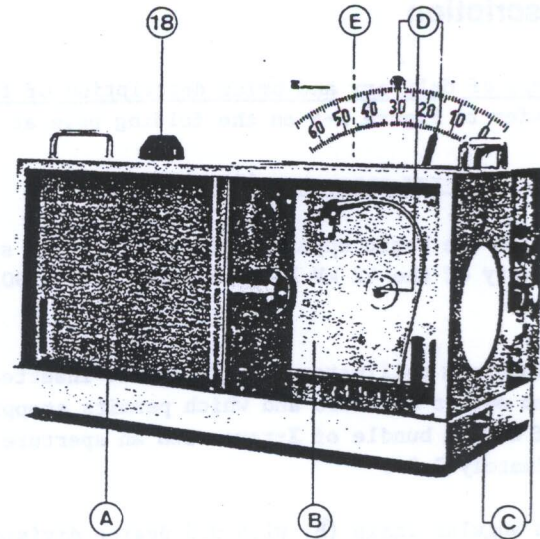


Figure 6

- (18) Large indicating lamp in the safety circuit
- (A) Radiation generation chamber
- (B) Experimenting chamber
- (C) Control panel
- (D) Shafts and pointers*) of the coaxial 2-fold swivel attachment for the counter tube holder (C) and sample holder (D); these comprise a goniometer in conjunction with the angular scale (B).
- (E) Housing for the electrical power supply and mechanical facilities

X-ray tube with spherical cooling head (554 94), see Figure 5.

The tube is not included in the scope of delivery of the basic X-ray unit (554 90). Please refer to Sections 1.4 and 2.2.2 for technical data and a description.

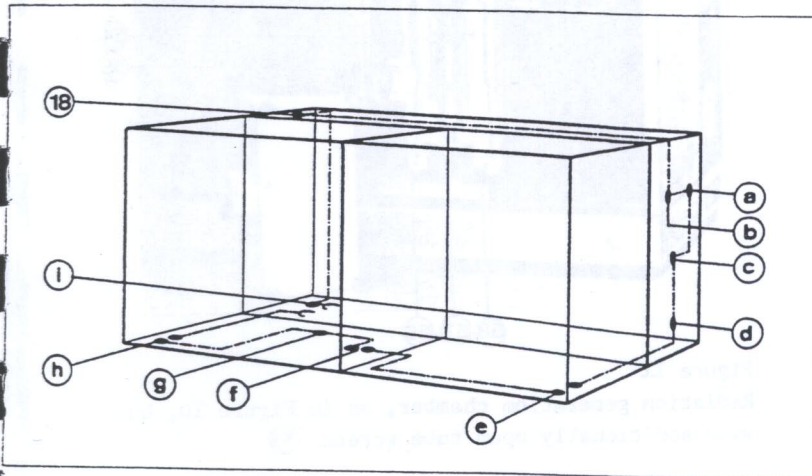
The "X-ray unit" equipment range also includes the following parts which are not illustrated:

- Lithium fluoride monocrystal (554 77) and sodium chloride monocrystal (554 78) for Bragg reflection
- Lithium fluoride crystal (554 87) and sodium chloride crystal (554 88) for Laue photography.

* When the apparatus is delivered, the pointers (14) and (15) are located within a recess in the housing and can be moved to their proper operating position by turning the knobs (5) and (6) to the left.

2.2.1 Safety circuit

the apparatus is used in accordance with specifications, the safety circuit guarantees completely reliable protection against high-voltage or radiation injury. It consists of the elements shown schematically in Figure 7.



Elements of the safety circuit (schematic)

- (a) Pushbutton "high voltage off"
- (b) Pushbutton "high voltage on"
- (c) Stepped switch for high voltage
- (d) Time selector switch
- (e) Safety contacts, actuated by the closed glass sliding door (22)
- (f) Safety contacts, actuated by the X-ray tube screen
- (g) Bridge in the X-ray tube base
- (h) Safety contacts, actuated by the closed steel sliding door (21)
- (i) 1 A slow-blow fuse link
- (18) Large indicating lamp

Figure 7

2.2.2 Radiation generation chamber

X-ray tube: vacuum X-ray tube with directly heated cathode and molybdenum anode

Operating mode: half wave (half-wave rectification of the applied AC anode voltage by the tube itself)

Operating voltage: alternating voltage from the high-voltage transformer (Figures 10 and 11) adjustable from 21 kV to 42 kV in 8 steps of approximately 3 kV each^p (refer also to 1.4 and 1.5).

Cooling: The solid copper block of the anode transfers the dissipated heat of the anode to the cooling head; for this reason, this must not sit loosely in the anode thread when the X-ray tube is inserted. The tube and cooling head dissipate heat to an air flow produced by a fan. In this case, the tube screen serves as the flow duct.

Safety: The following serves the purpose of protection against high-voltage and radiation injury: the tube screen consisting of plastic material containing lead, the metal housing of the basic apparatus lead glass window and lead glass sliding door of the experimentation chamber.

The socket for the X-ray tube is firmly fitted on the bracket plate (57). With a vertical adjustment screw (17), the radiation source can be externally raised and lowered without the need for access to the radiation generation chamber. Three locking

screws (24) on the left-hand inside wall of the experimentation chamber fix the respective vertical adjustment (see Figure 12).

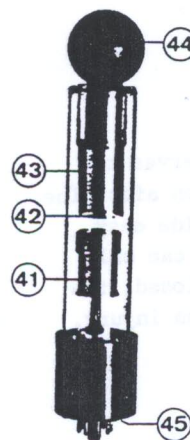


Figure 8

X-ray tube with cooling head

- (41) cathode system
- (42) molybdenum anode lining
- (43) anode block of copper
- (44) cooling head
- (45) base

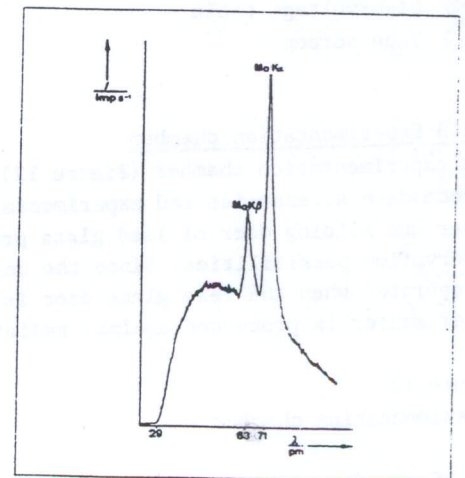


Figure 9

X-ray spectrum of the radiation source at maximum operating data (see also 1.4)

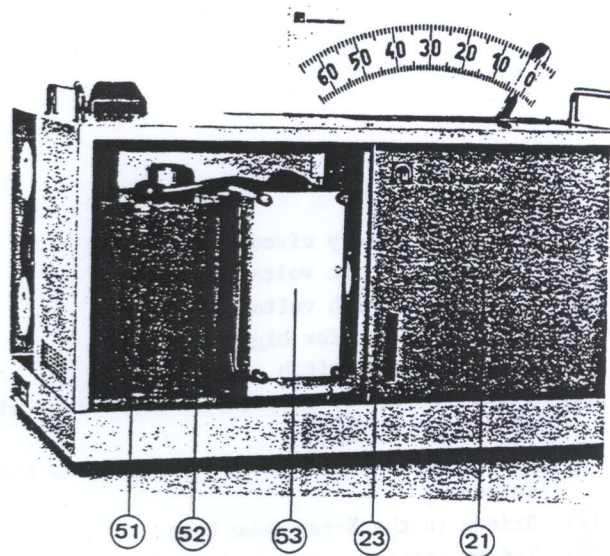


Figure 10

Radiation generation chamber with open metal sliding door ②

- ② Metal sliding door
- ③ Release pushbutton for the metal and lead glass sliding door ① and ②
- ④ Cooling head of the X-ray tube
- ⑤ High-voltage transformer
- ⑥ High-voltage cable
- ⑦ Tube screen

2.2.3 Experimentation chamber

The experimentation chamber (Figure 12) serves to accommodate accessories and experimentation aids. The cover and sliding door of lead glass provide easy observation possibilities. Since the unit can only be operated when the lead glass door is closed, the experimenter is protected against radiation injury.

Figure 12

Experimentation chamber

- ① Screw for vertical adjustment of the X-ray tube (can only be actuated when the screws ② are undone; refer to 3.3).
- ② 1) Locking screws for the goniometer adjusted by manufacturer (Adjusting screws! Do not undo!)
2) Open lead glass door
- ③ Locking screws for the bracket plate ④ with socket ⑤ for the X-ray tube (Figure 11); can only be actuated during vertical adjustment of the tube with screw ① !
- ⑥ Cable for counter tubes with socket for end-window counter (559 05 or 01)

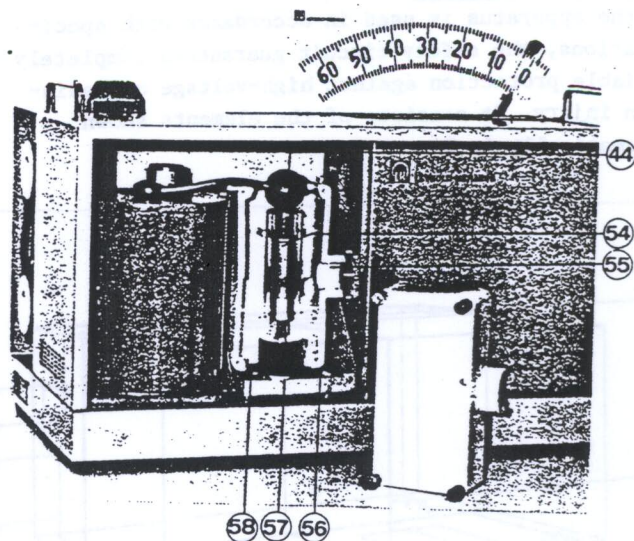


Figure 11

Radiation generation chamber, as in Figure 10, but with additionally open tube screen ③

- ④ X-ray tube
- ③ Radiation outlet aperture
- ⑥ Two contacts of the safety circuit which are actuated by the tube screen ③
- ⑦ Bracket plate as chassis of the radiation source; for vertical adjustment of the tube, this can be adjusted vertically with an externally accessible screw ① after undoing 3 locking screws ②
- ⑤ Socket for X-ray tube

- ③ Sockets for plugging in experimentation equipment; an electrical voltage can be fed in from the control panel through the insulated pair of sockets; the remaining sockets are earthed by the housing.
- ④ Luminescent screen of zinc cadmium sulphite, diameter 150 mm, located behind a round lead glass window.
Important: The luminescent screen must be protected against direct sunlight as otherwise it will become discolored.
- ⑤ Radiation outlet aperture, ϕ 42 mm, serving at the same time as the mount for the slit diaphragm collimator (A).
The aperture allows a cone of X-radiation to enter the experimentation chamber with an aperture angle of approximately 23° .
- ⑥ Coaxial γ_1 and γ_2 shafts with attachments for securing the shaft with sample holder (D) and the counter tube holder (C), e.g. for setting up an adjusted counter tube goniometer (refer to 2.2.5).

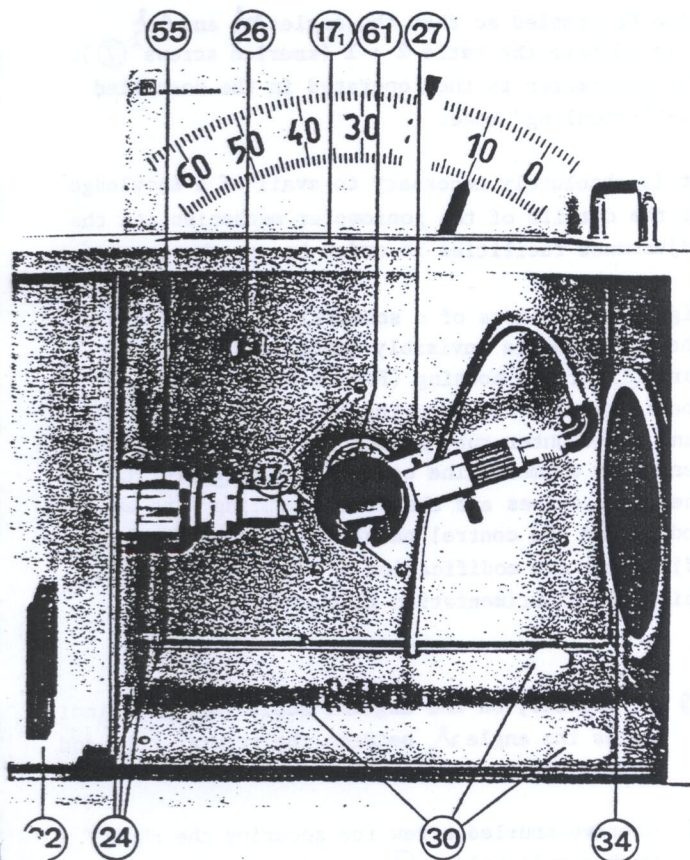


Figure 12

- ⑤ Rotary knob for ϑ_2 -drive for setting the angle ϑ_2 between the counter tube and optical axis; with cable drum for winding up the stranded steel wire when the goniometer is connected to the TY-recorder (575 60) or a suitable motor.
- ⑥ Rotary knob for ϑ_1 -drive for setting the angle ϑ_1 between the sample and optical axis.
- ⑦ Metallic knurled screw for so-called "2 ϑ -coupling"
- ⑧ Socket with 0.63 A slow-blow fuse link for the primary circuit of the high-voltage U_H
- ⑨ Pilot lamp "High voltage on"
- ⑩ "Off" pushbutton for the high-voltage U_H
- ⑪ Stepped switch for the high-voltage U_H ; High voltage values adjustable in 8 steps of approximately 3 kV each between approximately 21 kV and approximately 42 kV
- ⑫ "On" pushbutton for the high-voltage U_H
- ⑬ Slide control for adjusting the emission current I_{EM} ; adjustable from 0.05 mA to 1.0 mA
- ⑭ Coaxial socket for a current-sensitive measuring amplifier (532 91), especially for measuring the ionization current in the plate capacitor (554 91)
- ⑮ Input sockets for the low voltage for the plate capacitor (554 91) in which a 0-250 V DC transformer is incorporated.
- ⑯ Counter tube output coaxial socket for connection of the rate meter (575 52).

2.2.4 Control panel

The switching elements for the basic apparatus are provided on the control panel (see also Figure 1).

Figure 13

Control panel

- ① Toggle switch for the mains voltage; pilot lamp
- ② Pair of sockets for equivalence measurement of the high voltage U_H with demonstration moving coil instrument (531 86) or a different unit with a comparable internal resistance $R_i \geq 2.2 \text{ k}\Omega/\text{V}$; measurement range 30 V AC; $30 \text{ V}_{\text{rms}} \approx 30 \text{ kV}_{\text{rms}} \approx 30 \text{ p} = 42.4 \text{ kVp}$
- ③ Pair of sockets for measuring the emission current I_{EM} with the demonstration multi-range meter (531 86) or a corresponding unit, measurement range 1 mA DC. Time selector for preselection of the duty cycle of the high-voltage U_H

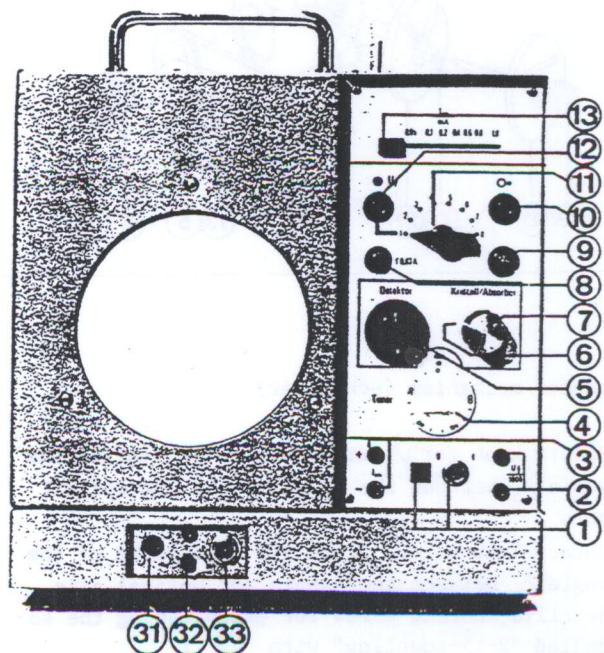


Figure 13

2.5 Goniometer (2-fold swivel attachment with angular scale); see Figure 14 and Figure 1

In conjunction with the angular scale (C), a coaxial 2-fold swivel attachment for the sample holder (D) and counter tube holder (C) comprises a two pointer goniometer which is included in the scope of delivery of the basic apparatus. By means of the goniometer mechanism, it is possible to place samples (e.g. monocrystals, absorbers or scattering elements) centrally into a concentrated beam of X-rays stopped down by the slit diaphragm collimator (A) and to incline it by defined angles ψ_1 with respect to the optical axis while at the same time swivelling the end-window counter tube with angles ψ_2 with respect to the optical axis concentrically around the sample.

The counter tube holder and sample holder can be moved irrespective of each other; however, they can

also be coupled so that the angles $\Delta\psi_2$ and $\Delta\psi_1$ covered have the ratio 2 : 1 (knurled screws (7)). The goniometer is then operated in the so-called "2- ψ -coupling" mode.

It is absolutely necessary to avail of a knowledge of the details of the goniometer mechanism and the adjustment facilities in order to use the apparatus.

Figure 14 consists of a schematic diagram. The mechanism is invisibly concealed in the rear part (E) of the housing (Figure 6); only the two coaxial shafts for securing the sample holder (D) and the counter tube holder (C) jut into the experimentation chamber. The control knobs (5), (6), (7) for the angle drives and the "2- ψ -coupling" are accommodated on the control panel in order to facilitate adjustment and modification of the angles ψ_1 and ψ_2 while the experimentation chamber is closed.

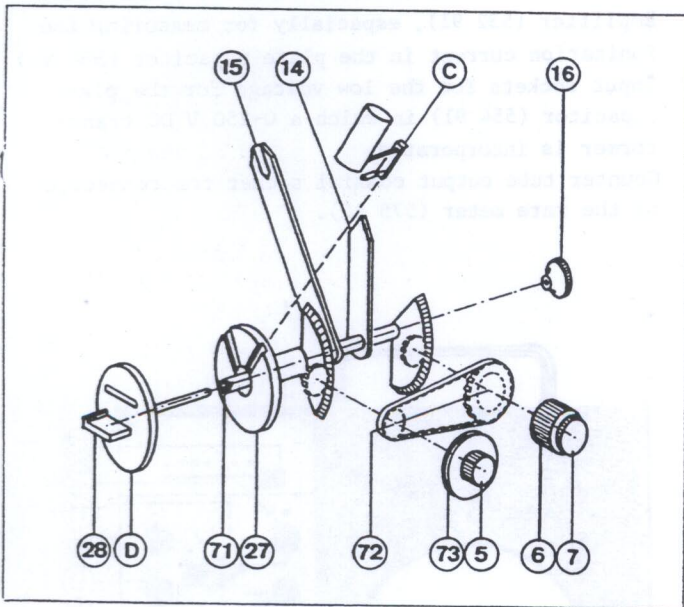


Figure 14

Goniometer mechanism (schematic)

- (5) Rotary knob for ψ_2 -drive for adjustment of the angle ψ_2 between the counter tube and optical axis
- (6) Rotary knob for ψ_1 drive for adjustment of the angle ψ_1 between the sample and optical axis.
- (7) Metallic knurled screw for establishing the so-called "2- ψ -coupling" with (72) :
 ψ_1 -pointer; on the angular scale (B), this indicates the angle ψ_1 between the sample and optical axis

- (15) ψ_2 -pointer; on the angular scale (B), this indicates the angle ψ_2 between the counter tube and optical axis.
- (16) Captive knurled screw for securing the shaft with sample holder (D)
- (17) Retaining disk on the ψ_2 -shaft designed as a hollow shaft, coaxially to (71) provided by two 60° mutually offset guide grooves for fitting the counter tube holder (C) (see also Figure 12).
- (18) Rotary table which can be secured to the sample holder (D).
- (19) ψ_1 -shaft, coaxial to (27), with front notch and bore for insertion of the shaft with the sample holder
- (20) 2 : 1 angular transmission for coupling both ψ -shafts so that $\Delta\psi_2 : \Delta\psi_1 = 2 : 1$
- (21) Cable pulley on the ψ_2 -rotary knob for driving the goniometer with an external motor; suitable for connection of the TY recorder (575 60).
- (22) Counter tube holder for the end-window counter (559 05 or 01) which can be optionally inserted in one of the two guide grooves of the retaining disk (27).
- (23) Sample holder with securing attachment for the rotary table (28) and slot for accommodation of the absorber holder (from 554 92).

3 Handling

3.0 General notes

Every unit is carefully adjusted by Messrs. Leybold Heraeus, but is delivered without an X-ray tube. The X-ray tube (554 94) with molybdenum anode belonging to the unit is not included in its scope of delivery.

After insertion of the X-ray tube (or after replacement should this become necessary later; see Section 3.1), the unit is ready for use for all experiments which can be carried out without a slit diaphragm collimator (A).

Due to unavoidable production tolerances, the X-ray tube must be vertically adjusted once (see Section 3.3) for experiments with the slit diaphragm collimator (A) (refer to experiments 4.6 ff).

If the path rays has become maladjusted due to improper handling of the unit (e.g. inadmissible actuation of the adjustment screws (17.1), (17.2)), readjustment should be carried out only by the servicing agents of Messrs. Leybold Heraeus if the measures described in Sections 3.3, 3.4 and 3.5 are of no avail.

3.1 Inserting the X-ray tube (554 94)

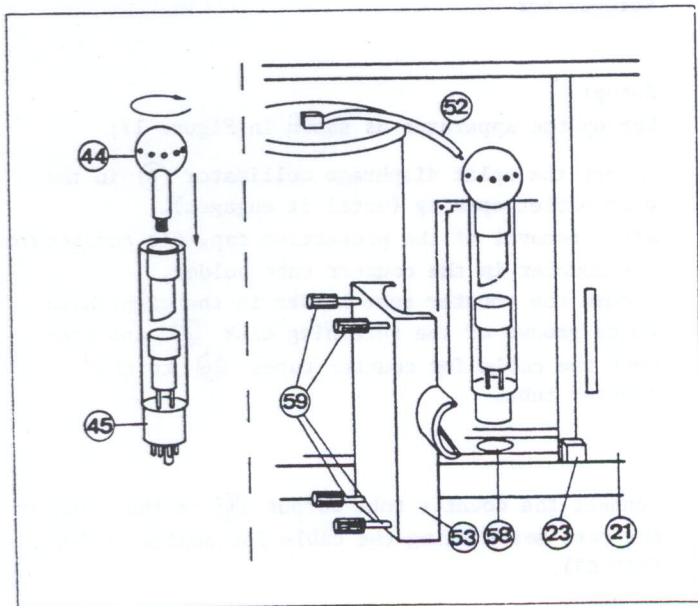


Figure 15 Inserting the X-ray tube

Open the steel sliding door (21) after operating the release pushbutton (23), undo the knurled screws (59) on the tube screen (53) and remove its front section.

Very thoroughly clean dust, fingerprints and persistent soiling from the interior and exterior of the

tube screen (53), the tube socket (58), the jacketing of the high-voltage transformer, the high-voltage cable (52) and, above all, the X-ray tube and the cooling head (44) with a dry, lint-free cloth in order to avoid high-voltage arcing-over and creepage currents.

Do not use aggressive liquids (alcohol or solvents, etc.) for cleaning!

In order to remove persistent soiling (e.g. grease), moisten a cloth with detergent; after treating parts in this way, carefully rub them dry with a dry cloth to ensure that no detergent residues remain.

Carefully screw the cooling head into the anode hole of the X-ray tube and tighten it slightly, at the same time making sure that, as far as possible, you touch the tube only with a cloth; hold the tube by the cooling head (44) and the base (45) and, with the anode in the correct position (see Figure 15), firmly insert it into the socket (58) and plug the high-voltage cable (52) onto the cooling head (44); once again screw the tube screw into place and close the chamber (the locking element must engage).

3.2 Activating X-radiation (see Figure 1)

Check that the mains voltage selector (20) is set to a value which agrees with the mains voltage in the room you are working; if necessary, change the setting accordingly (see Section 3.6).

Connect the apparatus to the mains socket with the mains cable and switch it on with switch (1); the pilot lamp lights up.

On the time selector (4), set the desired time or any time up to 2 hours (the high-voltage can otherwise not be activated because the time selector switch lies in the electrical safety circuit); set the stepped switch (11) for the high-voltage U to Stage 1 and set the slide control (13) for the emission current I_{EM} to 0.05 mA (minimum value).

Activate the high-voltage with the "on" pushbutton (12).

Once all safety precautions have been taken:

- X-ray tube correctly inserted and tube screen properly installed (see Section 3.1),
- Sliding doors (21) and (22) internally locked (by engaging),
- Time selector (4) operated,
- Stepped switch (11) for high-voltage set to Stage 1,

When the high-voltage pilot lamp (9) and the other more visible large indicating lamp (18) light up.

The X-ray tube emits a pulsating X-ray beam with a spectral distribution corresponding to the peak voltage 21 kV_p.

If the emission current I_{EM} and anode high-voltage $U_{\frac{1}{2}}$ are to be determined, connect two suitable measuring instruments such as demonstration multi-range meter (531 86) to the foreseen pair of sockets (3) and (2).

Measuring range for emission current I_{EM} : 1 mA DC
for high-voltage $U_{\frac{1}{2}}$: 30 V AC;
 $R_i \geq 2.2 \text{ k}\Omega/\text{V}$.

The high-voltage is measured at a coil coupled inductively to the primary coil of the high-voltage transformer. Multiplied by $10^3 \sqrt{2}$, the average rms voltage indicated by the measuring instrument indicates the peak value of the high-voltage $U_{\frac{1}{2}}$:
 $1 \text{ V}_{\text{rms}} \approx 10^3 \text{ V}_{\text{rms}} \approx 10^3 \sqrt{2} \text{ V}$ (slight deviations from this mean value are possible, among other things due to production tolerances of the high-voltage transformer, differing operating temperatures and loads).

When the high-voltage $U_{\frac{1}{2}}$ has been switched on, this can be increased with the stepped switch (11) to approximately 42 kV (Stage 8); approximately 30 V_{rms} are then indicated on the voltmeter.

The emission current I_{EM} can be continuously adjusted up to 1.0 mA with the slide control (13). An electronic regulation circuit limits and stabilizes the emission current to the set value.

In a dimmed room, a green luminescence caused by the emitted invisible X-radiation can now be observed on the fluorescent screen. The apparatus is now ready for use in experiments without slit diaphragm collimator (A).

3.3 Vertical adjustment of the X-ray tube

A fine concentrated beam of X-rays is required for various experiments. This is produced with the slit diaphragm collimator (A) (see Figure 1). The divergence of the beam of rays amounts to approximately 0.5°.

The longitudinal axis of the collimator defines the optical axis of the path of rays. Vertical adjustment of the X-ray tube means: moving the cathode spot of the tube to the optical axis (see Figure 16.1).

Figure 16.1

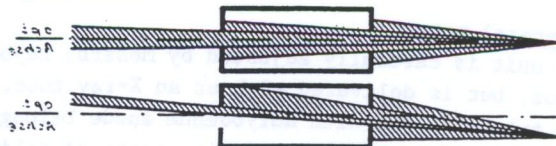
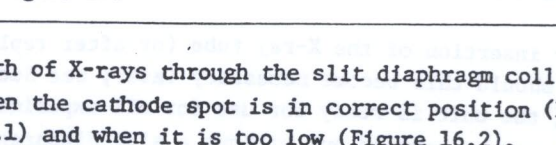


Figure 16.2



Path of X-rays through the slit diaphragm collimator when the cathode spot is in correct position (Figure 16.1) and when it is too low (Figure 16.2).

An indicator of the correct height of the X-ray tube is the intensity maximum of the beam of rays measured with the end-window counter tube. This maximum is found in a test setup as shown in Figure 17 by raising and lowering the X-ray tube.

Apparatus:

X-ray apparatus with split diaphragm collimator (A)	
and end-window counter (C)	554 90/94
End-window counter for	
beta and gamma rays	559 05 or 01
Cable for counter tubes, 100 cm	559 07
Rate meter	575 52
Demonstration multi-range meter	531 86
Additionally:	
Screwdriver	

Setup:

Set up the apparatus as shown in Figure 17;

Insert the split diaphragm collimator (A) in the beam outlet opening (until it engages). After removal of the protective cap, fit and secure the counter in the counter tube holder, secure the counter tube holder in the right-hand guide groove of the retaining disk (27) and connect the cable for counter tubes (26) to the counter tube.

Connect the counter tube output (33) to the input of the rate meter using the cable for counter tubes (559 07).

Connect the demonstration multi-range meter to the output of the rate meter; measuring range of the instrument: 10 V DC.

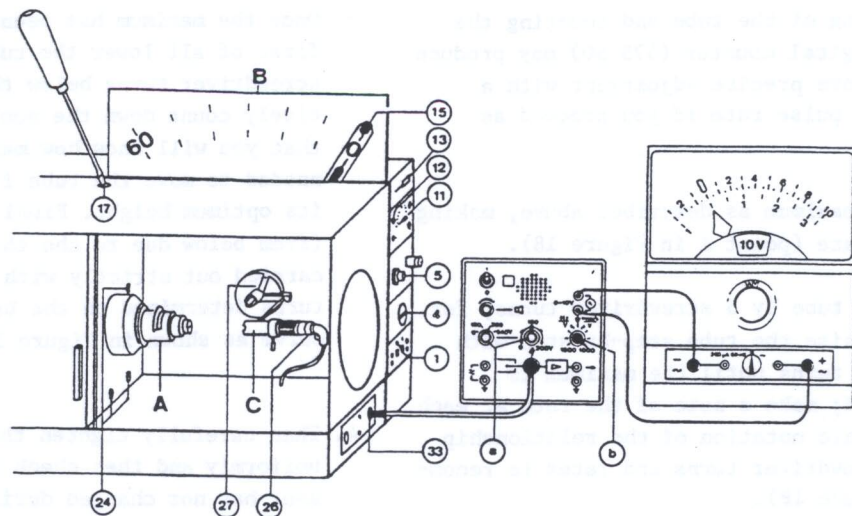


Figure 17

Make the following settings on the rate meter:

- At the pushbuttons (a), set the counter tube voltage to approximately 460 V (on older counter tubes, it may be additionally necessary to redefine the counter tube plateau)
- Rate meter measuring range (Knob (b)): 1,000 imp./s per volt;
- Drive an audible signal generator as required.

Execution:

In order to measure the intensity, set the counter tube with the rotary knob (5) for $\frac{1}{2}$ -drive to $0^\circ \pm 0.2^\circ$ on the angular scale (B) (pointers (15)) and switch on the counting apparatus (rate meter) and X-ray apparatus; set the stepped switch (11) for the high-voltage $U_{\frac{1}{2}}$ to Stage 1; with the slide control (13), preselect an emission current I_{EM} of 0.05 mA and set a time of approximately 15 minutes on the time selector switch (4); do not switch on the high-voltage yet.

Loosen the locking screws (24) just enough to move the tube fixture; completely lower the tube with fixture by turning the slotted screw (17) to the left.

Note:

With a view to well-defined adjustment, it is recommended always to set the required height only from the same side (best from below) due to the slight thread play of the screw (17) and the required friction in the tube fixture.

Close the lead glass sliding door (22) and activate the high voltage with pushbutton (12).

For a rough adjustment of the intensity maximum, continuously raise the tube by slowly turning the screw (17) to the right until the intensity maximum is clearly exceeded.

For fine adjustment of the vertical position, lower the tube to just below the intensity maximum and then raise it to the now known maximum as carefully as possible; carefully and uniformly tighten the three locking screws (24) and then check that the vertical adjustment has no longer changed. When using this procedure, please remember that the indicated rates are constantly subject to slight, irregular fluctuations due to the pulse statistics.

Precision adjustment:

The previously described procedure leads to satisfactory axes adjustment of the cathode spot, thus making it possible to carry out all experiments requiring the slit diaphragm collimator.

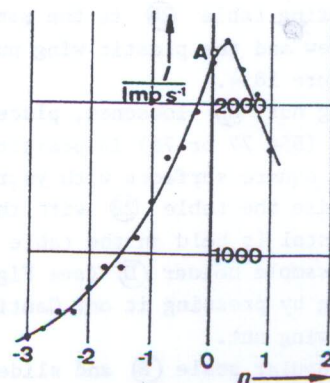


Figure 18

Step-by-step raising of the tube and counting the pulses with the digital counter (575 50) may produce an even slightly more precise adjustment with a slightly increased pulse rate if you proceed as follows:

1. Search for the maximum as described above, making a note of the rate (point A in Figure 18).
2. Lower the X-ray tube by 3 screwdriver turns, for instance, and raise the tube step-by-step with 1/4 screwdriver turns until the maximum is clearly exceeded; make a note of the rate at each setting. A graphic notation of the relationship between 1/4 screwdriver turns and rates is recommended (see Figure 18).

3. Once the maximum has been reliably recognized, first of all lower the tube once again (3 full screwdriver turns below the maximum) and also precisely count down the number of quarter turns so that you will know how many quarter turns are then needed to move the tube from the lower position to its optimum height. Final adjustment of the tube (from below due to the thread play) can now be carried out strictly with the number of quarter turns determined on the basis of the table (or curve as shown in Figure 18).

4. Then carefully tighten the 3 locking screws (24) uniformly and then check that the vertical adjustment has not changed during this time.

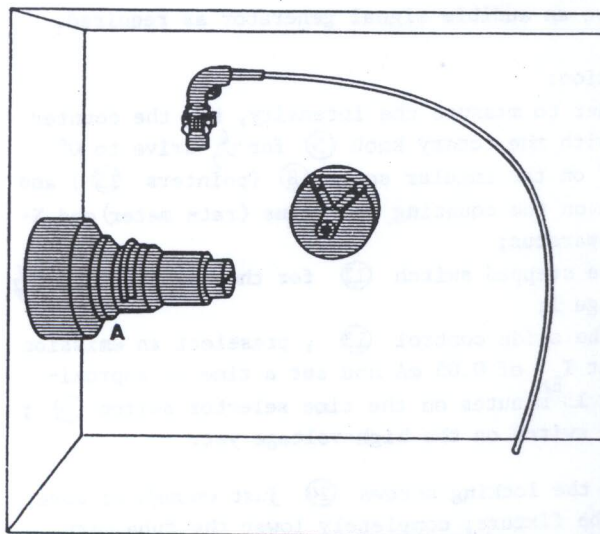
3.4 Assembly of the goniometers for experiments with the Bragg configuration

Carry out installation in the following sequence (see Figures 19.1-19.5 and Figure 1).

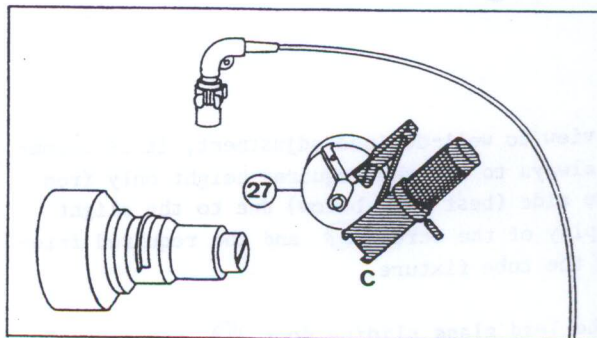
- a) Insert the slit diaphragm collimator (A) in the beam outlet opening (until it engages), see Figure 19.1.

After removal of the protective cap, insert the end-window counter tube (559 05 or 01) into the counter tube holder (C) and screw it tight.
- c) Insert the counter tube holder with end-window counter tube in the right-hand guide groove of the retaining disk (27) and secure it as shown in Figure 19.2.
- d) Connect the counter tube cable (26) to the counter tube as shown in Figure 19.3.
- e) Insert the shaft of the sample holder (D) into the hole of the ψ_1 -axis and, by firmly tightening the captive knurled screw (16) on the rear of the X-ray apparatus, fix it in the experimentation chamber as shown in Figure 18.4 (the face notch in the ψ_1 -axis holds the sample holder in a defined position).
- f) Fit the rotating table (28) to the sample holder with the screw and the plastic wing nut (83) as shown in Figure 18.4.
- g) With the wing nut (83) loosened, place the monocrystal (82) (554 77 or 78) in position without touching its square surfaces with your fingers, carefully raise the table (28) with the crystal so that the crystal is held on the table by the stop (81) of the sample holder (D) (see Figure 19.5); avoid tilting by pressing it on! Cautiously tighten the wing nut.
- h) Attach the angular scale (B) and slide it to the right until it moves no further.

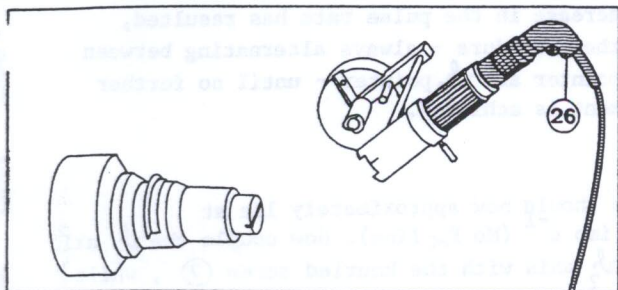
- i) With the ψ -coupling (screw (7)) undone, set the short ψ_1 -pointer (14) to 20° , for instance, with the rotary knob (6) and set the long ψ_2 -pointer (15) to $2\psi_1 = 40^\circ$ with the knob (5).



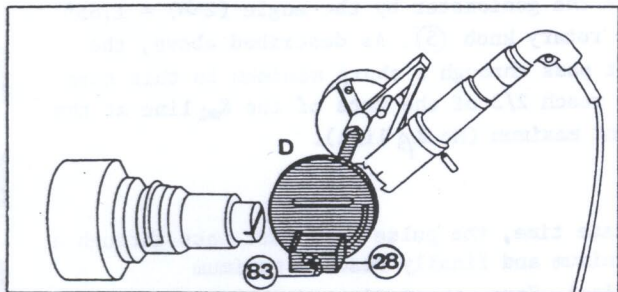
19.1



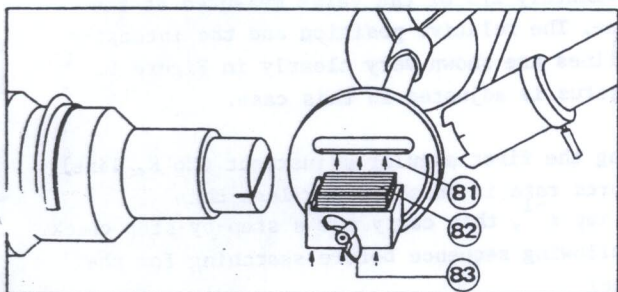
19.2



19.3



19.4



19.5

Important: Carry out angular setting very carefully; observe parallaxes!

Establish 2- θ coupling by firmly tightening the screw (7) :

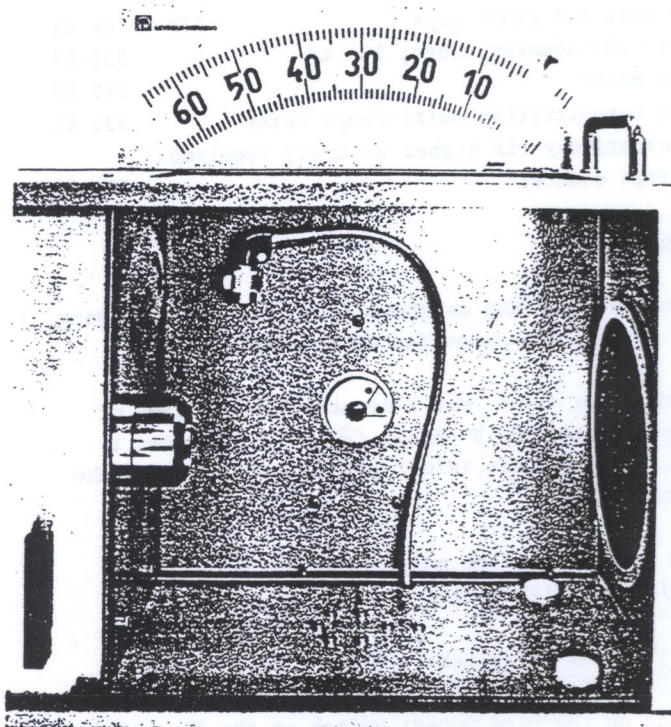
Important: Hold the rotary knob (6) when tightening the screw (7) !

3.5 Functional checking of the goniometer

The X-ray apparatus is delivered with the goniometer adjusted. Thus, within the framework of the scope of performance of the configuration, optimum conditions have been provided for angular adjustment and indication and for the registration of sufficiently high counting rates. If the X-ray apparatus (with vertically adjusted and hardened tube, see Sections 3.6 and 3.7) is operated properly, these can only be impaired by unavoidable production tolerances which can lead to differences between the indicated and set angles. Such deviations can be determined

Figure 20

Experimentation chamber prepared for experiments with the counter tube goniometer



After connecting an apparatus for the power supply of the end-window counter tube (559 05 or 01) and for measurement of the pulses registered by the counter tube (e.g. rate meter 575 52, with digital counter 575 50 or the moving coil instrument 531 86) to the coaxial socket (33), the counter tube goniometer is ready for operation.

during functional checking of the counter tube goniometer. For this purpose, find the diffraction maxima of the first order of the molybdenum- K_{α} and $-K_{\beta}$ lines in a Bragg configuration and ascertain whether or not the following criteria are fulfilled:

- 1) Separation of the lines $Mo K_{\alpha}$ and $Mo K_{\beta}$ (see Figure 9),
- 2) Correct indication of the diffraction angles,
- 3) The expected amplitude of the pulse rate at the diffraction maximum of the first order (approximately 2×10^3 imp./s) for the $Mo K_{\alpha}$ line at maximum X-ray apparatus operating data.



Apparatus:

Slit diaphragm collimator (A))	
Angular scale (B))	from
Counter tube holder (C))	554 90
Sample holder (D) with table (28))	
NaCl monocrystal (without yellow marking)		554 78
End-window counter tube		
for beta and gamma rays		559 05 or 01
Cable for counter tubes, 100 cm		559 07
Rate meter		575 52
with demonstration multi-range meter		531 86
Alternatively (if higher accuracy required):		
Digital counter		575 50

Setup:

Assemble the setup as shown in Figure 21, observing the instructions provided in Section 3.4:

On the rate meter, set a counter tube voltage of approximately 460 V (Knobs (a) if the plateau is guaranteed at this value; if necessary, record the characteristic).

Rate meter range for pulse counting (Knob (b)):
 0 imp./s per Volt.

Carrying out the check:

Switch on the rate meter; switch on the X-ray apparatus with switch (1); on the time selector (4), pre-select an operating time of ≥ 15 min; switch on the high-voltage with pushbutton (12).

Set the high-voltage U_H to Stage 8 (42 kV) with the stepped switch (11) and set the emission current I_{EM} to 1.0 mA with the slide control (13).

Set the coupled goniometer to the angles $\gamma_1 = 7.25^\circ$ and $\gamma_2 = 14.5^\circ$ with the rotary knob (5).

With this setting, a pulse rate of approximately 2×10^3 imp s^{-1} should be measured on the Mo K_{α} line.

If this is the case, slowly adjust the goniometer to smaller angles with the rotary knob (5), down to the position of the Mo K_{β} line ($\gamma_2 = 12.85^\circ$ and $\gamma_1 = 6.43^\circ$);

Observe the rate meter indication during movement.

If an increase in the pulse rate has resulted, repeat the procedure - always alternating between the γ_1 -pointer and γ_2 -pointer - until no further improvement is achieved.

The rate should now approximately lie at 2×10^3 imp s^{-1} (Mo K_{α} line). Now couple the γ_1 axis and the γ_2 axis with the knurled screw (7), while the two pointers are in this position, and slowly turn back the goniometer by the angle $(2\gamma) = 1.65^\circ$ with the rotary knob (5). As described above, the rate must pass through a sharp minimum in this case and must reach 2/3 of the rate of the K_{α} line at the subsequent maximum (Mo K_{β} line).

At the same time, the pulse rate must pass through a sharp minimum and finally reach a maximum (Mo K_{β} line). Here, the indicated pulse rate should be approximately 2/3 of the value measured at the Mo K_{α} line. The relative position and the intensity of both lines are shown very clearly in Figure 9. The apparatus is adjusted in this case.

If, during the first angular adjustment (Mo K_{α} line), the measured rate is considerably less than 2×10^3 imp s^{-1} , then carry out a step-by-step check in the following sequence before searching for the Mo K_{β} line:

- a) Turn the NaCl crystal to the remaining 7 possible positions on the rotary table one after the other and measure the rate anew each time (mark the optimum position of the crystal by means of adhesive strips on the narrow side).
 If, even in this case, a satisfactory rate can still not be measured,
- b) search for the intensity maximum in the proximity of the set angles (7.25° and 14.5°):

After undoing the 2- γ -coupling (knurled screw (7)), search for an intensity maximum in the proximity of the 7.25° setting by slowly moving the short γ_1 -pointer to and fro with the rotary knob (6). Once such a maximum has been found, an improved maximum must be sought in the proximity of 14.5° by accordingly varying the γ_2 setting with the rotary knob (5).

- rf
- 1) there is a sharp separation of the lines $Mo K_{\alpha}$ and $Mo K_{\beta}$,
 - 2) the angles at which the lines were found also do not deviate by more than $\pm 0.2^{\circ}$ from the theoretical ν_1 or ν_2 value and if
 - 3) the pulse rates at the determined optimum angle settings approximately reach the specified values, then the apparatus is adjusted well.

Angular deviations can be noted down and used, if necessary, for calculatory corrections (this is also possible at deviations greater than $\pm 0.2^{\circ}$).

A rate which is too low (even if the angular indications are satisfactory!) may be caused by:

- a) an X-ray tube which is not hardened (see Section 3.7) or
- b) inadequate vertical adjustment of the X-ray tube (see Section 3.3) or
- c) maladjustment of the goniometer axes which cannot be remedied using the measures described in Sections 3.4 and 3.5 (inform our servicing agency in this case).

If there is no separation of the two lines $Mo K_{\alpha}$ and $Mo K_{\beta}$, then the goniometer is also maladjusted.

If only the angle indications no longer lie within the specified tolerance range, then it may be necessary to adjust the pointers; it is difficult to do this and, in this case, it is thus necessary to contact our servicing agency.

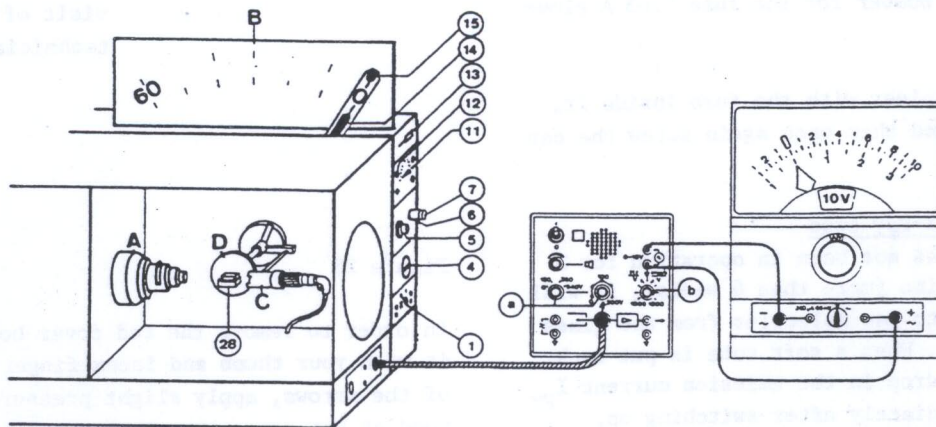


Figure 21

3.6 Conversion to mains voltages other than 220 V AC; replacing fuses

Important:

Remove the mains plug before replacing fuses!

3.6.1

In order to convert to mains voltages other than 220 V AC, replace the 1.25 A slow-blow mains voltage fuse used for 220/240 V AC (2.0 A slow-blow for 110/125/150 V AC) in the mains voltage selector ② as shown in Figure 1.

Replacement order numbers for fuses; 1.25 A, slow-blow: ET 69 816

2.0 A slow-blow: ET 69 808

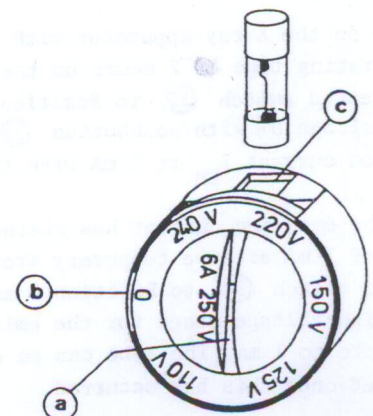


Figure 22



X-ray apparatus 42 kV

In order to replace the mains voltage fuse, insert a coin in the slot (a) and turn it until the "0" is next to the white marking (b) as shown in Figure 22. Catch hold of the fuse which has sprung out of the opening (c) in this position; slide a new fuse (chosen dimensioning in accordance with the mains voltage) into opening (c) and, using the tip of a ballpoint pen or similar, push it downwards while turning the coin in slot (a) at the same time; set the voltage selector so that the value specified on it for the local mains AC voltage lies next to the marking (b).

3.6.2

Replace the 0.63 A slow-blow, high-voltage fuse in socket (8) as shown in Figure 1.

Replacement order number for the fuse 0.63 A slow-blow: ET 69 813

Unscrew the fuse holder with the fuse inside it, replace the fuse and then once again screw the cap tight.

3.7 Hardening the X-ray tube

If an X-ray tube has not been in operation for a longer period of time (more than 6 weeks), it will become "soft" due to gas molecules from the glass and metal surfaces. When a soft tube is put back into operation, a drop in the emission current I_{EM} is discovered immediately after switching on. This effect is particularly disadvantageous during quantitative experiments. If this is the case, then you should proceed as follows:

Connect a suitable measuring instrument to the pair of sockets (3) in order to measure the emission current I_{EM} (e.g., the demonstration multi-range meter 531 86) and put the X-ray apparatus into operation:

Switch on the X-ray apparatus with switch (1), set an operating time of 2 hours on the timer (4), set the stepped switch (11) to Position 1, switch on the high-voltage U_H with pushbutton (12) and set the emission current I_{EM} to 1 mA with the slide control (13).

Once the emission current has reached the first set value of 1 mA after a temporary drop, set the stepped switch (11) to Position 8 and now wait at this high-voltage stage for the emission current to stabilize to 1 mA. The tube can be considered as hardened once this has occurred.

3.8 Fault-finding

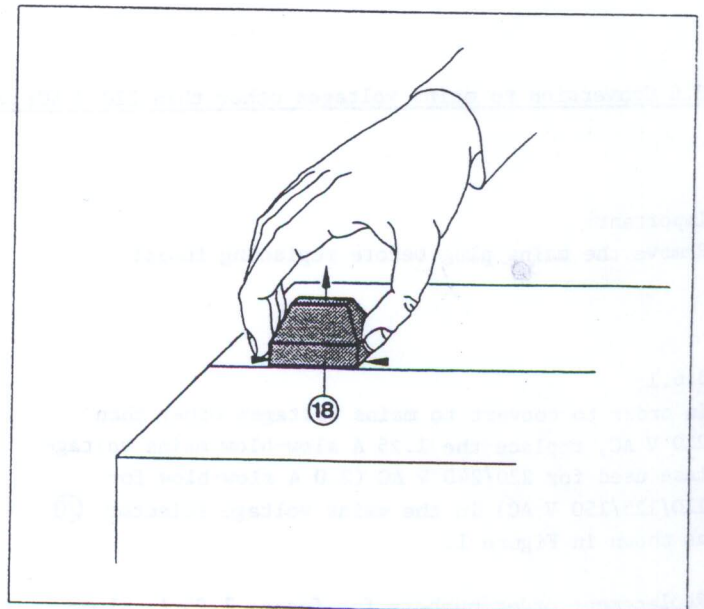
3.8.1 Activation problems

The main pilot lamp (1) does not light up after switching on:

Possible causes	Remedy
a) No mains voltage	Determine and eliminate the cause,
b) Fuse (20) defective	Replace the fuse (see Section 3.6)
c) Incandescent bulb in (1) defective	This does not impair operability of the apparatus; have the incandescent bulb replaced during the next visit of the servicing technician.

Figure 23

In order to remove the red cover hood, take hold of it with your thumb and index finger in the direction of the arrows, apply slight pressure and lift up the hood at the same time. Replace the double-ended tubular 12 V, 3 W incandescent bulb (replacement order No. ET 69 760).





X-ray apparatus 42 kV

The large indicating lamp (18) does not light up when the high-voltage is switched on with push-button (12):

Reason:

The safety circuit is not closed and one of the functional elements shown in Figure 7 is switched off. No high-voltage can be applied to the tube.

Possible causes	Remedy
a) Time selector (4) set to zero	Preselect a time
b) Stepped switch for high-voltage (11) not set to Stage 1	Set switch to Stage 1
c) Sliding doors (21) or (22) not locked	Close doors properly
d) Tube screen (53) (Figure 10) not installed or not properly fitted	Determine and eliminate the cause (see Section 3.1).
e) X-ray tube not installed or is not correctly fitted	Determine and eliminate the cause (see Section 3.1)
f) Incandescent bulb in (18) defective	Replace as shown in Figure 23
Malfunctions other than a)-f)	Inform the servicing agency. The 1 A slow-blow fuse permanently installed in the interior of the apparatus ((i) in Figure 7) must not be replaced by the user since, when it blows, it indicates a defect which, in certain circumstances, may be a grave one.

3. The high-voltage pilot lamp (9) does not light up although the large indicating lamp (18) is bright.

Important:

The high-voltage may still be applied to the X-ray tube despite a faulty indication of the lamp (9)!

Possible causes	Remedy
a) Fuse in (8) defective	Replace (see Section 3.6)
b) Incandescent bulb in (9) defective	This does not impair operability of the apparatus; have the incandescent bulb replaced during the next visit of our servicing technician.
c) Malfunctions other than a) and b)	Inform our servicing agency

3.8.2 Loud crackling in the ray generation chamber
Sometimes loud crackling occurs in the ray generation chamber during operation of the X-ray apparatus with a very high voltage. This can be ascribed to high-voltage arcing-over in the area of the high-voltage cable due to soiling (e.g. due to slight accumulation of dust). This effect is not only an annoying accompanying phenomenon during operation of the apparatus, but also considerably stresses the electrical systems. Immediate elimination of the cause is therefore necessary.

First of all, carefully clean the coverplate of the transformer, the high-voltage cable and the cooling head of the X-ray tube with a clean, lint-free cloth soaked in alcohol. In certain circumstances, it may be necessary to clean the X-ray tube if the X-ray apparatus is stored in dusty rooms; however, this should not be done unless the first measure produces no considerable improvement because, after removal of the X-ray tube, readjustment cannot be avoided in most cases (see Section 3.3).

3.8.3 Unsatisfactory experimental results:

1. During screen investigations (high-voltage Stage 8!):

Possible causes	Remedy
a) Soft X-ray tube (emission current has dropped)	Reharden the X-ray tube (see Section 3.7)
b) X-ray tube too old (after more than 300 hours of operation)	Replace the X-ray tube (see Section 3.1)

2. During plateau determination in a capacitor experiment:

Possible causes	Remedy
a) Soft X-ray tube (emission current has dropped)	Reharden the X-ray tube (see Section 3.7)
b) X-ray tube too old (after more than 300 hours of operation)	Replace the X-ray tube (see Section 3.1).
c) Voltage transformer in the capacitor defective	Carry out a check in accordance with experiment 4.4.1; if defective, send in the capacitor for repair



X-ray apparatus 42 kV

3. In the case of Laue or Debye-Scherrer photographs:

Possible causes	Remedy
a) Soft X-ray tube (emission current has dropped)	Reharden the X-ray tube (see Section 3.7)
b) X-ray tube too old (after more than 300 hours of operation)	Replace the X-ray tube (see Section 3.1)
c) Height of the X-ray tube maladjusted	Adjust the height of the X-ray tube (see Section 3.3)

4. During the examination of spectograms in a Bragg configuration:

In a Bragg configuration, the Mo K_{α} and Mo K_{β} lines are not correctly resolved with the goniometer or measured at incorrect diffraction angles.

Possible causes	Remedy
Path of rays maladjusted (e.g. X-ray tube not vertically adjusted) or goniometer maladjusted	If necessary, vertically adjust the X-ray tube (see Section 3.3) and carry out a functional check of the goniometer (see Section 3.5); If the apparatus is otherwise maladjusted, inform our servicing agency

5. During counter tube measurements

Too low or irreproducibly fluctuating pulse rates are measured with the counting tube:

Possible causes	Remedy
a) Soft X-ray tube (emission current has dropped)	Reharden the X-ray tube (see Section 3.7)
b) X-ray tube too old (after more than 300 hours of operation)	Replace the X-ray tube (see Section 3.1)
c) X-ray tube not vertically adjusted	Vertically adjust the X-ray tube (see Section 3.3)
d) Fault in the counting apparatus	Pursue the fault further there

Important:

Should malfunctions or faults occur which cannot be remedied with the measures listed in Section 3.8, please make use of our servicing agency in all cases!



KLINGER
EDUCATIONAL
PRODUCTS CORP.

112-19 14TH ROAD
COLLEGE POINT, NEW YORK 11356
(718) 461-1822

The Hall effect for silver

Verifying the proportional relationship between Hall voltage U_H and magnetic flux density B , determining the polarity of the charge carriers which are mainly responsible for charge transport in silver. Calculating the charge carrier density n .

If a current-carrying metallic conductor band is in a magnetic field perpendicular to the direction of current, a transverse electrical field and a potential difference are produced (Hall effect).

The following equation is valid for the Hall voltage U_H :

$$U_H = \frac{1}{n \cdot e} \cdot \frac{B \cdot I}{d} \quad (1)$$

- B: Magnetic flux density
- I: Current
- d: Thickness of the band-shaped conductor
- e: Elementary charge
- n: Concentration of charge carriers

$\frac{1}{n \cdot e}$ is called the Hall constant R_H . R_H is a value which is dependent on material and temperature:

$$R_H = \frac{1}{n \cdot e} \quad (2)$$

The conductor band consists of silver in the following experiment. First, it will be proved that $U_H \sim B$.

The polarity of the charge carriers which are mainly responsible for the current (polarity of the Hall constants) can be determined from the direction of the Hall voltage. The concentration of the charge carriers is established experimentally since all the values in "1" except for n can be measured. The Hall voltage U_H is caused by deflection of the moving charge carriers in the magnetic field by the Lorentz force, whose direction may be predicted by the "right-hand rule".

Apparatus:

1	Hall effect apparatus, silver	586 81
1	U-core with yoke	562 11
1	Clamping device	562 12
1	Pair of bored pole pieces	560 31
2	Coils, 250 turns	562 13
1	Extra-low variable transformer	522 39
2	Interchangeable scale demonstration meters, basic units	530 50
1	Measuring module 0 to 1000 mT/3000 mT	530 75
1	Measuring module 0-3 A/10 A	530 65
1	Shunt resistor 30 A	530 90
3	Connecting leads, red, 50 cm	501 25
2	Connecting leads, blue, 50 cm	501 26
3	Connecting leads, black, 50 cm	501 28
1	Connecting lead, black, 25 cm	501 23
1	Microvoltmeter	532 13
1	Pole probe	516 501
1	Power supply unit 0-12 V/20 A, regulated	522 47

Recommended:

1	Calibrating magnet for pole probe ...	516 53
1	Multimeter 2H (15 A -)	531 53
2	Batteries 1.5 V/IEC R6	685 44

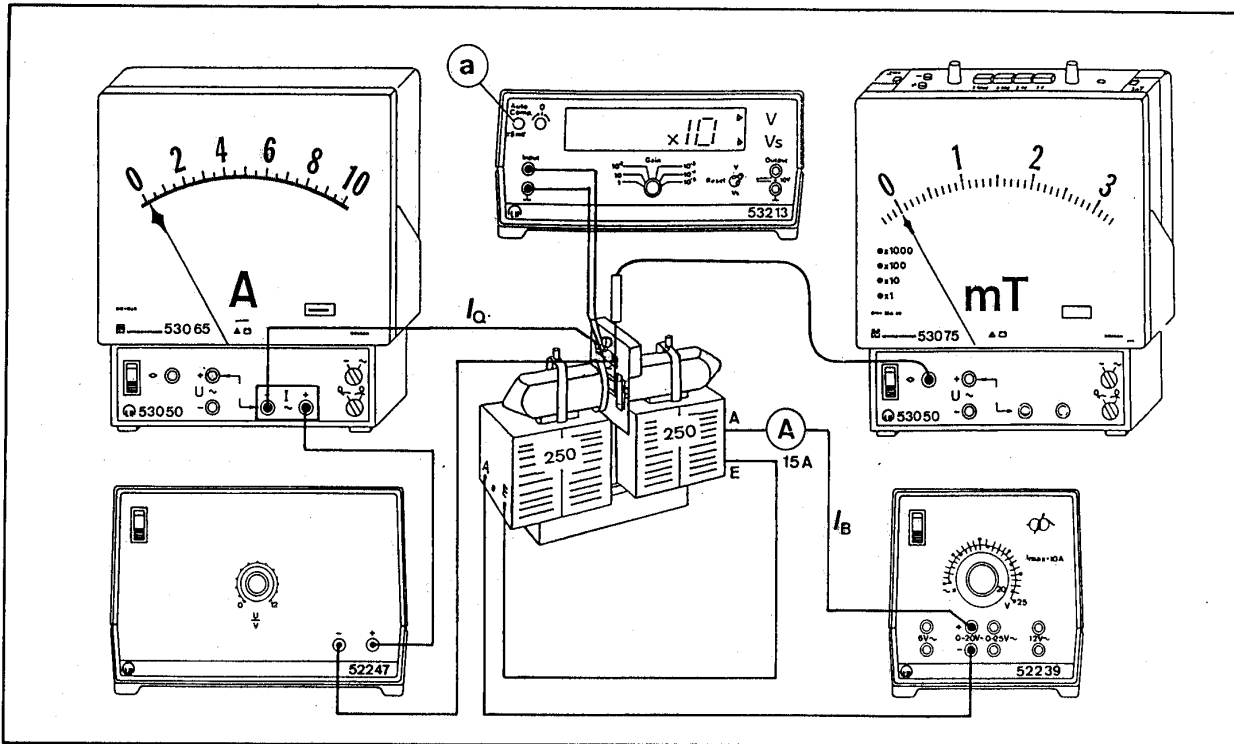


Fig. 1: Experiment setup for the Hall effect.

I_B : Field current

I_Q : Transverse current

b) U_H is a function of B for constant transverse current I_Q :

Setting up:

Note:

Only switch on circuits for a short time for a transverse current above 15 A or magnetic currents above 5 A because the connecting leads will heat up and the coils designed for 5 A will overload.

In the transverse circuit, use leads which permit a load of 20 A (e.g. connecting leads 501 20-29 or safety connecting leads 500 65-74).

Set up the apparatus as in Fig. 1, initially without the Hall effect apparatus. Set up the electromagnet with exactly the pole piece spacing that is given by the thickness of the support plate of the Hall effect apparatus. To do this, loosen the clamping device and place one edge of the Hall effect apparatus between the pole pieces. Then push the latter as close as possible to the support plate.

Calibrate the Hall probe with the calibrating magnet as described in the instructions for use 516 501. Remove the protective sleeving from the pole probe.

Carrying out the experiment:

a) $I_B - B$ calibrating curve:

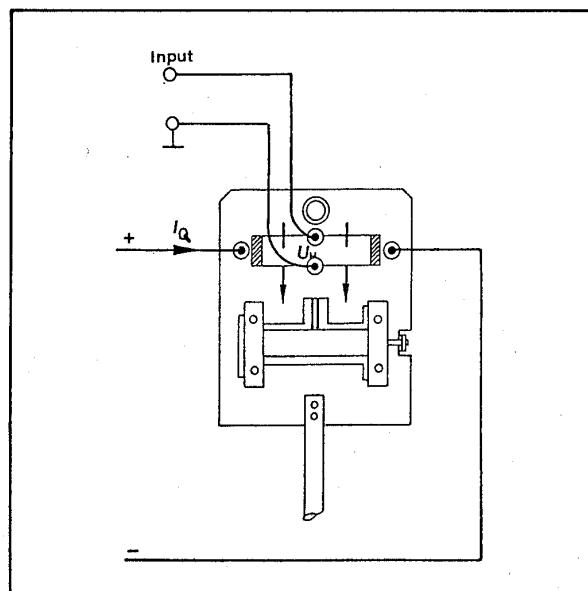
Demagnetize the iron of the electromagnets before recording the $I-B$ calibrating curve and before determining B from this curve (allow 5 A \sim to flow through the coils for a short time).

Measure the magnetic flux density B as a function of magnetic current I_B ; to do this, increase I_B in steps of 0.5 A (Fig. 3).

Mount the Hall effect apparatus in the electromagnet as shown in Fig. 1, with the pole pieces pushed as close as possible to the support plate (air gap as narrow as possible and of the same width as for the recording of the calibrating curve).

Connect the Hall effect apparatus to the microvoltmeter and the power source as shown in Fig. 2. The field direction should be as printed on the support plate (current direction I_B ; coil connections).

Fig. 2: Electrical connections of the pole effect apparatus; I_Q : transverse current.



Reset the measuring instrument display for the Hall voltage U_H to zero before switching on the magnetic current I_F , but with the transverse current switched on. Correct the zero point by means of button (a) (Fig. 1) on the microvoltmeter.

After switching off the magnetic current, check the zero point again and, if necessary, take into account any fluctuations which have occurred.

Read off the respective zero voltage U_H for each

set current I_B . Read off the effective field strength from the I_B -B calibrating curve for each current I_B . Transverse current $I_Q = 15$ A and $I_Q = 20$ A (Fig. 4).

Polarity of the charge carriers:

To determine the polarity of the Hall voltage for the chosen current direction.

Determination of the charge carrier concentration n and Hall constant R_H :

Set a transverse current $I_Q = 15$ A, and a field current $I_B = 8.5$ A ($\approx B = 0.805$ Tesla, in accordance with calibrating curve). Measure U_H .

Repeat measurement for $I_Q = 20$ A, $I_B = 8.5$ A.

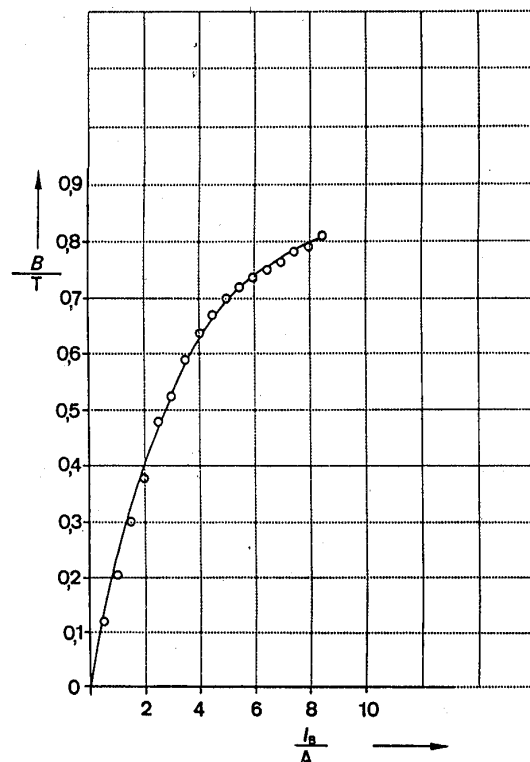


Fig. 3: I_B - B calibrating curve; pole piece

distance the same as the thickness of the support plate

I_B : Coil current

B: Magnetic flux density of the field produced by I_B . Saturation at large

field currents.

Measurement example:

a) Table 1/Fig. 3

Table 1:

I in A	B in T
0	0
0,5	0,118
1	0,200
1,5	0,295
2	0,374
2,5	0,455
3	0,520
3,5	0,585
4	0,630
4,5	0,665
5	0,695
5,5	0,715
6	0,735
6,5	0,748
7	0,760
7,5	0,780
8	0,790
8,5	0,800
9	0,810

b) Fig. 4

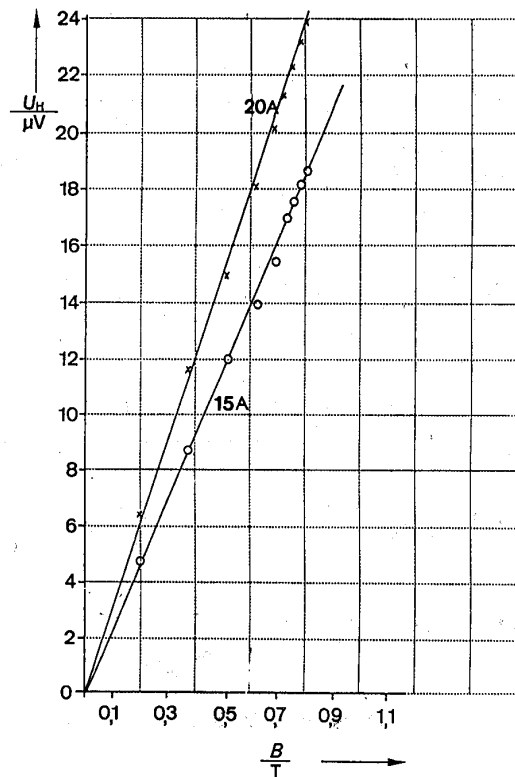


Fig. 4: U_H as a function of B; parameter I_Q

B in accordance with calibrating curve in Fig. 3 from I_B ;

Hall foil made of silver.

c) The microvoltmeter indicates negative voltage values for the setup chosen in Fig. 2. The upper side of the Hall foil is thus charged negatively with respect to the lowest side.

d₁):

$I_Q = 15 \text{ A}$; $B = 0.805 \text{ T}$; foil thickness $d = 5 \cdot 10^{-5} \text{ m}$;
 10^{-5} m ;

$e = 1.602 \cdot 10^{-19} \text{ C}$; $U_H = 1.87 \cdot 10^{-5} \text{ V}$.

d₂):

$I_Q = 20 \text{ A}$; $B = 0.805 \text{ T}$; $U_H = 2.4 \cdot 10^{-5} \text{ V}$.

Evaluation and results:

For b)

The graphs in Fig. 4 show that $U_H \sim B$ and that U_H increases with increasing transverse current I_Q .

Note:

Experimental proof of the proportional relationship $U_H \sim I$ may easily be obtained by

measuring U_H for various I_Q (for constant field current I_B).

For c)

Negative Hall voltages are obtained for the setup of current and field direction chosen in Fig. 2. If the "right-hand rule" is used, we find that the conduction mechanism for silver is mainly effected by negative charge carriers.

Note:

In 1916, Tolman obtained certain proof that electrons are the charge carriers in metals.

For d₁)

Evaluation in accordance with (1) and (2):

$$R_H = 7,74 \cdot 10^{-11} \text{ m}^3 \cdot \text{C}^{-1}$$

$$n = 8,06 \cdot 10^{28} \text{ m}^{-3}$$

For d₂)

$$R_H = 7,45 \cdot 10^{-11} \text{ m}^3 \text{ C}^{-1}$$

$$n = 8,37 \cdot 10^{28} \text{ m}^{-3}$$

Note:

Theoretical value: $R_H = 8.9 \cdot 10^{-11} \text{ m}^3 \text{ C}^{-1}$

$$n = 6.6 \cdot 10^{28} \text{ m}^{-3}$$

(atoms density $5.8 \cdot 10^{22} \text{ cm}^{-3}$)

Investigating the Hall effect in silver

Objects of the experiment

- Validation of the proportionality of the Hall voltage and the magnetic flux density.
- Determining the polarity of the charge carriers.
- Calculating the Hall constant R_H and the charge carrier concentration n .

Principles

If a current-carrying metallic conductor strip is located in a magnetic field B perpendicular to the direction of the current I , a transverse electrical field E_H and a potential difference is produced (Hall effect).

The following equation holds for the Hall voltage U_H (Fig. 1):

$$U_H = \frac{1}{n \cdot e} \frac{B \cdot I}{d} \quad (I)$$

B : magnetic flux density

I : current through the metallic conductor

d : thickness of the band-shaped conductor

n : concentration of charge carriers

$e = 1.602 \cdot 10^{-19}$ C: elementary charge

The Hall voltage U_H is caused by the deflection of the moving charge carriers in the magnetic field due to the Lorentz force, whose direction may be predicted by the right hand rule. The

factor $\frac{1}{n \cdot e}$ is called Hall constant R_H :

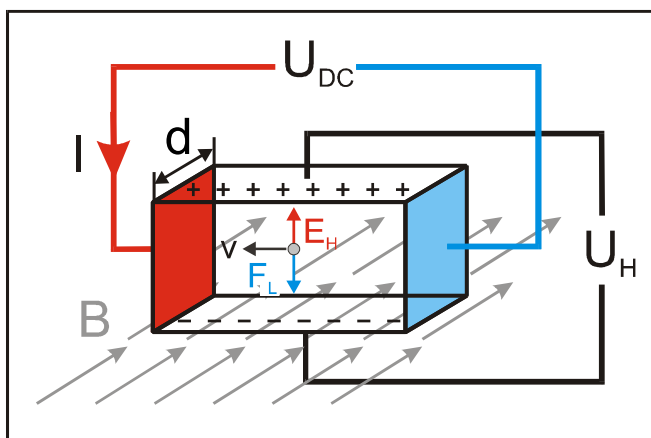
$$R_H = \frac{1}{n \cdot e} \quad (II)$$

The sign of the Hall constant R_H is determined by the polarity of the charge carriers.

The Hall constant depends on the material and the temperature. For metals R_H is very small, however, for semiconductors R_H becomes significantly large (compare experiments P7.2.1.3 and P7.2.1.4).

The polarity of the charge carriers can be determined from the direction of the Hall voltage. The concentration of the charge carriers n can be determined experimentally by measuring the Hall voltage U_H as function of the magnetic field B for various currents I .

Fig. 1: Hall Effect schematically: Inside a charge carrying metallic conductor which is located in the magnetic field B the Lorentz force F_L is causing an electrical field E_H resulting in a Hall voltage U_H . (I denotes the transverse current).



Apparatus

1 Hall effect apparatus (silver)	586 81
1 U-core with yoke	562 11
1 Pair of bored pole pieces	560 31
2 Coil with 250 turns	562 13
1 High current power supply	521 55
1 Variable extra low-voltage transformer	521 39
1 Multimeter LD analog 30	531 130
4 Pair cables 100 cm, red/blue	501 46
2 Connecting lead 100 cm black	501 33
1 Leybold multiclamp	301 01
1 Stand rod, 25 cm	300 41
1 Stand base, V-shape, 20 cm	300 02

Option (a)

1 Microvoltmeter	532 13
1 Universal Measuring Instrument Physics	531 835
1 Combi B-Sensor S	524 0381
1 Extension cable, 15-pole	501 11

Option (b)

2 Mobile-CASSY	524 009
1 μ V-Box	524 040
1 Combi B-Sensor S	524 0381
1 Extension cable, 15-pole	501 11

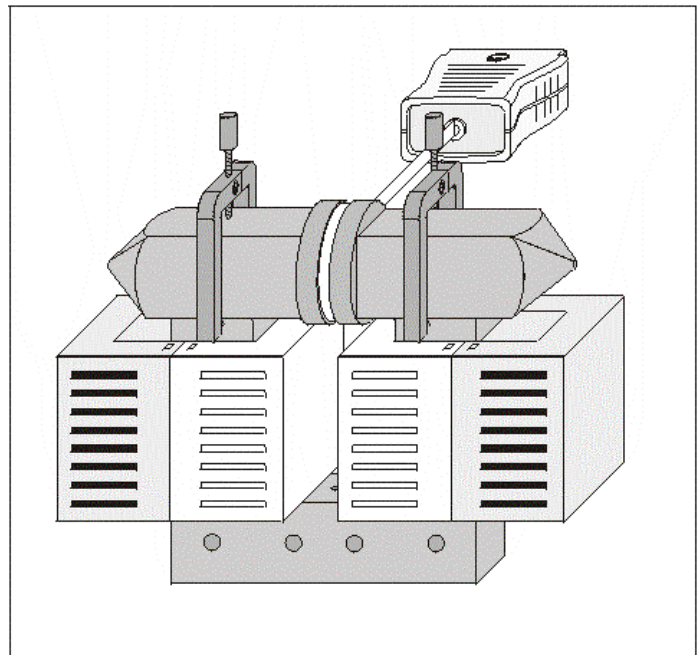


Fig. 2: Calibration of the magnetic field schematically

b) Measuring the Hall voltage as function of the magnetic field

After recording the calibration curve mount the Hall effect apparatus in the electromagnet. The pole pieces have to be pushed as close as possible to the support plate (i.e. the air gap between the pole pieces as narrow as possible and of the same width as for recording the calibration curve).

Safety notes

- For transverse currents over 15 A or magnet currents above 5 A, only switch on the device briefly (overheating of leads or overloading of the coils, which are designed for a maximum load of 5 A).
- In the transverse current circuit, use cables which are rated for a maximum load of 20 A (e.g. connecting leads 501 20 ff or safety connecting leads 500 610).
- Protect the experiment setup from drafts while measuring the Hall voltage.

Setup

The experiment is performed in two steps:

a) Calibration of the magnetic field

Set up the U-core with yoke, the pair of bored pole pieces and the coil with 250 turns as shown in Fig 2. Set the pole piece spacing of the electromagnet exactly to the thickness of the support plate of the Hall effect apparatus. To do this loosen the clamping devices and place one edge of the Hall effect apparatus between the pole pieces. Then push the latter as close as possible to the pole pieces.

Connect the coils with 250 turns in series to the extra low-voltage transformer and locate the Combi B-Sensor S between the pole pieces.

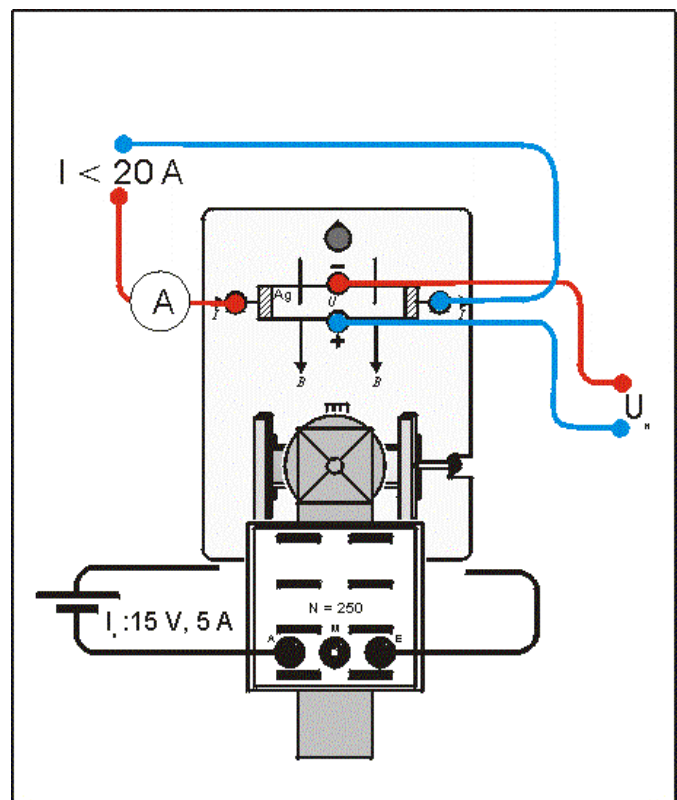


Fig. 3: Experimental setup (wiring diagram) for the Hall effect.

To measure the Hall voltage connect either the Micro-voltmeter or the Mobile CASSY with the μV -Box to the support plate of the Hall effect apparatus.

Connect the Hall effect apparatus to the high current power supply as shown in Fig. 3. The B-field direction should be as printed on the support plate. For measuring the current I through the coils the Multimeter LD analog 30 is used.

Carrying out the experiment

Note: For further notes to the experiment see also instruction sheet 586 81/84.

a) Calibration of the magnetic field

- Demagnetize the iron of the electromagnets before recording the magnetic field as function of the current I by allowing to flow a $I = 5$ A AC current through the field coils 250 turns for a short time; then steadily reduce the current to zero.
- To measure the current I through the coils connect the ammeter between the positive pole of the voltage transformer and the coil.
- Measure the magnetic flux density B as function of the current I by increasing the current I in steps of 0.5 A DC.

b) Measuring the Hall voltage as function of the magnetic field

- Mounting the Hall effect apparatus between the pole pieces (Fig. 3.).
- Before exposing the Hall effect apparatus to the magnetic field, adjust the zero point: Apply a transverse current I of e.g. 10 A and set the indicator of the meter for measuring the Hall voltage U_H to zero using the adjusting knob 4 (see instruction sheet 588 81/84). If the display changes after switching off, switch the transverse current back on and repeat the zero-point adjustment.
- Apply a transverse current $I = 15$ A to the Hall effect apparatus and measure the Hall voltage U_H as function of magnetic field B (Read off the effective field value from the calibration curve of part a)). Carry out several measurements to determine a mean value for the Hall voltage U_H . For further measurement hints see also the instruction sheets 568 81/84 (Hall effect apparatus) and 532 13 (Microvoltmeter).
- Repeat the measurement for a transverse current $I = 20$ A.

Measuring example

a) Calibration of the magnetic field

Table. 1: Magnetic field B as function of the current I through the coils.

$\frac{I}{\text{A}}$	$\frac{B}{\text{T}}$
0.0	0.000
0.5	0.118
1.0	0.200
1.5	0.295
2.0	0.374
2.5	0.455
3.0	0.520
3.5	0.585
4.0	0.630
4.5	0.665
5.0	0.695
5.5	0.715
6.0	0.735
6.5	0.748
7.0	0.760
7.5	0.780
8.0	0.790
8.5	0.800
9.0	0.810

The data of table 1 are plotted in Fig. 4.

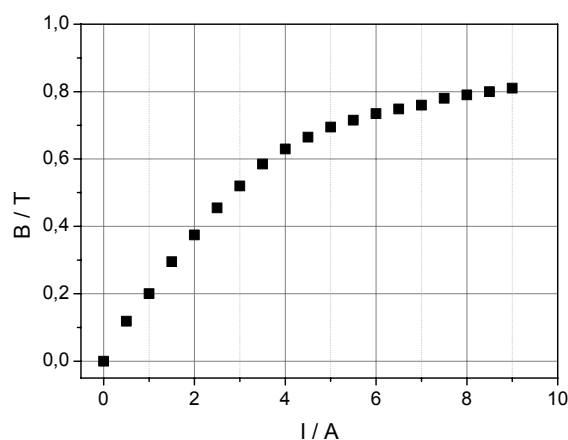


Fig. 4: Calibration curve magnetic field as function of current I .

b) Measuring the Hall voltage as function of the magnetic field

Table. 2: Hall voltage U_H (absolute value) as function of the magnetic field B for constant transverse currents I .

$\frac{B}{T}$	$\frac{U_H}{\mu V}$ ($I = 15 \text{ A}$)	$\frac{B}{T}$	$\frac{U_H}{\mu V}$ ($I = 20 \text{ A}$)
0.20	4.6	0.20	6.25
0.35	8.2	0.38	11.7
0.51	12.0	0.50	15.0
0.62	14.1	0.61	18.1
0.70	16.1	0.68	20.5
0.73	17.0	0.70	21.0
0.76	17.7	0.72	21.6
0.78	18.1	0.76	22.7
0.80	18.6	0.80	24.0

The polarity of the Hall voltage U_H was determined to be negative.

Results

b) Measuring the Hall voltage as function of the magnetic field

The recorded data of Table 2 for the transverse currents $I = 15 \text{ A}$ and $I = 20 \text{ A}$ are plotted in Fig. 5.

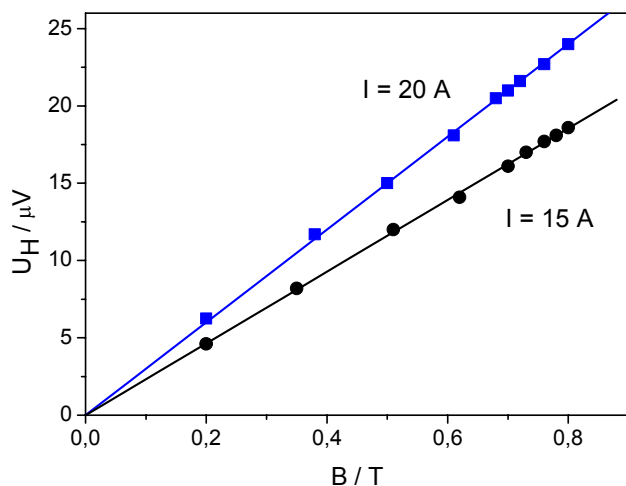


Fig. 5: Hall voltage U_H as function of the magnetic field B for currents $I = 15 \text{ A}$ (circles) and $I = 20 \text{ A}$ (squares). The solid lines correspond to a fit of equation (I).

Evaluation

Form Fig. 5 follows that the Hall voltage U_H is proportional to the magnetic field B :

$$U_H \sim B \tag{III}$$

Form Fig. 5 also follows that the Hall voltage U_H increases with increasing transverse current I :

$$U_H \sim I \tag{III}$$

Note: The proportionality between the Hall voltage U_H and transverse current I can be determined experimentally by measuring the Hall voltage U_H as function of the transverse current I for a constant magnetic field B .

From the fit of equation (I) to the experimental data is resulting the slope

$$A_H = \frac{1}{n \cdot e} \cdot I$$

$$A_H (I = 15 \text{ A}) = 23.2 \frac{\mu V}{T}$$

$$A_H (I = 20 \text{ A}) = 30.4 \frac{\mu V}{T}$$

With the thickness $d = 5 \cdot 10^{-5} \text{ m}$ the Hall constant can be determined (absolute value):

$$R_H (I = 15 \text{ A}) = 7.7 \cdot 10^{-11} \frac{\text{m}^3}{\text{C}}$$

$$R_H (I = 20 \text{ A}) = 7.6 \cdot 10^{-11} \frac{\text{m}^3}{\text{C}}$$

Literature value: $R_H = 8.9 \cdot 10^{-11} \frac{\text{m}^3}{\text{C}}$

The Hall voltage is determined to be negative. This shows that in silver the conduction mechanism is mainly effected by negative charge carriers.

With elementary charge $e = 1.602 \cdot 10^{-19} \text{ C}$ follows the concentration of charge carriers:

$$n (I = 15 \text{ A}) = 8.1 \cdot 10^{28} \frac{1}{\text{m}^3}$$

$$n (I = 20 \text{ A}) = 8.2 \cdot 10^{28} \frac{1}{\text{m}^3}$$

Literature value: $6.6 \cdot 10^{28} \frac{1}{\text{m}^3}$

(atoms density $5.8 \cdot 10^{22} \frac{1}{\text{m}^3}$)

Supplementary information

In 1916, Tolman obtained certain proof that electrons are the charge carriers in metals.